

Montana Tech Library

Digital Commons @ Montana Tech

Graduate Theses & Non-Theses

Student Scholarship

Spring 2020

MODELING UNCONVENTIONAL WATER PRODUCTION IN THE NORTHEAST ELM COULEE FIELD, BAKKEN FORMATION

Jan Branning

Follow this and additional works at: https://digitalcommons.mtech.edu/grad_rsched



Part of the [Petroleum Engineering Commons](#)

MODELING UNCONVENTIONAL WATER PRODUCTION IN THE NORTHEAST ELM COULEE FIELD, BAKKEN FORMATION

by
Jan Branning

A thesis submitted in partial fulfillment of the
requirements for the degree of

Master of Science in Petroleum Engineering

Montana Tech

2020



Abstract

Wells within the Northeast (NE) Elm Coulee produce significantly higher water cuts than wells within Elm Coulee Proper. The purpose of this work was to identify the source of produced water in the NE Elm Coulee. An area within the NE Elm Coulee was selected for a numerical flow simulation analysis, and a total of three models of the project area were constructed by isolating production mechanisms to determine the source of produced water in the NE Elm Coulee. A Separate Tank model was constructed to determine if the source of the produced water was matrix water saturation in the Middle Bakken. Two Vertical Migration models were constructed to determine if the source of the produced water was from vertical migration from the Three Forks formation into the Middle Bakken via hydraulic fracture flow paths or natural fracture networks in the Lower Bakken shale member. The models were constructed using data from various sources, and each model was history matched by matching simulated and observed fluid rates and cumulative volumes. The impact of natural fracture networks in the Middle Bakken on fluid production was determined in the modeling process through the use of a discrete fracture network (DFN) modeling technique. The modeling and history matching processes identified matrix water saturation in the Middle Bakken as the most likely source for the produced water in the NE Elm Coulee.

Keywords: Elm Coulee, Bakken, water production, water cut, unconventional simulation, discrete fracture network, DFN

Acknowledgements

My academic success would not have been possible without the help and support of the Montana Board of Oil and Gas, Montana Technological University, and my family and friends.

First and foremost, I would like to thank Dr. B. Todd Hoffman for being my academic advisor throughout my graduate studies. Dr. Hoffman's wisdom and guidance helped me to achieve my academic goals through his mentorship and support. In addition, I would like to thank my committee members, David Reichhardt and Dr. Glenn Shaw, for their participation and input during my graduate studies. I have greatly enjoyed my time at Montana Tech, and it has been a pleasure to work with the entire Montana Tech Petroleum Engineering department.

My family has provided immense emotional and financial support during my studies at Montana Tech. A special thank you to my mom, April, and my sister, Ashton, for helping me to stay focused and determined to achieve my goals as an engineer. I would also like to thank my brother-in-law, Jasen, and my stepfather, Scott, for always being available and willing to help with anything throughout my academic career. The support of my family made my accomplishments possible – thank you all!

Finally, thank you to the Montana Board of Oil and Gas and the Montana Tech Graduate School for the financial support during my graduate studies. I am grateful for the tuition waiver, project funding, and stipend. I am honored to have worked on an oil and gas project within Montana as a Montana native.

Table of Contents

ABSTRACT	II
ACKNOWLEDGEMENTS	III
LIST OF TABLES	VII
LIST OF FIGURES.....	VIII
 1. INTRODUCTION.....	 1
1.1. Bakken Petroleum System	1
1.1.1. Stratigraphy.....	2
1.1.2. Structure	4
1.1.3. Formation Thickness	5
1.1.4. Porosity and Permeability	6
1.2. Elm Coulee Field.....	6
1.2.1. Natural Fractures.....	7
1.2.2. Water Production	9
1.3. Study Objectives.....	11
1.4. Data Sources	11
2. PROJECT AREA	12
2.1. Sundheim 21-27 Well Evaluation	12
2.1.1. Well Construction	13
2.1.2. Well Production.....	14
3. NUMERICAL FLOW SIMULATION	16
3.1. Geologic Model Structure	17
3.2. Model Discretization	20
3.2.1. Grid Block Size	20
3.2.2. Model Layering.....	21
3.3. Fluid Properties.....	23

3.4.	<i>Rock Properties</i>	25
3.4.1.	Matrix Grid	26
3.4.1.1.	Vertical Porosity Trend Model	26
3.4.1.2.	Matrix Permeability	29
3.4.1.3.	Matrix Relative Permeability Curves	30
3.4.2.	Fracture Grid	32
3.4.2.1.	Discrete Fracture Network (DFN)	32
3.4.2.2.	Fracture Relative Permeability Curves	34
3.5.	<i>Initialization</i>	35
3.6.	<i>Well Construction</i>	37
3.6.1.	Well Trajectories	37
3.6.2.	Hydraulic Fracture Completions	38
3.6.2.1.	Discrete Fracture Network (DFN) Completions	39
3.6.3.	Well Production Constraints	39
4.	<i>HISTORY MATCHING</i>	40
4.1.	<i>Separate Tank Model</i>	41
4.1.1.	Separate Tank (ST) Base Case	41
4.1.2.	Matrix Permeability	43
4.1.3.	Relative Permeability Curves	45
4.1.4.	Water Saturation	50
4.1.5.	Discrete Fracture Network (DFN) Optimization	52
4.1.6.	Pressure Dependent Permeability (T_m)	58
4.2.	<i>Vertical Migration Models</i>	62
4.2.1.	Hydraulic Fracture Vertical Migration (HFVM) Base Case	62
4.2.1.1.	Hydraulic Fracture Vertical Migration Initial Changes	63
4.2.1.2.	Hydraulic Fracture Permeability	65
4.2.1.3.	Matrix Permeability	68
4.2.2.	Natural Fracture Vertical Migration (NFVM) Base Case	71
4.2.2.1.	Natural Fracture Vertical Migration Initial Changes	71

4.2.2.2. Lower Bakken DFN Adjustments.....	75
5. RESULTS	79
5.1. <i>Separate Tank Model</i>	79
5.1.1. Separate Tank Results.....	79
5.2. <i>Vertical Migration Models</i>	81
5.2.1. Hydraulic Fracture Vertical Migration (HFVM) Model.....	81
5.2.1.1. Hydraulic Fracture Vertical Migration Results	81
5.2.2. Natural Fracture Vertical Migration (NFVM) Model.....	83
5.2.2.1. Natural Fracture Vertical Migration Results	83
5.3. <i>Discussion</i>	85
5.3.1. Study Question 1	85
5.3.1.1. Separate Tank Evidence	85
5.3.1.2. Vertical Migration Evidence.....	86
5.3.2. Study Question 2	88
5.3.3. Study Question 3	90
6. CONCLUSIONS.....	91
7. REFERENCES	93
8. APPENDIX A: ADDITIONAL TABLES AND FIGURES.....	96

List of Tables

Table I: Average Water Cuts of Sundheim 21-27 Well Cluster	14
Table II: Number of Vertical Layers per Interval	21
Table III: Horizontal Matrix Permeability for Both Model Cases.....	30
Table IV: Property Uncertainty Identification.....	41
Table V: Initial Pressure Dependent Transmissibility Table	59
Table VI: Modified Pressure Dependent Transmissibility Table	59
Table VII: History Matched Pressure Dependent Transmissibility Table	60
Table VIII: Sundheim 21-27-1H Simulated Cumulative Volumes DFN Comparison...	107
Table IX: Sundheim 21-27-2H Simulated Cumulative Volumes DFN Comparison	107
Table X: Sundheim 21-27-3H Simulated Cumulative Volumes DFN Comparison.....	107

List of Figures

Figure 1: Location of Bakken Formation, Williston Basin (Bakken Oil Business Journal, n.d.)	
.....	2
Figure 2: Stratigraphic Column of the Bakken Petroleum System.....	3
Figure 3: Structure of the Bakken Petroleum System (Sonnenberg and Pramudito, 2009)	4
Figure 4: Thickness of Bakken and Upper Three Forks Members (Hamlin et al., 2017)...	5
Figure 5: Location of the Elm Coulee Field, Bakken	7
Figure 6: Conceptual Elm Coulee Fracture Model (Khatri, 2017)	8
Figure 7: Water Production in the Elm Coulee Field.....	9
Figure 8: Average Water Cut of Bakken Wells in the Elm Coulee based on IP (MBOG, 2018)	
.....	10
Figure 9: Location of Sundheim 21-27 Well Cluster, NE Elm Coulee	12
Figure 10: Sundheim 21-27-1H Calculated Water Cut.....	15
Figure 11: Sundheim 21-27-2H Calculated Water Cut.....	15
Figure 12: Sundheim 21-27-3H Calculated Water Cut.....	15
Figure 13: Geologic Model Vertical Log Locations in Relation to Project Area.....	18
Figure 14: Identifying Formation Tops using GR Logs.....	18
Figure 15: Generated Surfaces of Geologic Model	19
Figure 16: Project Area Discretized into 100' by 100' Grid Blocks.....	21
Figure 17: Project Area Discretized into 24 Vertical Layers	22
Figure 18: Oil Formation Volume Factor Curves.....	24
Figure 19: Oil Viscosity Curves	24
Figure 20: Neutron Porosity Log Example	27

Figure 21: Upscaled Neutron Porosity Log Values	28
Figure 22: Porosity Distribution in Model Space	29
Figure 23: Initial Oil-Water Relative Permeability Curves.....	31
Figure 24: Initial Gas-Oil Relative Permeability Curves	31
Figure 25: Example DFN of the Middle Bakken Member	33
Figure 26: Linear Relative Permeability Curves for Fracture Fluids	34
Figure 27: Average Middle Bakken Water Saturation in Elm Coulee Proper (Almanza, 2011)	36
Figure 28: Sundheim 21-27 Well Cluster Trajectories	37
Figure 29: DFN Hydraulic Fracture Completion on Sundheim 21-27-1H	39
Figure 30: Separate Tank Base Case Rates	42
Figure 31: Separate Tank Base Case Volumes	42
Figure 32: Matrix Permeability Sensitivity Analysis on Sundheim 21-27-2H Oil Rate ..	44
Figure 33: Matrix Permeability Sensitivity Analysis on Sundheim 21-27-2H Cumulative Oil Volume.....	44
Figure 34: Initial Adjustment to the Oil-Water Relative Permeability Curve.....	46
Figure 35: Oil and Water Rates for Sundheim 21-27-1H After Reducing S_{wcr}	46
Figure 36: Relative Permeability Curves After Altering Corey Exponents	47
Figure 37: Oil and Water Rates for Sundheim 21-27-1H After Adjusting Corey Exponents	48
Figure 38: History Matched Oil-Water Relative Permeability Curves	49
Figure 39: Oil and Water Rates for Sundheim 21-27-1H After Relative Permeability History Matching	49

Figure 40: Separate Tank Matrix Water Saturation Sensitivity Analysis	51
Figure 41: Initial Middle Bakken DFN	53
Figure 42: Sundheim 21-27-1H Oil and Water Rates using Initial DFN	53
Figure 43: Permeability in the Middle Bakken Fracture Grid	54
Figure 44: DFN Representing Dual Fracture Systems in the Middle Bakken Member ...	55
Figure 45: Initial Middle Bakken DFN	56
Figure 46: Sundheim 21-27-1H Oil and Water Rates Post DFN Modeling	57
Figure 47: Sundheim 21-27-1H Oil and Water Rates with Initial T_m Modification	60
Figure 48: Sundheim 21-27-1H Oil and Water Rates with History Matched T_m	61
Figure 49: Tall Hydraulic Fractures Penetrating into the Three Forks Formation	63
Figure 50: Sundheim 21-27-1H Hydraulic Fracture Vertical Migration Model Base Case Rates	64
Figure 51: Lower Bakken Initial Fracture Grid Permeability	65
Figure 52: Lower Bakken Fracture Grid Permeability After Increasing Hydraulic Fracture Permeability	66
Figure 53: Sundheim 21-27-1H Oil and Water Rates After Increasing Hydraulic Fracture Permeability	67
Figure 54: Sundheim 21-27-1H Oil and Water Rates After Reducing Middle Bakken Permeability	69
Figure 55: Final Lower Bakken Fracture Grid Permeability	70
Figure 56: Final Simulated Oil and Water Rates for Hydraulic Fracture Vertical Migration Case	71
Figure 57: Initial DFN for the Lower Bakken Shale Member	72

Figure 58: Fracture Grid of the Lower Bakken After Upscaling DFN Properties	73
Figure 59: Natural Fracture Base Case Sundheim 21-27-1H Oil and Water Rates.....	74
Figure 60: Fracture Grid of the Lower Bakken After Reducing DFN Intensity	75
Figure 61: Water Migration for Natural Fracture Vertical Migration Model in Sundheim 21-27-1H	76
Figure 62: History Matched Lower Bakken Fracture Grid Permeability.....	77
Figure 63: Sundheim 21-27-1H History Matched NFVM Simulated Oil and Water Rates	78
Figure 64: Sundheim 21-27-1H Separate Tank History Matched Rates.....	80
Figure 65: Sundheim 21-27-1H Separate Tank History Matched Cumulative Volumes .	80
Figure 66: Sundheim 21-27-1H HFVM History Matched Rates.....	82
Figure 67: Sundheim 21-27-1H HFVM History Matched Cumulative Volumes	82
Figure 68: Sundheim 21-27-1H NFVM History Matched Rates.....	84
Figure 69: Sundheim 21-27-1H NFVM History Matched Cumulative Volumes	84
Figure 70: Sundheim 21-27-1H Simulated Cumulative Water Recovery in HFVM Model with 50 Percent Middle Bakken Matrix Water Saturation	87
Figure 71: Sundheim 21-27-1H Simulated Oil Rates in the ST Model with and without Middle Bakken DFN.....	88
Figure 72: Sundheim 21-27-1H Simulated Cumulative Volumes in the ST Model with and without Middle Bakken DFN.....	89
Figure 73: DFN Hydraulic Fracture Completion on Sundheim 21-27-2H	96
Figure 74: DFN Hydraulic Fracture Completion on Sundheim 21-27-3H	96
Figure 75: DFN Completions on Sundheim 21-27 Wells	97

Figure 76: Middle Bakken Matrix Permeability Sensitivity Analysis on Sundheim 21-27-2H Oil Rates	98
Figure 77: Middle Bakken Matrix Permeability Sensitivity Analysis on Sundheim 21-27-3H Oil Rates	98
Figure 78: Sundheim 21-27-2H Separate Tank History Matched Cumulative Volumes .	99
Figure 79: Sundheim 21-27-2H Separate Tank History Matched Cumulative Volumes .	99
Figure 80: Sundheim 21-27-3H Separate Tank History Matched Rates.....	100
Figure 81: Sundheim 21-27-3H Separate Tank History Matched Cumulative Volumes	100
Figure 82: Sundheim 21-27-2H HFVM History Matched Rates.....	101
Figure 83: Sundheim 21-27-2H HFVM History Matched Cumulative Volumes	101
Figure 84: Sundheim 21-27-3H HFVM History Matched Rates.....	102
Figure 85: Sundheim 21-27-3H HFVM History Matched Cumulative Volume	102
Figure 86: Sundheim 21-27-2H NFVM History Matched Rates.....	103
Figure 87: Sundheim 21-27-2H NFVM History Matched Cumulative Volumes	103
Figure 88: Sundheim 21-27-3H NFVM History Matched Rates.....	104
Figure 89: Sundheim 21-27-3H NFVM History Matched Cumulative Volumes	104
Figure 90: Sundheim 21-27-2H Simulated Oil Rates in the ST Model with and without Middle Bakken DFN.....	105
Figure 91: Sundheim 21-27-2H Simulated Cumulative Volumes in the ST Model with and without Middle Bakken DFN.....	105
Figure 92: Sundheim 21-27-3H Simulated Oil Rates in the ST Model with and without Middle Bakken DFN.....	106

Figure 93: Sundheim 21-27-3H Simulated Cumulative Volumes in the ST Model with and without Middle Bakken DFN.....	106
Figure 94: Initial vs History Matched ST Model Relative Permeability Curves	107

1. Introduction

The Elm Coulee field, located primarily within Richland county, northeastern Montana, is part of the Bakken Petroleum System (Sonnenberg and Pramudito, 2009). Field development and economic production in the Elm Coulee began in 2000, motivated by improved horizontal drilling capabilities and multi-stage hydraulic fracturing (Sonnenberg and Pramudito, 2009). The realized potential of the Elm Coulee was instrumental in the large-scale development of the Bakken within North Dakota, and it also helped to form the foundation of the global oil-shale industry. The Elm Coulee consists of two main areas of production: Elm Coulee Proper and the Northeast (NE) Elm Coulee. To date, more than 1,200 wells have been drilled in the Elm Coulee field, with approximately 1,100 wells active in 2020. The Elm Coulee field highlights the production potential of the Bakken Petroleum System, and it can be studied to understand the mechanics and challenges of water and oil production from unconventional petroleum reservoirs.

1.1. Bakken Petroleum System

The Bakken Petroleum System is composed of three stratigraphic intervals: the Lodgepole formation, the Bakken formation, and the Three Forks formation, and it is classified as a continuous petroleum accumulation (Nordeng, 2009; Sonnenberg, Theloy, and Jin, 2017). The Bakken Petroleum System is one of North America's largest accumulations of unconventional oil and gas, and estimates for the technically recoverable volume of hydrocarbons in the Bakken Petroleum System is nearly 7.4 billion barrels of oil and 6.7 trillion cubic feet of gas (Sonnenberg et al., 2017). The Bakken Petroleum System spans across the U.S. states of Montana and North Dakota and the Canadian provinces of Saskatchewan and Manitoba (Stroud and Sonnenberg, 2011). A map with the location of the Bakken formation within the Williston Basin in relation to the U.S. and Canada can be seen in Figure 1.

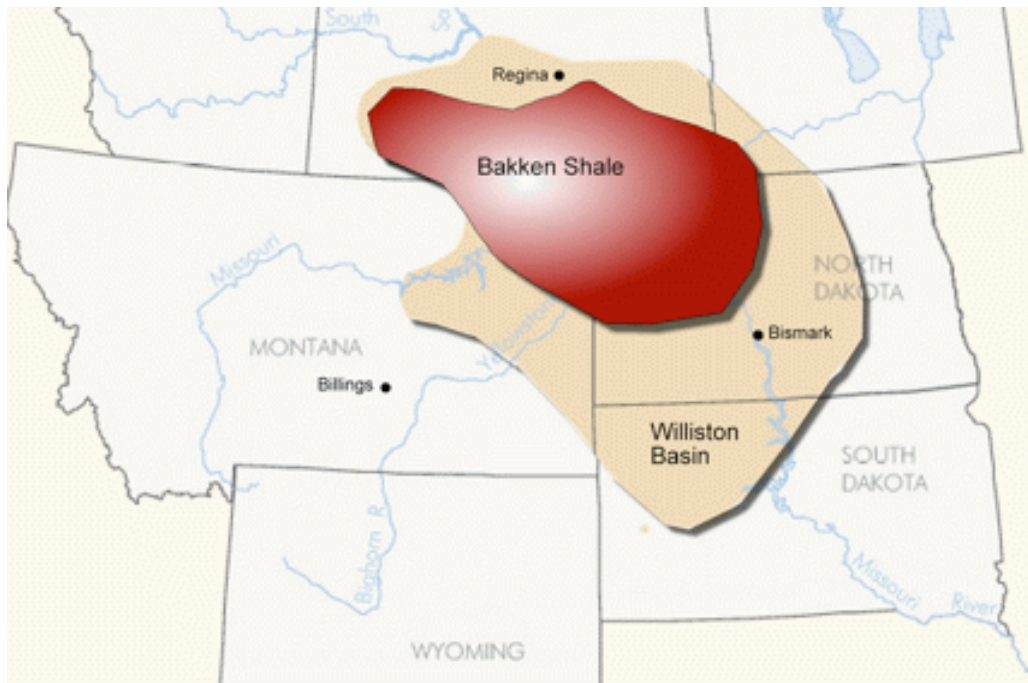


Figure 1: Location of Bakken Formation, Williston Basin (Bakken Oil Business Journal, n.d.)

1.1.1. Stratigraphy

The Bakken formation is bounded by the Lodgepole shale and limestone unit above, and the Three Forks dolomite unit below (Sonnenberg, 2014). The Bakken Petroleum System is late Devonian, early Mississippian in age, and it was deposited roughly 400 million years ago (Sonnenberg, 2014). The main source of hydrocarbon production within the Bakken Petroleum System is from the Bakken formation; however, production from the Three Forks formation is economic in some areas of the Williston Basin.

The Bakken formation is located at depths of 8,500 ft to 11,500 ft depending on location within the Williston Basin, and it consists of three main stratigraphic members: the Upper shale member, Middle dolomite member, and Lower shale member (Sonnenberg and Pramudito, 2009). The Upper and Lower shale members bounding the Middle Bakken member are the source rocks for the Bakken Petroleum System, and the Upper shale member of the Bakken was

previously targeted for production in the late 1970's through the early 1990's with vertical and horizontal wells (Sonnenberg, 2014). The target zone for most wells completed in the Bakken Petroleum System today are within the Middle member of the Bakken formation; however, the upper bench of the Three Forks formation is commonly targeted, and it is estimated to contain 3.7 billion barrels of technically recoverable oil (Sonnenberg, 2015). Because the Bakken Petroleum System is a continuous hydrocarbon accumulation, some influx of hydrocarbons from the Upper shale member has been speculated to contribute to the overall production in the Bakken's Middle member, and Sonnenberg and Pramudito estimated that up to 20 percent of the Elm Coulee's total production could be coming from hydrocarbon migration from the Upper Bakken shale member (2009). Figure 2 shows the stratigraphic sequence of the Bakken Petroleum System (Sonnenberg and Pramudito, 2009).

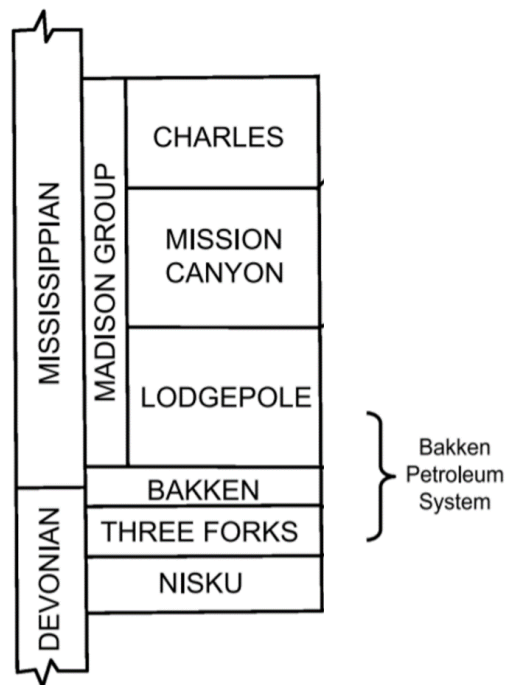


**Figure 2: Stratigraphic Column of the Bakken Petroleum System
(Sonnenberg and Pramudito, 2009)**

1.1.2. Structure

The overall structure of the Bakken Petroleum System is shown in Figure 3 as a cross-section from west to east. The structure of the system follows the structure of the Williston Basin, with the Lodgepole, Bakken, and Three Forks formations being at their deepest point in the central portions of the basin, located near Williston, North Dakota. The depth of the system is at the shallowest points near the western and eastern portions of the Williston Basin, where the Bakken formation pinches out. The most notable structural feature within the Bakken Petroleum System is the Nesson Anticline, seen in the central portions of the system; however, the system contains additional anticlines such as the Billings, TR, Little Knife, and Cedar Creek anticlines (Sonnenberg, 2014; Sonnenberg and Pramudito, 2009). The Elm Coulee field is located in the western portion of the Bakken Petroleum System, and it is pictured in relation to the structure of the system in Figure 3.

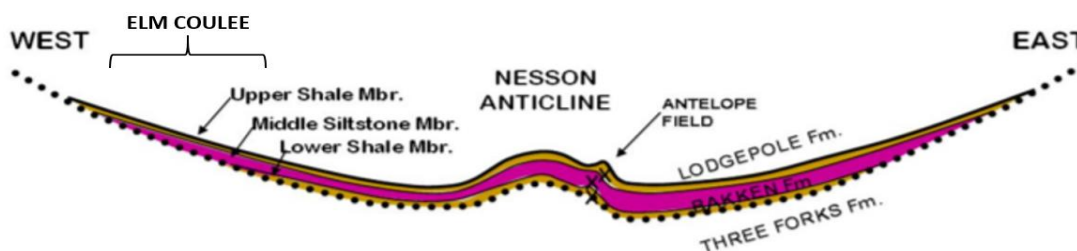


Figure 3: Structure of the Bakken Petroleum System (Sonnenberg and Pramudito, 2009)

The three stratigraphic members of the Bakken are characterized by relatively thin bedding, with the Middle and Lower Bakken shale members pinching out in the southwest portion of the Elm Coulee field (Sonnenberg, 2014; Todd, Reichhardt, and Heath, 2017). The Bakken reaches its maximum thickness in the central portion of the Williston Basin near the Nesson Anticline. East of this area, the total thickness of the formation approaches 140 feet (Sonnenberg, et al., 2017). The total thickness of the Bakken formation in the Elm Coulee field is approximately 50 feet to 70 feet (Todd et al., 2017).

1.1.3. Formation Thickness

Both Bakken shales, the Upper and Lower members, are thinner than the Middle Bakken dolomite member. The Upper shale member has a thickness ranging from 0.5 feet to 46 feet depending on location in the basin (Price, 1999). Within the Elm Coulee, the Upper shale member in the ranges from 6 feet to 10 feet (Sonnenberg and Pramudito, 2009). The Bakken's Middle dolomite member has a thickness ranging from 10 feet to 92 feet across the Williston Basin, and a thickness ranging from 10 feet to 40 feet in the Elm Coulee field (Todd et al., 2017; Tran, Sinurat, and Wattenbarger, 2011). The Lower shale member has thicknesses ranging from 2 feet to 14 feet across the Williston Basin, and a thickness range of 2 feet to 6 feet within the Elm Coulee field (Sonnenberg and Pramudito, 2009; Steptoe, 2012). The Lower member of the Lodgepole formation and the Upper member of the Three Forks formation are considered part of the Bakken Petroleum System (Khatri, 2017; LeFever, LeFever, and Nordeng, 2013). Figure 4 shows the thickness of the Bakken and upper Three Forks members across the Williston Basin (Hamlin et al., 2017).

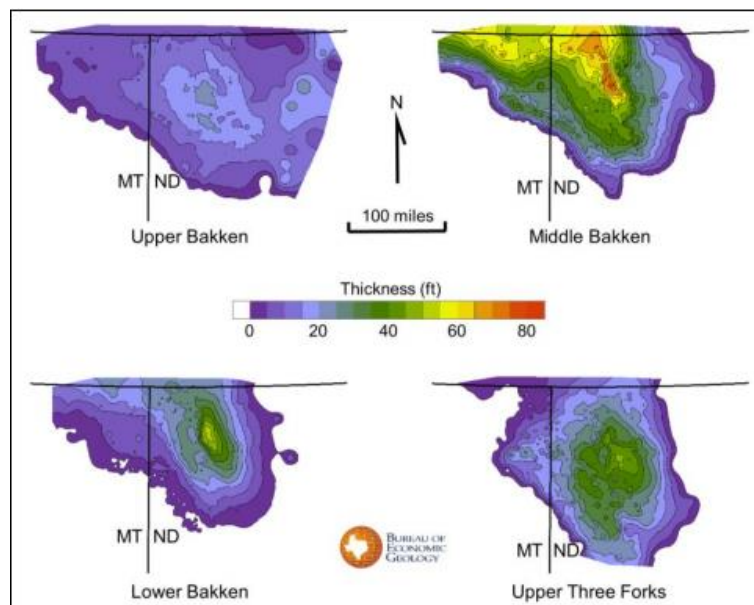


Figure 4: Thickness of Bakken and Upper Three Forks Members (Hamlin et al., 2017)

1.1.4. Porosity and Permeability

All members of the Bakken Petroleum System are characterized as unconventional reservoir rocks with low matrix porosity and permeability (Sonnenberg and Pramudito, 2009). Oil bearing Waulsortian-like mounds in the Lodgepole have porosity and permeability values ranging from 2 percent to 5 percent and 0.01 md to 0.5 md, respectively (Burke, 1996). The Upper and Lower Bakken shale members have porosities ranging from 0 percent to 8.5 percent, and permeability values ranging from 0.01 md to 0.03 md (Hamlin et al., 2017; Tran et al., 2011). Upper and Lower Bakken shale porosity percentages in the Elm Coulee may be higher than these values, with porosities approaching 30 percent in some areas. Porosity for the Bakken Middle member ranges from 3 percent to 9 percent, with permeability in the sub-millidarcy range at an average value of 0.04 md (Sonnenberg and Pramudito, 2009). Porosities in the upper bench of the Three Forks range from 2 percent to 9.5 percent, and permeability values average less than 0.25 md (Hamlin et al., 2017; Sonnenberg, 2015). The Middle Bakken in the Elm Coulee has a highly dolomitic facies, and porosity and permeability in the Elm Coulee have been observed to be higher than other areas of the Bakken due to dissolution (Cox et al., 2008).

1.2. Elm Coulee Field

The Elm Coulee field is located in and around Richland county, eastern Montana, and is comprised of the production wells, colored by operator, in Figure 5. The wells in the Elm Coulee are broken down into two main production areas: Elm Coulee Proper and the NE Elm Coulee. The wells outlined in black in Figure 5 represent the Elm Coulee Proper area, and the wells outlined in red represent the NE Elm Coulee area. Wells in the Elm Coulee Proper were drilled first starting in 2000, and the NE Elm Coulee was subsequently developed in the early 2010's. The majority of wells within the Elm Coulee field target the Middle Bakken member for

economic production, but some Three Forks wells have also been drilled in the Elm Coulee. Oil production in the Elm Coulee has been categorized by initial production rates ranging from 200 barrels of oil per day (BOPD) to 1,900 BOPD, with noticeable areas of higher initial production, labeled as “sweet spots” within the field (Sonnenberg and Pramudito, 2009).

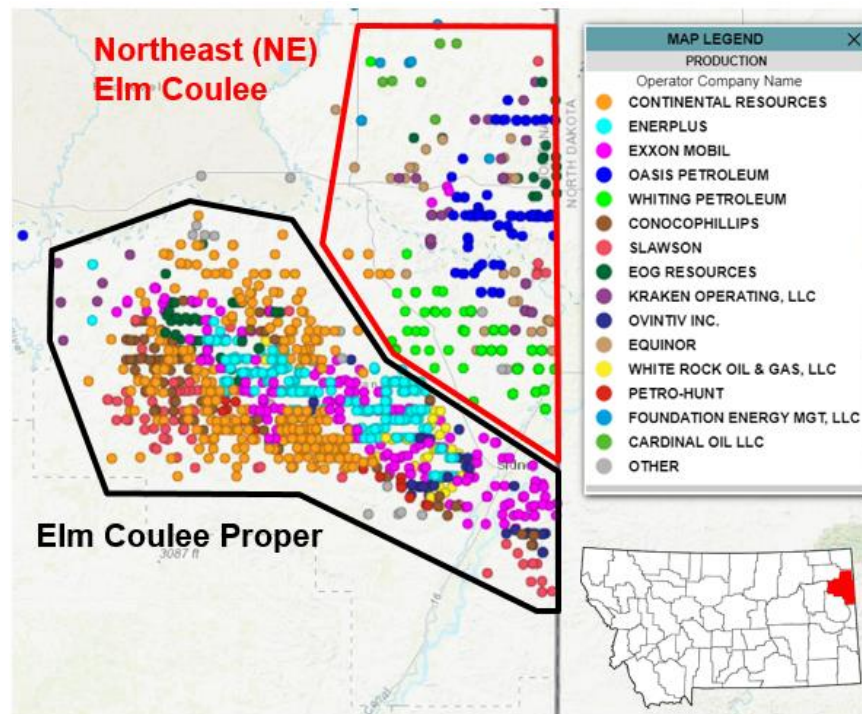


Figure 5: Location of the Elm Coulee Field, Bakken

1.2.1. Natural Fractures

The Bakken formation is slightly overpressured with an observed pressure gradient of 0.52 psi/ft, and fractures have been observed in cores because of the reservoir’s overpressured nature (Messner, 1978). The overpressure in the Bakken is a result of in-situ oil maturation, and the fractures generated from overpressure are classified as expulsion fractures. Additional tectonic fractures exist in the Bakken as a result of structural influence (Borglum and Todd, 2012). “Sweet spots,” or areas where initial production rates have been observed to be high, combined with seismic measurements, have been used to locate and quantify the natural fractures

and their parameters within the Elm Coulee, and it has been determined that Elm Coulee Proper has two main fracture networks: one with fractures oriented $\sim 45^\circ$ NE, and a secondary set with fractures oriented $\sim 60^\circ$ NW (Almanza, 2011; Khatri, 2017). Khatri (2017) also used seismic interpretation to identify structural faults and fracture networks within the Elm Coulee, and a figure summarizing the two natural fracture systems within the Elm Coulee can be seen below.

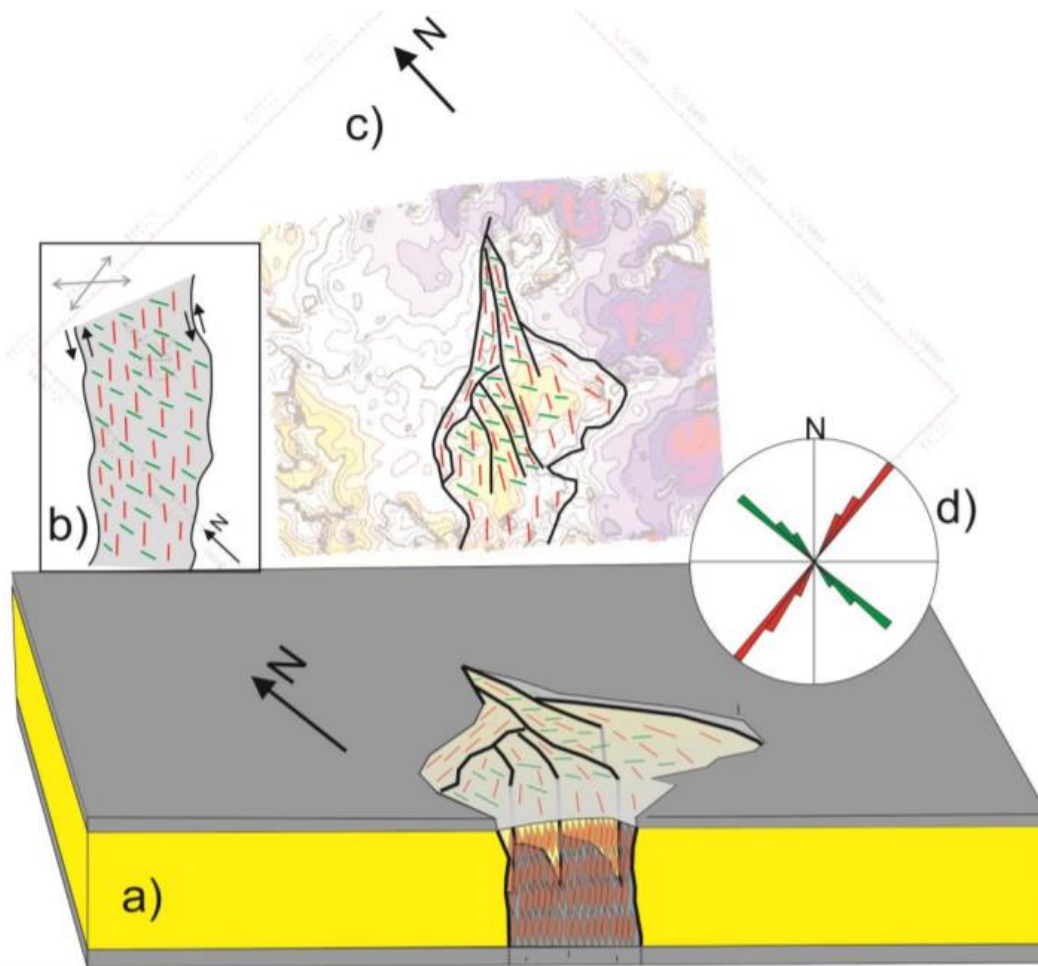


Figure 6: Conceptual Elm Coulee Fracture Model (Khatri, 2017)

The grey layers in Figure 6 represent the Upper and Lower Bakken shales, while the yellow layer represents the Middle Bakken member. Identified faults are shown in the figure with heavy black lines (Khatri, 2017). The fractures oriented NE-SW are represented by red, and the fractures oriented NW-SE are represented by green lines. The fracture networks in the

Bakken enhance reservoir permeability and porosity, and the fractures contribute to the initial production rates and recovery volumes for wells in the Elm Coulee (Almanza, 2011).

1.2.2. Water Production

Operators in the Elm Coulee have observed a significant difference in water cuts between wells in Elm Coulee Proper and the NE Elm Coulee. The wells within Elm Coulee Proper have average water cuts of 0 percent to 30 percent, whereas wells within the NE Elm Coulee produce higher water cuts of 50 percent to 70 percent. The boundary between the two areas in the Elm Coulee cannot be explained through significant structures or faults that have been identified. Figure 7 shows the difference in observed cumulative water production between the Elm Coulee Proper and the NE Elm Coulee, where cumulative water production volumes are visualized by color for wells in the Elm Coulee.

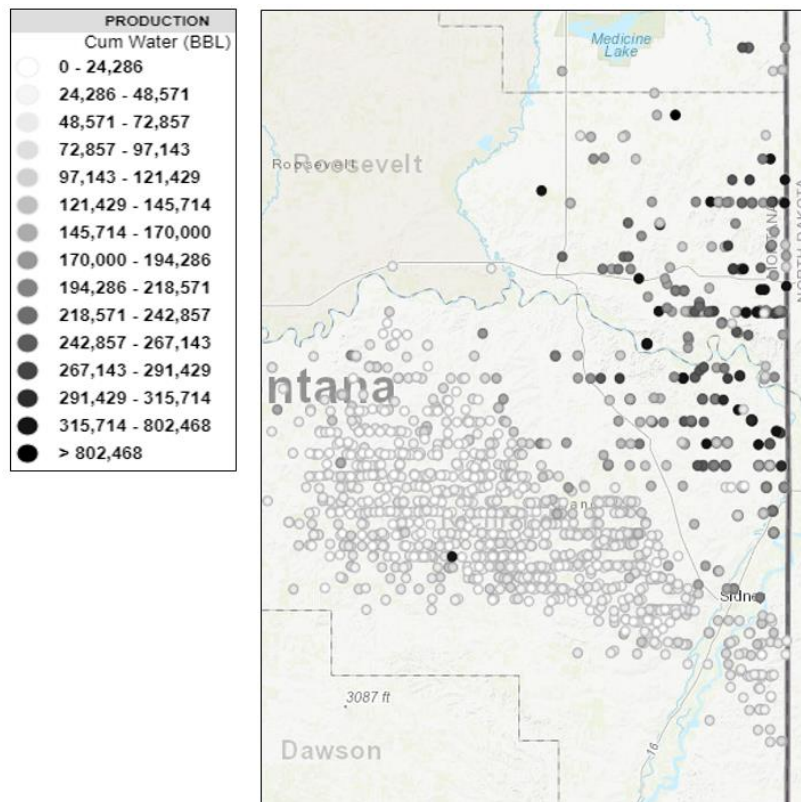


Figure 7: Water Production in the Elm Coulee Field

A map showing the average water cut for Bakken wells in Elm Coulee Proper and the NE Elm Coulee based on initial production (IP) is shown in Figure 8 (Montana Board of Oil and Gas [MBOG], 2018). The thick black line in Figure 8 depicts the boundary of Elm Coulee Proper, and contours showing the thickness of the Middle Bakken within Elm Coulee Proper are shown in the figure. Figure 8 highlights the distinct difference in produced water cuts that operators in the Elm Coulee have observed since drilling and completing wells in the NE Elm Coulee.

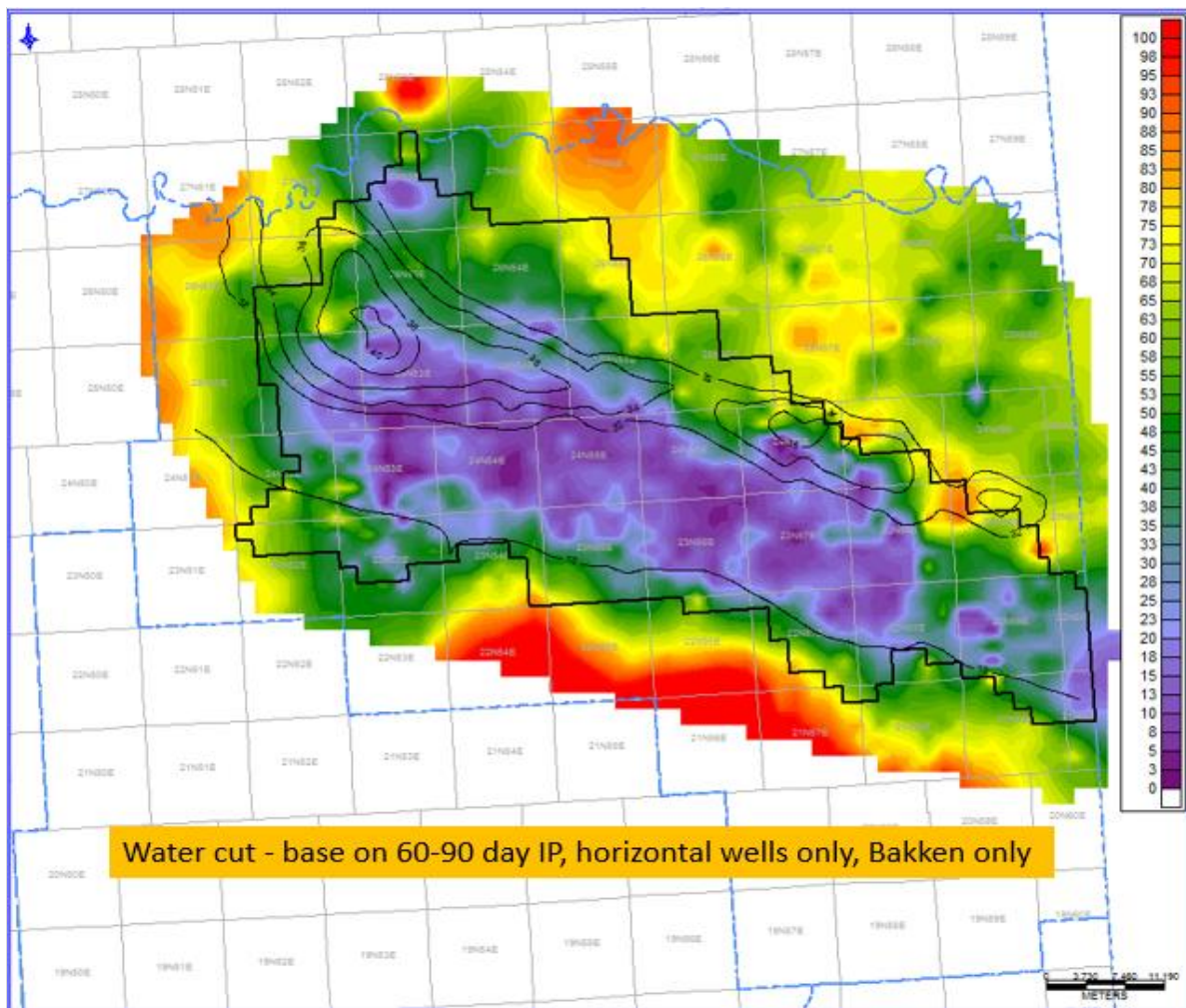


Figure 8: Average Water Cut of Bakken Wells in the Elm Coulee based on IP (MBOG, 2018)

1.3. Study Objectives

The research in this paper answers the following questions by creating numerical flow simulations of the Sundheim 21-27 well cluster, located in the NE Elm Coulee field:

- (1) What is the source of the produced water in the NE Elm Coulee?
- (2) How much production influence do natural fracture systems have on wells in the NE Elm Coulee?
- (3) Can operators minimize water production-related expenses and increase profitability in the NE Elm Coulee?

1.4. Data Sources

Data for the project was obtained through public records from the Montana Board of Oil and Gas, peer-reviewed literature sources, and Drillinginfo. Maps, production data, core data, PVT measurements, and well logs were used from the data sources to construct three numerical flow simulations of the project area to determine the source of produced water in the NE Elm Coulee.

2. Project Area

Project data was collected from wells within Township 25N, Range 58E to construct a geologic model of the area. The Sundheim 21-27 well cluster was selected for numerical flow simulation to determine the source of produced water in the NE Elm Coulee. The group of wells is located in sections 27 and 34 of T25N, R58E. There is a total of 4 wells within the two-section area; however, only 3 of the wells are active and producing as of 2020. The wells are located on the southwest edge of the NE Elm Coulee field, and the wells are operated by Whiting Petroleum Corporation. Figure 9 shows the location of the Sundheim 21-27 well cluster within the NE Elm Coulee.

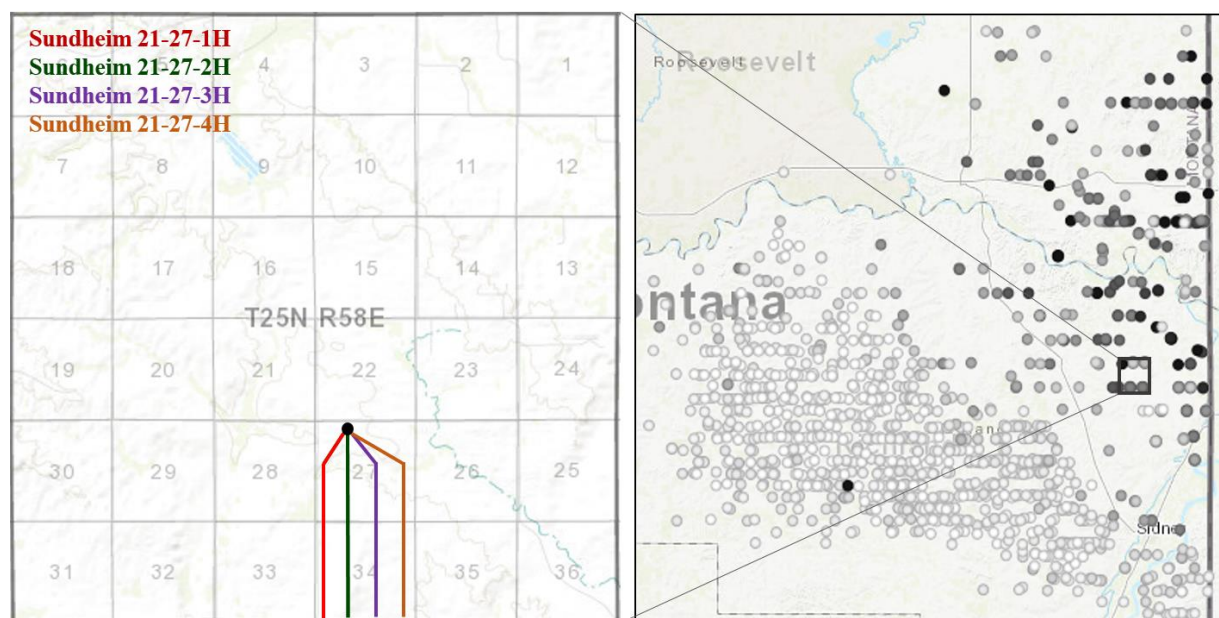


Figure 9: Location of Sundheim 21-27 Well Cluster, NE Elm Coulee

2.1. Sundheim 21-27 Well Evaluation

There are four wells in the Sundheim 21-27 well cluster: Sundheim 21-27-1H, Sundheim 21-27-2H, Sundheim 21-27-3H, and Sundheim 21-27-4H. Sundheim 21-27-4H is a nonproductive well due to issues in wellbore construction and integrity, so the well group consists of 3 active production wells as of 2020. Sundheim 21-27-1H was drilled and completed

in 2013, whereas Sundheim 21-27-2H and Sundheim 21-27-3H were drilled and completed in 2014. All three wells, 1H, 2H, and 3H, are still active and producing economically as of 2020.

2.1.1. Well Construction

The Sundheim 21-27 wells target the Middle Bakken member. The wells are vertical down to a depth of approximately 9,900 feet, and horizontal for approximately 10,500 feet in a southern direction. The true vertical depth (TVD) for the wells is approximately 10,500 feet, with total measured depths (MD) of around 20,500 feet. Surface elevation in the area where the Sundheim wells are drilled is approximately 2,200 feet above sea level.

The wells use 4 strings of casing in their design: conductor pipe, surface casing, intermediate casing, and a perforated cemented liner. The conductor casing for the wells runs to a depth of approximately 100 feet below surface level with a 16-inch outer diameter (OD), 65.00 pound per foot casing. The surface casing in the wells is 9 5/8-inch OD down to 1,800 feet with a weight of 36.00 pounds per foot. The intermediate casing is 7-inch OD, 29.00 pound per foot weight, set at a depth of approximately 2,700 feet down to 10,800 feet. The lateral sections of the wells are completed using cemented liners and multi-stage hydraulic fractures. The liners used in the lateral section of the Sundheim wells are set at approximately 9,900 feet to 20,500 feet MD with 4 1/2-inch OD casing, and the weight of the liners range from 11.60 to 13.50 pound per foot. Casing designs between the wells in the Sundheim cluster are similar; however, the depths for the casing intervals vary slightly for each well.

The Sundheim 21-27 wells were completed with cemented liners and perforations using a plug and perforate method. The perforation density in the wells was 6.0 shots per foot, and the wells used an average of 25-30 stages of hydraulic fractures. Each well completion used 60,000-200,000 barrels of water and approximately 4 million pounds of proppant.

2.1.2. Well Production

Initial oil production rates in the Sundheim 21-27 wells ranged from 700 BOPD to 1,300 BOPD. The initial water production rates for the wells were observed to be much higher, with rates ranging from 4,400 barrels of water per day (BWPD) to over 6,000 BWPD. The production data for the wells was obtained for the post-flowback period, so the production data did not include water from the completion processes. Water cuts for the wells were determined by dividing daily water production volume by total daily fluid volume.

Initial water cuts for the Sundheim 21-27 wells are high, with water cut values approaching upwards of 96 percent; however, the average water cuts for the wells over their entire production periods range from 57 percent to 60 percent. The high initial water cut values are most likely a result of additional water drainage from hydraulic fractures and natural fracture networks, whereas the late-time and average water cut percentages more closely represent water production from the reservoir matrix rock within the Middle Bakken or Three Forks formations. Figures 10-12 show the calculated water cuts for the wells over their entire production period with a red line representing a water cut of 50 percent. Table I summarizes the average water cuts for the three producing Sundheim 21-27 wells over their entire production periods from 2013/2014 to 2019.

Table I: Average Water Cuts of Sundheim 21-27 Well Cluster

Well	Average Water Cut (%)
Sundheim 21-27-1H	59.8
Sundheim 21-27-2H	57.9
Sundheim 21-27-3H	57.3

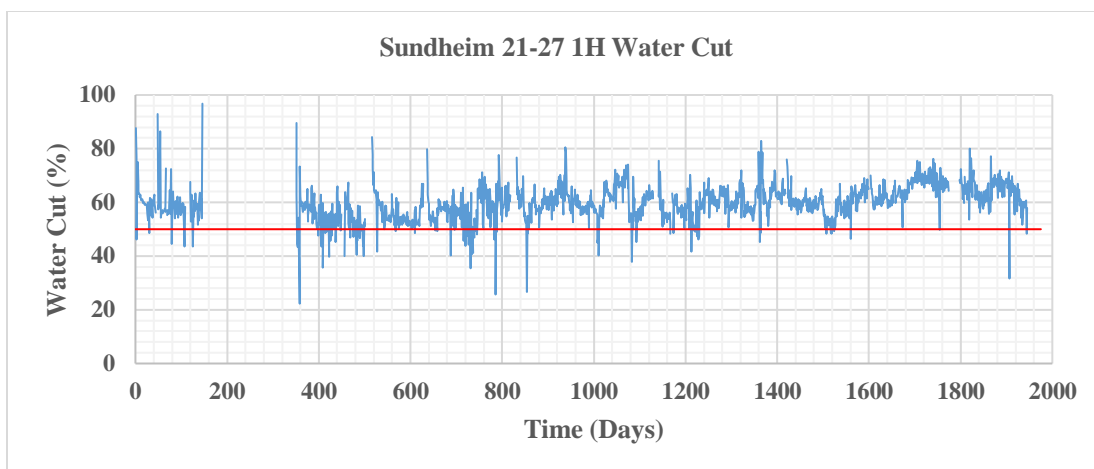


Figure 10: Sundheim 21-27-1H Calculated Water Cut

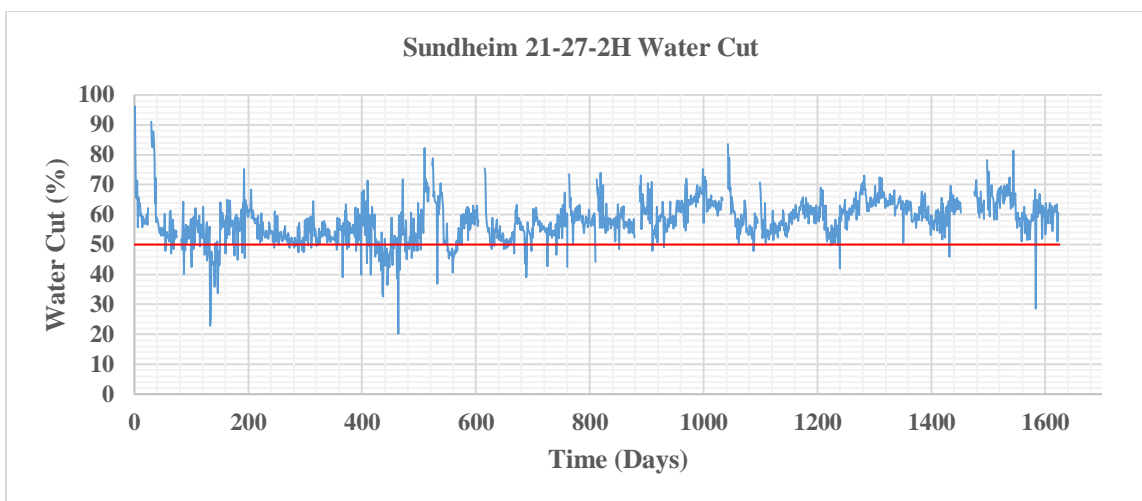


Figure 11: Sundheim 21-27-2H Calculated Water Cut

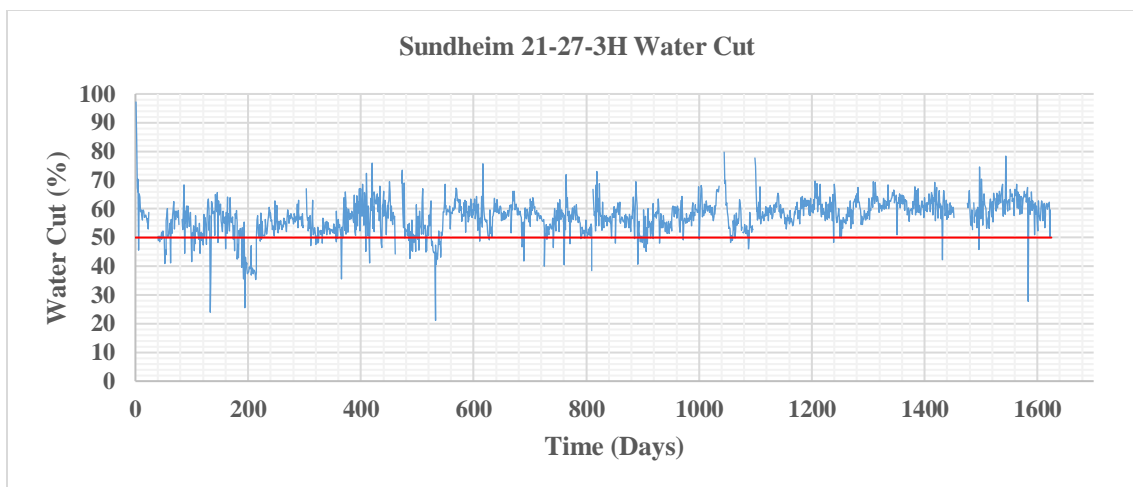


Figure 12: Sundheim 21-27-3H Calculated Water Cut

3. Numerical Flow Simulation

A numerical flow simulation, also often referred to as a reservoir model, is digital representation of the subsurface environment that uses flow equations to make predictions about downhole pressures and production rates. Reservoir engineers use numerical flow simulations to gain an understanding of the interaction between the reservoir and wells within a petroleum system. Reservoir properties and well data must be formatted and input into simulation software to initialize a numerical flow simulation. Reservoir models are commonly used to determine reservoir properties, analyze project economics, determine production mechanics, optimize field development, and forecast well performance.

There are two main types of numerical flow simulation that are used in industry: black oil models and compositional models. Both black oil models and compositional models can model three-phase fluid flow. Black oil models predict fluid flow by modeling three main phases in the reservoir: oil, gas, and water. Black oil models rely on correlations and material balance equations to determine oil and gas phase changes as a result of pressure. A compositional model uses equations of state to determine the flow of each separate hydrocarbon component. Compositional models are typically used in cases where injection processes or phase changes are prominent. Black oil models are generally less intensive on computing power than compositional models. A black oil simulation method was used to model the project area and to determine the source of the produced water in the NE Elm Coulee.

Constructing the reservoir model was broken down into 7 main steps:

1. Building a geologic model of the area to define reservoir structure
2. Discretizing model grid into blocks and layers
3. Populating fluid properties

4. Populating rock properties
5. Initializing the model with pressures and saturations
6. Well construction
7. History matching

Schlumberger's Petrel software package was used to generate the reservoir model. The model was constructed for the purpose of determining the source of produced water in the NE Elm Coulee, and the sections below describe each of the main steps in the modeling process.

3.1. Geologic Model Structure

Modeling the project area started with creating a geologic model of Township 25N, Range 58E. The purpose of the geologic model was to capture the structure and vertical porosity trend within the area of interest using logs from vertical wells adjacent to the Sundheim 21-27 well cluster. A total of 17 vertical well logs were used to generate the geologic model. Figure 13 shows the locations of the vertical wells in relation to the geologic model's areal extent. The location of the project area is located in the southern portion of the geologic model, shown by the yellow rectangle in Figure 13.

Gamma ray (GR) logs were used to identify the boundaries of each stratigraphic interval. The GR logs were used to identify the depths of the Lodgepole formation, Upper Bakken member, Middle Bakken member, Lower Bakken member, and Three Forks formation. To correct for any discrepancies in the log datums, the logs were hung off the top of the Upper Bakken, which was set at a depth of 8,200 feet below sea level in all vertical logs. The Lodgepole formation was assigned a thickness of 50 feet using the contours generated from the Upper Bakken member. The Three Forks was assigned a thickness of 50 feet to model the upper bench of the formation. A three-well example of identifying stratigraphic surfaces based on the

GR logs is shown in Figure 14; however, all 17 vertical well logs were used to generate the surfaces within the geologic model.

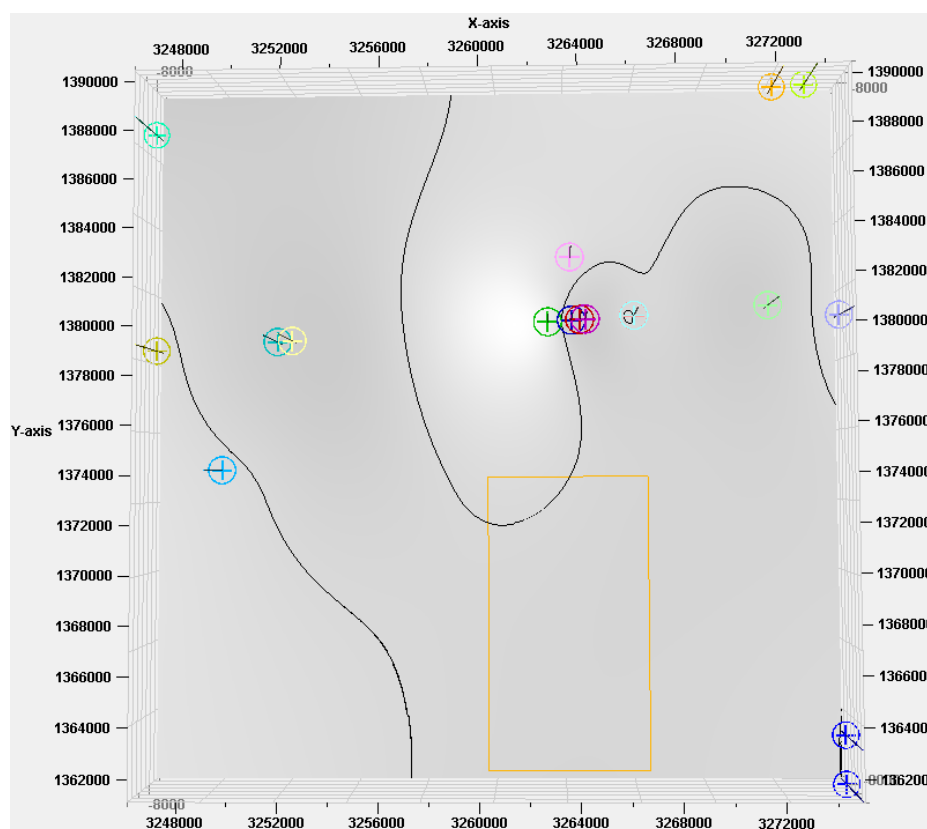


Figure 13: Geologic Model Vertical Log Locations in Relation to Project Area

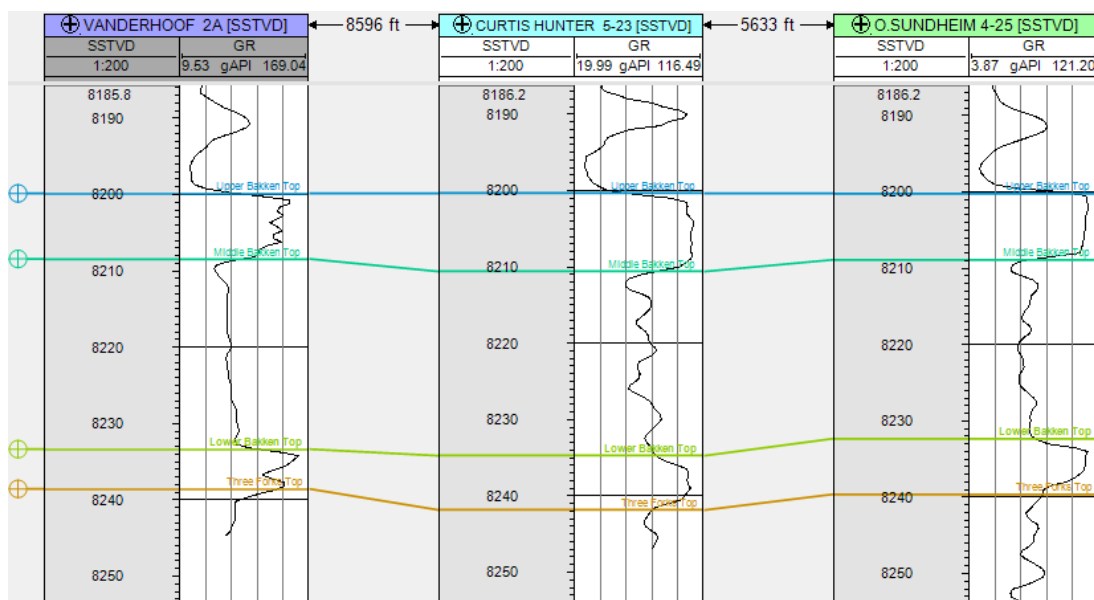


Figure 14: Identifying Formation Tops using GR Logs

The stratigraphic surfaces in areas between the vertical wells were generated using the formation tops identified from the GR logs. Petrel's surface generation function estimates surface depth between wells based on the depth at which the formation tops were identified from the logs and the distance between logged well locations. The geologic model covers a very small area when compared to the area of the entire basin; thus, the model's structure is mostly flat. Figure 15 shows the resulting surfaces for the Lodgepole formation, Upper Bakken member, Middle Bakken member, Lower Bakken member, and Three Forks upper bench formation with a 50 times vertical exaggeration to emphasize surface separation. The Z-axis in Figure 15 shows formation depth below sea level. The Sundheim 21-27 well cluster project area is denoted by the yellow rectangle in Figure 15, shown overlaid on the Lodgepole top surface. The geologic model was trimmed down to exclude areas outside of the Sundheim 21-27 project area for subsequent modeling steps and flow simulation. The suite of vertical logs used in the geologic model was also used to create a porosity distribution in model space, but this procedure is discussed in the 'Rock Properties' portion of the paper.

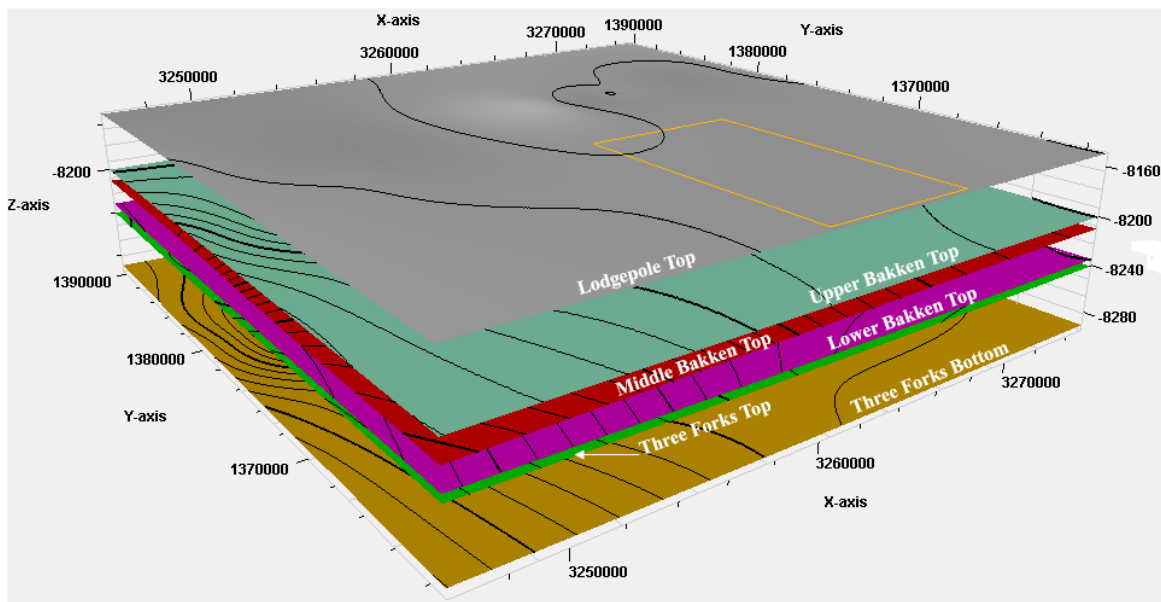


Figure 15: Generated Surfaces of Geologic Model

3.2. Model Discretization

After trimming down the geologic model to the Sundheim 21-27 project area, denoted by the yellow rectangle in Figure 15, the model was discretized into grid blocks and layers. The purpose of the grid and layer system in the model was to break down the model into small cubic volumes to be used in flow equations to determine pressures and saturations at various timestep intervals. The primary goal when discretizing model space is to maximize model resolution and capture reservoir heterogeneity; however, there is a limit to the amount of resolution that can be efficiently modeled. Fine grid systems require substantially more computing power than coarse grid systems, especially when flow simulation iterations are being performed on a local machine rather than on cloud-based computing.

3.2.1. Grid Block Size

The project area was discretized into 100 feet by 100 feet grid blocks in the X and Y directions. Most of the heterogeneity in unconventional reservoirs exists in the vertical direction, so capturing a high resolution of horizontal reservoir heterogeneity was determined to be less important for the project. The primary reason that grid blocks measuring 100 feet by 100 feet were chosen was to avoid placing multiple sets of hydraulic fractures in the same grid block, as this was observed to cause convergence problems in Petrel. The 100 feet by 100 feet grid block size was fine enough to observe pressure and saturation changes in model space with ample resolution, and simulation runs could be completed from start to finish in around one hour when performed on a local machine with limited computing power. The grid block dimensions for the project area model were 68 by 124 by 24 in the X, Y, and Z directions, respectively. The resulting total number of grid blocks in the model was 202,368. Figure 16 shows an aerial view of the project area discretized into the selected grid with the green arrow indicating North.

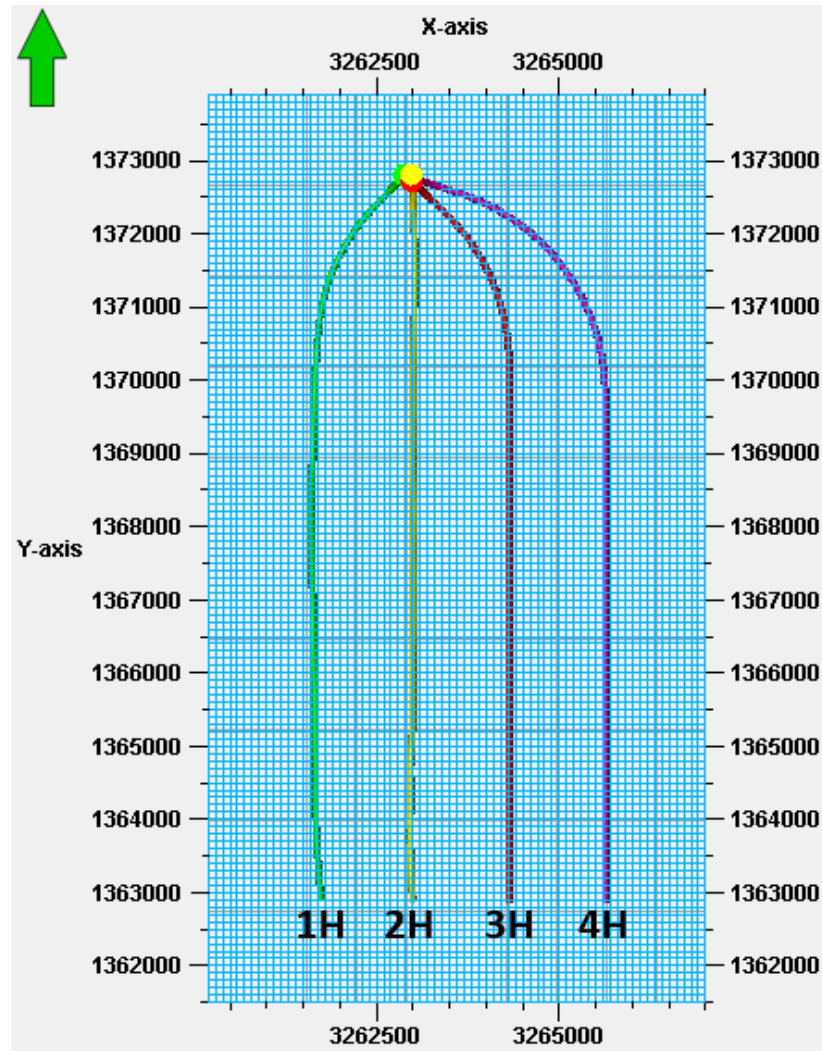


Figure 16: Project Area Discretized into 100' by 100' Grid Blocks

3.2.2. Model Layering

Vertical reservoir heterogeneity was captured in model space by creating layers. Table II shows the number of layers modeled within each stratigraphic interval.

Table II: Number of Vertical Layers per Interval

Interval	Number of Layers
Lodgepole	3
Upper Bakken	3
Middle Bakken	10
Lower Bakken	2
Three Forks	6

The Lodgepole was modeled into 3 layers, resulting in a layer thickness of approximately 17 feet. The reason for the coarse vertical layering in the Lodgepole was because the interval was of little importance to understand water production in the NE Elm Coulee. The Upper and Lower Bakken members were given 3 and 2 vertical layers, respectively. The resulting thickness for the layers was approximately 4 feet for the Upper Bakken member and 3 feet for the Lower Bakken member. The Middle Bakken was assigned 10 vertical layers, resulting in a layer thickness of approximately 2.5 feet. Capturing vertical resolution in the Middle Bakken member was important because the Sundheim 21-27 wells target the Middle Bakken member for production. The upper Three Forks was modeled using 6 layers. The thickness of the vertical layers in the Three Forks was approximately 8 feet. Figure 17 shows the vertical layers for each stratigraphic interval in the project area with the green and red arrow indicating North.

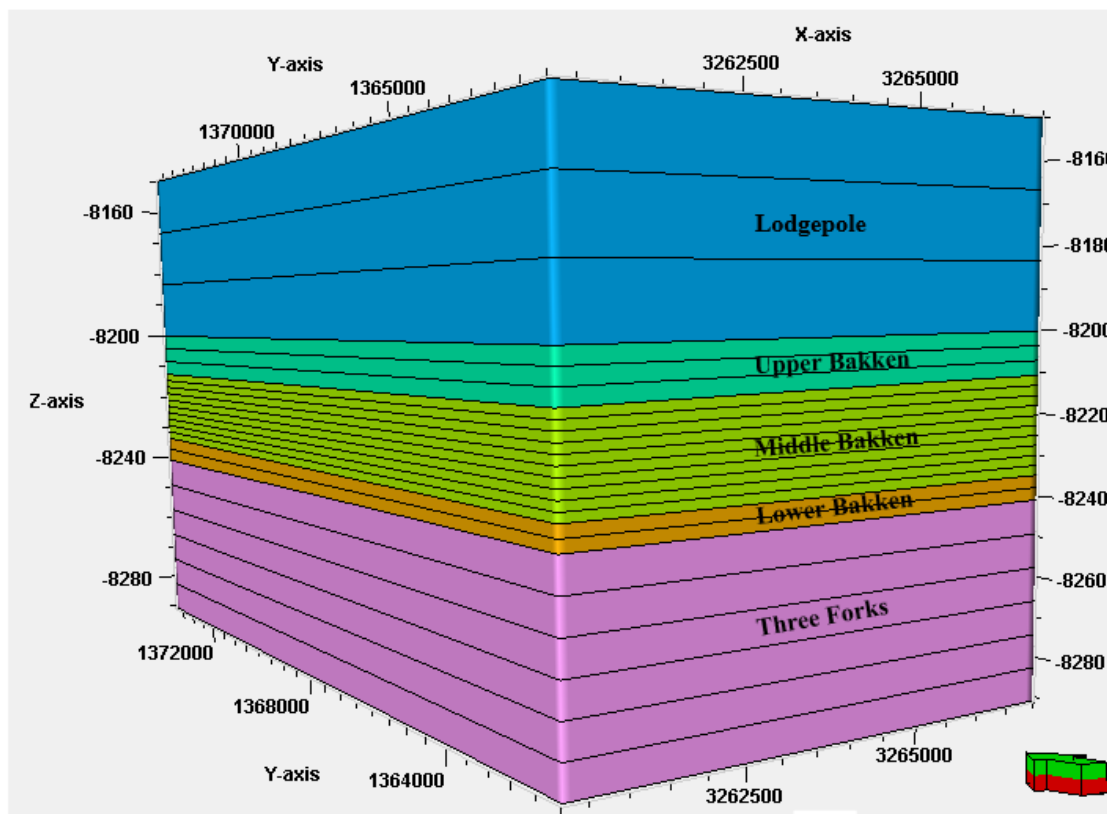


Figure 17: Project Area Discretized into 24 Vertical Layers

3.3. Fluid Properties

PVT data for the NE Elm Coulee was used to create a modified 'Light Oil and Gas' fluid model for the project area within Petrel. Input data for the fluid model included measured properties for all three active phases: oil, gas, and water. Petrel's default fluid correlations were used throughout the fluid model to fill gaps in data that were not accessible.

Temperature measurements in the NE Elm Coulee determined the reservoir temperature to be approximately 250 °F. Oil density was set at 42 °API in the fluid model with a bubble point pressure of 2465 psia. The oil in the NE Elm Coulee exists as an undersaturated fluid due to reservoir pressure being much higher than the fluid bubble point pressure at static reservoir conditions. The solution gas oil ratio (GOR) was set at 800 standard cubic feet per stock tank barrel. Petrel's default correlations were used to create formation volume factor and viscosity curves for the oil phase. The generated oil formation volume factor and viscosity curves can be seen in Figures 18 and 19, respectively. Gas density for the area was measured to be 0.069 pounds per cubic foot, resulting in a gas specific gravity of 0.901. There were no acid gasses reported in the PVT data, so H₂S, CO₂, and N₂ concentrations were left at zero. Petrel's default correlations were used to determine the gas formation volume factor and viscosity curves. The water density was determined to be approximately 77 pounds per cubic foot, based on a measured salinity concentration of 300,000 parts per million (PPM). Petrel's default correlations were used to determine water formation volume factor curve, compressibility, and viscosity curve. The resulting water viscosity was determined to be approximately 0.58 centipoise (cP).

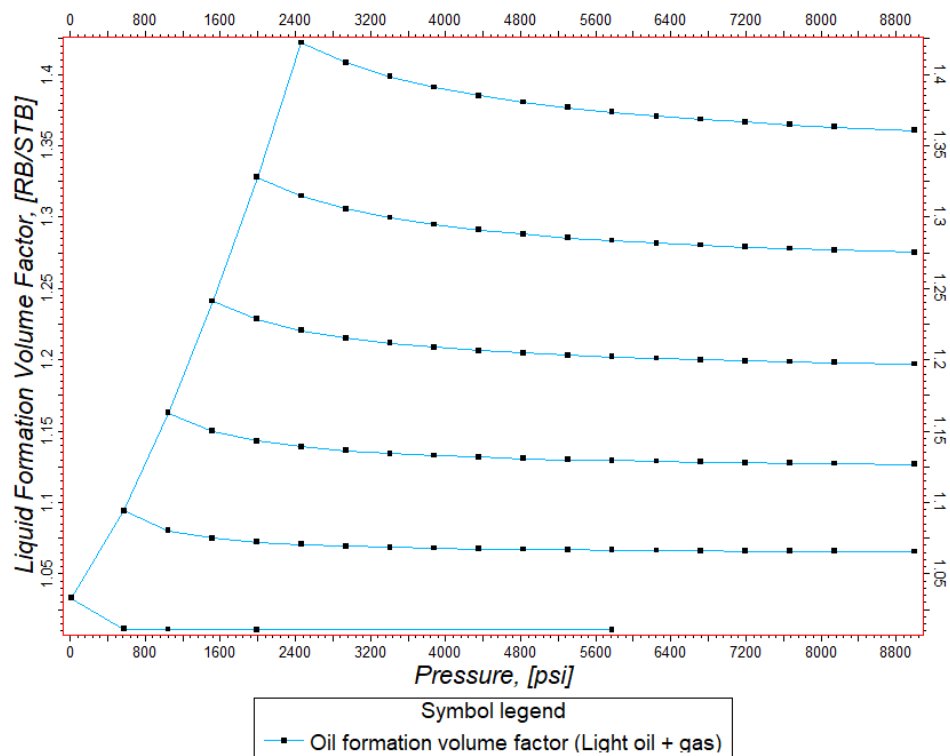


Figure 18: Oil Formation Volume Factor Curves

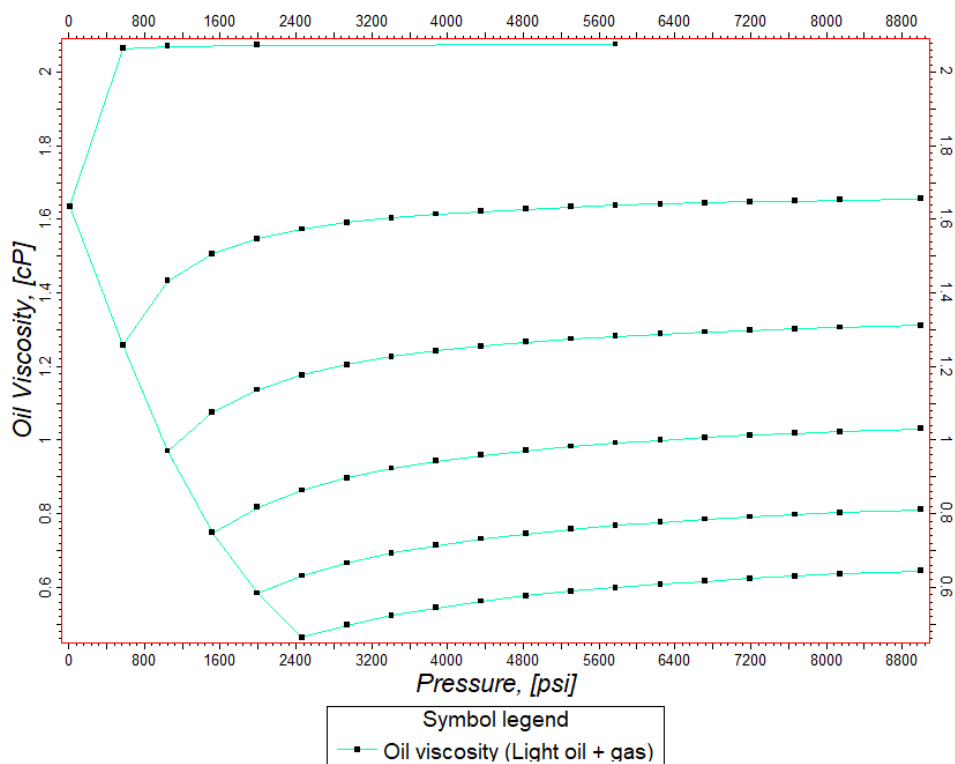


Figure 19: Oil Viscosity Curves

3.4. Rock Properties

A large majority of the time spent modeling the Sundheim 21-27 well cluster was focused on defining the rock properties of each stratigraphic interval. Porosity and permeability (horizontal and vertical) were input into model space to capture the complex geology of each stratigraphic interval within the NE Elm Coulee, except for the Lodgepole formation. The Lodgepole formation was assigned a porosity of zero percent because no fluid production from the Lodgepole was thought to be relevant for determining the source of produced water in the NE Elm Coulee. The rock properties for the model were gathered from available core reports and literature.

Three models were constructed to determine the source of produced water in the NE Elm Coulee. One model was a “Separate Tank model,” where the Bakken was isolated from the Three Forks. The other models allowed fluid from the Three Forks formation to migrate up to the Middle Bakken via hydraulic and natural fracture flow channels. The fluid migration models will be referred to as the “Vertical Migration models” throughout the paper.

A dual-permeability system was implemented into the models to account for the hydraulic fracture completions for the wells and the naturally fractured nature of the Bakken due to reservoir structure and overpressure. The dual-permeability model requires generating properties for two separate grids: the matrix grid and the fracture grid. The properties from both grids are combined in flow equations to simulate rates, saturations, and pressures of each grid block in the model. The rock properties were input into model space with initial values that were obtained from literature and core reports; however, these values contained a large amount of uncertainty. The uncertainty envelope in the rock properties values was used to history match the models to reproduce observed rates and volumes, and this process is described in the ‘History Matching’ section of the paper.

3.4.1. Matrix Grid

The matrix grid represents rock properties that are native to the matrix rock in each stratigraphic interval of interest: the Upper Bakken member, the Middle Bakken member, the Lower Bakken member, and the Three Forks formation. Examples of properties that were input into the matrix rock grid were matrix porosity, matrix permeability, matrix water saturation, and relative permeability curves that represented the fluid flow characteristics of the matrix rock. The process of creating a matrix porosity trend model, upscaling porosity well logs into the matrix grid, and inputting matrix permeability are outlined in the sections below. Inputting fluid saturations into the matrix grid are discussed in the ‘Initialization’ section of this paper.

3.4.1.1. Vertical Porosity Trend Model

The geologic model was used to create a vertical porosity trend model for the matrix rock within Township 25N, Range 58E. The goal of the porosity trend model was to capture the spatial distribution of porosity across the entire geologic model area within the stratigraphic intervals of interest. The 17 vertical well logs that were used to create the geologic model included a neutron porosity log. Neutron porosity logs were one of the only logs available to capture the heterogeneity of rock properties for the area of interest. The neutron porosity logs determined formation porosity by identifying the amount of hydrogen atoms in the formations, and the neutron porosity logs were used to determine porosity distribution across the project area. A three-well example of the neutron porosity logs that were used to create the porosity trend model can be seen in Figure 20. The vertical axis in Figure 20 is the subsurface vertical depth of the wells, and the horizontal axis in Figure 20 is the corresponding neutron porosity measurement in a decimal percent.

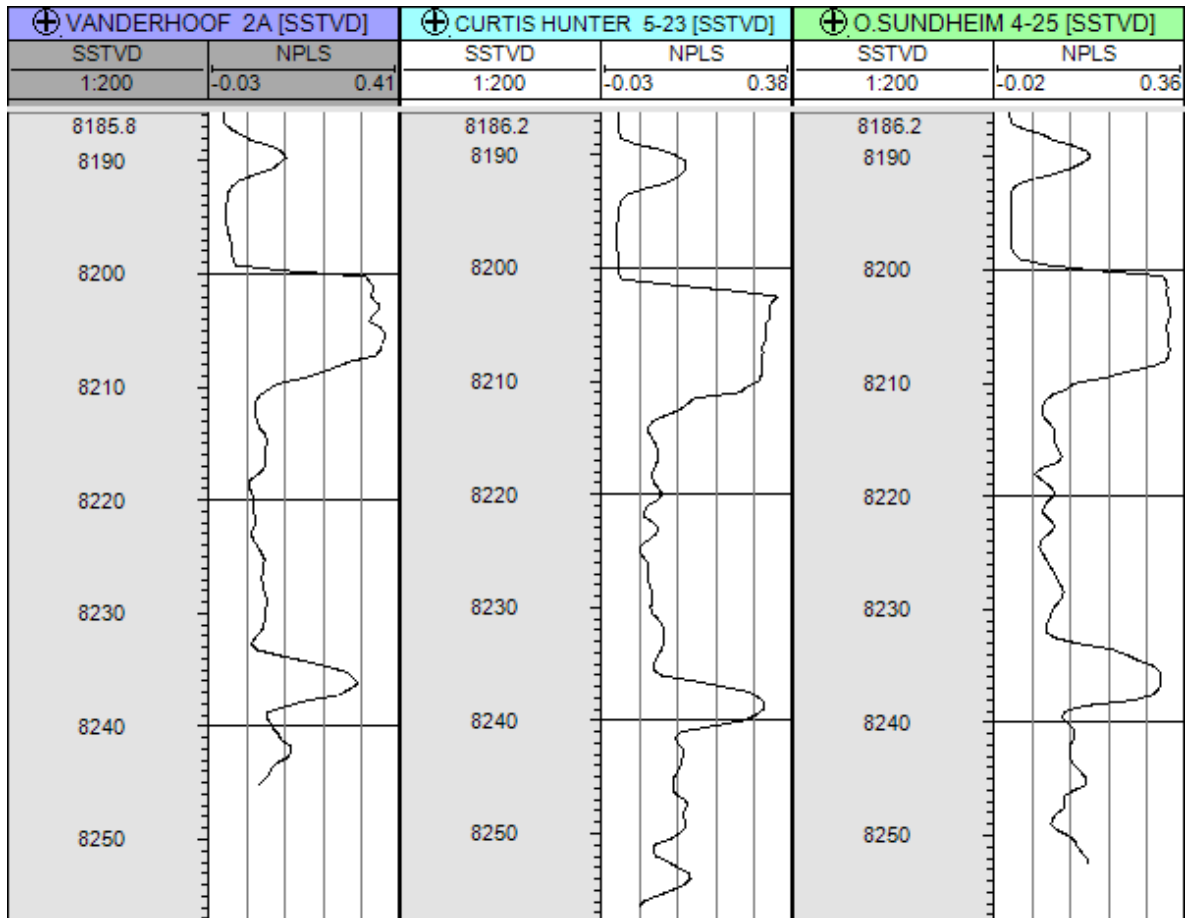


Figure 20: Neutron Porosity Log Example

Measured neutron porosity values for the logged wells were populated into the model's grid system using an upscaling process. Upscaling logs into the grid is a process that converts continuous log measurements into discrete values to be entered into the grid system of the model. The purpose of upscaling the porosity logs into the grid is to capture average porosity values for each vertical grid interval at logged well locations. The logged porosity values are averaged across the vertical thickness of each layer in the model, and the grid blocks surrounding the logged wells are populated with the averaged porosity values. Figure 21 shows an example of a single vertical well log where continuous neutron porosity log data was upscaled into discrete porosity values across each vertical layer surrounding the logged well location. The porosity upscaling process was completed on each of the 17 logged wells within the geologic model.

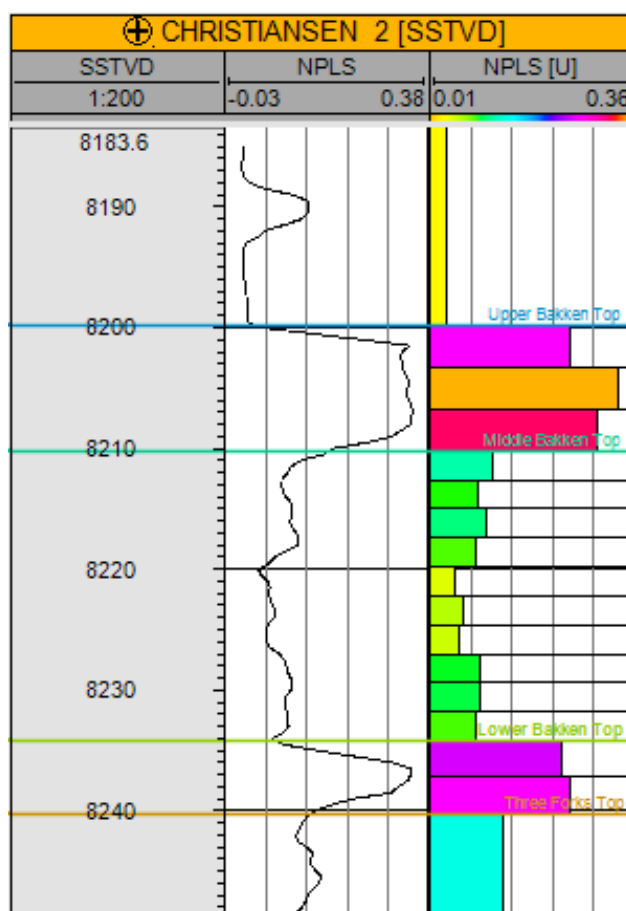


Figure 21: Upscaled Neutron Porosity Log Values

The goal of the vertical porosity trend model was to capture heterogeneity of porosity in the three Bakken members and the Three Forks formation for the Sundheim 21-27 project area. The neutron porosity log upscaling process resulted in porosity values for the grid blocks surrounding the vertical well locations. The vertical porosity trend model captures vertical porosity changes for logged well locations and incorporates the changes into the porosity model. Petrel populates horizontal porosity values in locations between logged wells using an arithmetic averaging technique to estimate the horizontal distribution of porosity in model space. The result of applying the vertical porosity trend model and estimated horizontal spatial distribution of porosity can be seen in Figure 22, where the black rectangle represents the Sundheim 21-27 project area and the arrow indicates North.

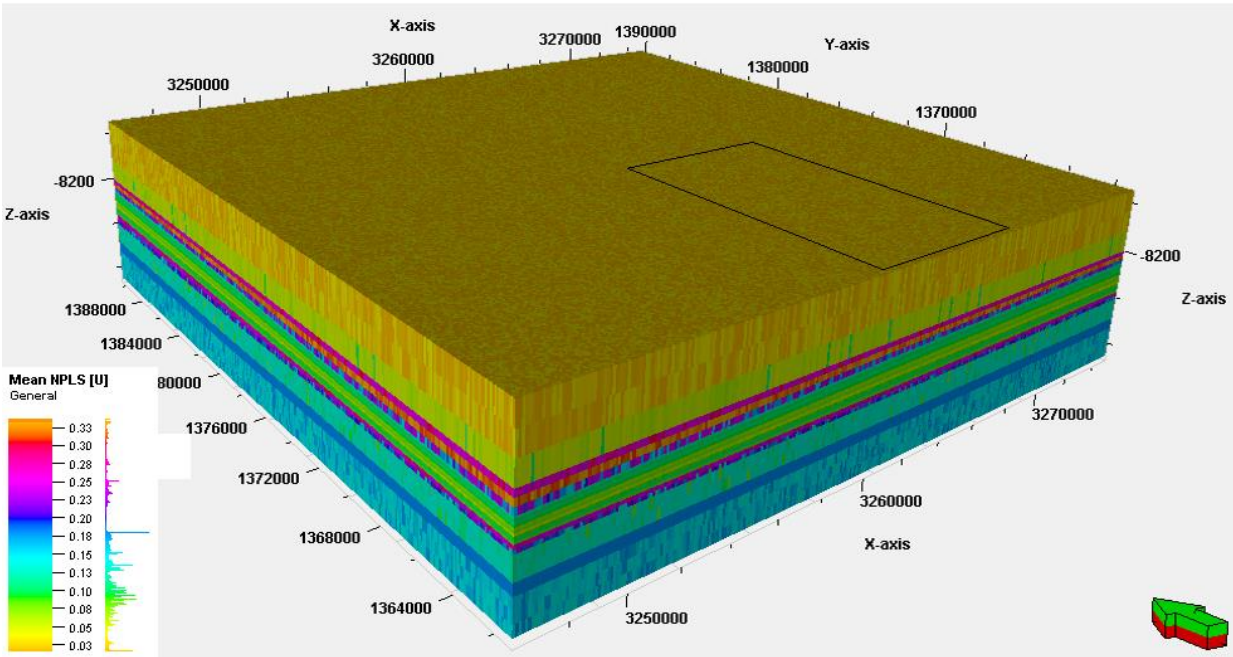


Figure 22: Porosity Distribution in Model Space

3.4.1.2. Matrix Permeability

Matrix permeability in the model was constructed for each stratigraphic interval based on core reports and literature. Core data was sparse for the project area, so the permeability of the stratigraphic intervals was modeled homogeneously, and most of the permeability values that were used in the model came from literature sources. Vertical matrix permeability anisotropy was incorporated into model space by reducing permeability in the Z direction by a factor of 10.

In the Separate Tank model, where fluid production from the Middle Bakken member was isolated, the Upper and Lower shale members were assigned a permeability value of 0 mD. The purpose of isolating the Middle Bakken was to simulate water production only from Middle Bakken matrix water saturation. In the Vertical Migration models, the Lower shale unit was assigned a horizontal permeability value of 0.01 mD to allow fluid flow from the Three Forks formation. Additional permeability for the Lower Bakken member was simulated using the fracture network, and this process is outlined in the ‘Fracture Grid’ section of the paper. A

summary of the initial permeability values that were used in the models can be seen in Table III; however, the permeability values were altered within the envelope of uncertainty throughout the history matching process. The changes in permeability from the values listed in Table III are identified in the ‘History Matching’ section of the paper.

Table III: Horizontal Matrix Permeability for Both Model Cases

Formation	Separate Tank Model	Vertical Migration Models
Upper Bakken	0.000 mD	0.010 mD
Middle Bakken	0.020 mD	0.020 mD
Lower Bakken	0.000 mD	0.010 mD
Three Forks	0.000 mD	0.200 mD

3.4.1.3. Matrix Relative Permeability Curves

The initial relative permeability curves for the matrix rock in the model were generated using the default ‘Rock Physics’ options in Petrel. The relative permeability curves for a “shaly sand” were selected as the most suitable option for the Bakken and Three Forks formations. An oil-water capillary pressure correlation was implemented into model space while modeling the initial relative permeability curves. The relative permeability curves were one of the most heavily modified parameters of the model during the history matching process. The process of optimizing the relative permeability curves for the model is discussed in the ‘History Matching’ portion of the paper. The initial oil and water relative permeability curves used in the model can be seen in Figure 23, and the initial gas and oil relative permeability curves can be seen in Figure 24.

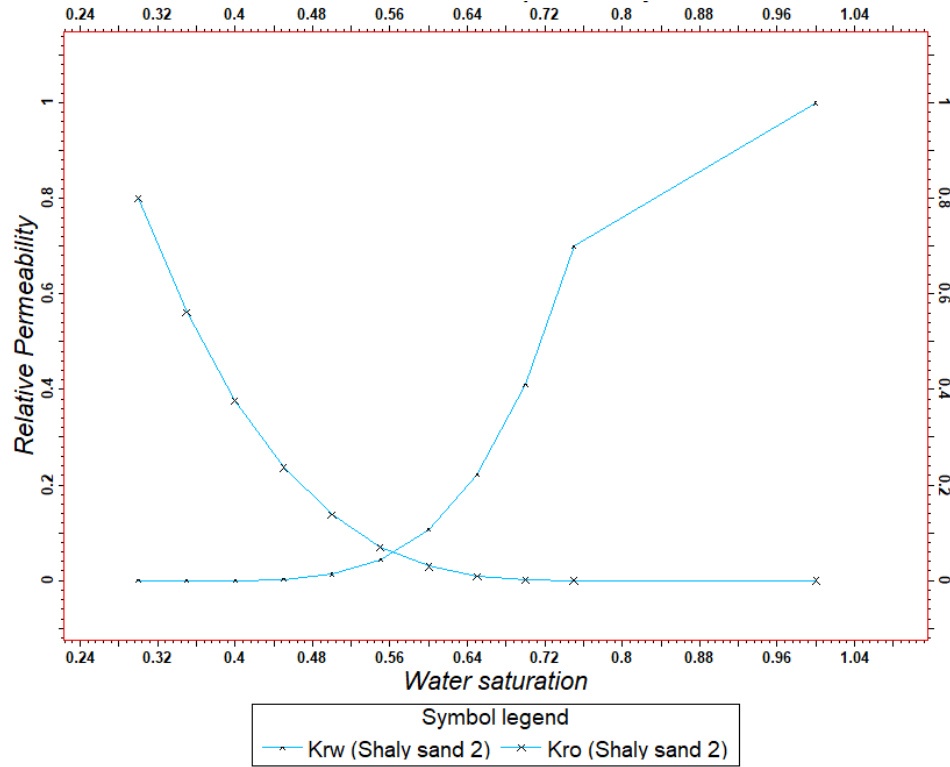


Figure 23: Initial Oil-Water Relative Permeability Curves

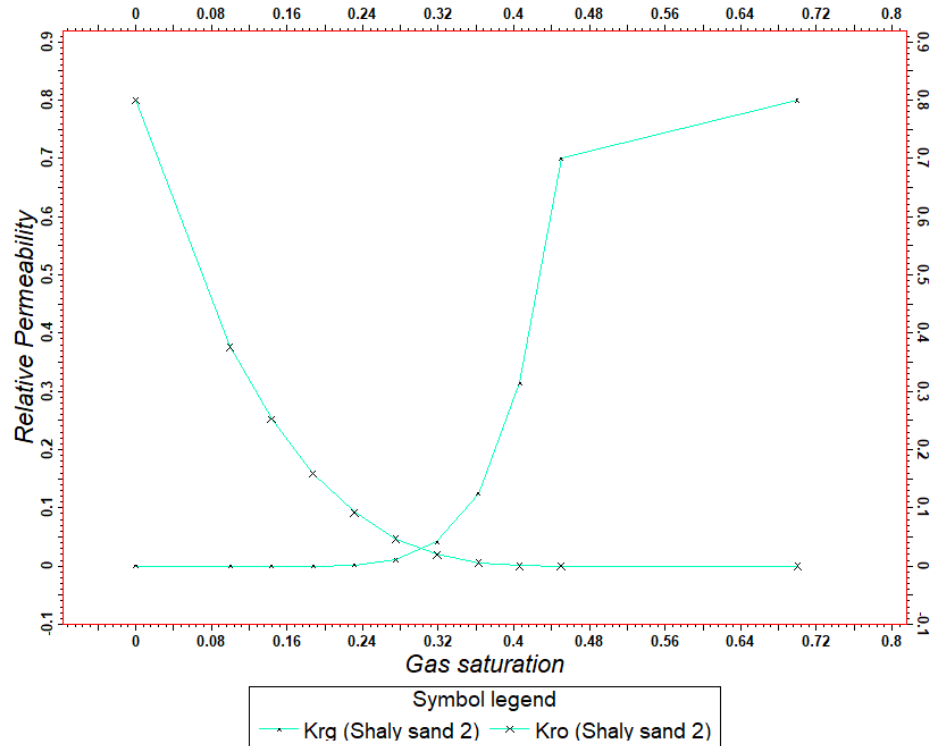


Figure 24: Initial Gas-Oil Relative Permeability Curves

3.4.2. Fracture Grid

Previous work on the geology of the Williston Basin identified the presence of natural fractures in the Bakken and Three Forks formations that contribute to fluid production (Almanza, 2011; Khatri, 2017; Sonnenberg, 2015). Both expulsion and tectonic fractures exist in the Bakken as a result of in-situ oil maturation and structural influence (Borglum and Todd, 2012). The fracture grid represents the rock properties of the natural fractures in the Bakken and Three Forks formations in model space. The dual permeability system in both the Separate Tank model and the Vertical Migration models required inputting properties of the natural fracture system so that the flow equations would account for increased pore space and overall permeability from the natural fracture system in pressure, saturation, and rate calculations. The fracture grid consisted of several discrete fracture networks (DFN) and fracture relative permeability curves.

3.4.2.1. Discrete Fracture Network (DFN)

A DFN is a simulation tool that is used to explicitly model natural fracture geometry within petroleum reservoirs. Natural fracture system properties such as fracture length, aperture, permeability, orientation, and density can all be captured using a DFN. A DFN was used to model the fracture networks within all three models of the project area. Natural fracture presence was quantified and found to influence the estimated ultimate recovery (EUR) for wells in the Elm Coulee Proper; however, the intensity of natural fracturing present in the NE Elm Coulee has not been explicitly quantified (Almanza, 2011). An initial DFN for the Middle Bakken member was generated, but the DFN properties were altered during the history matching process of the flow simulation to better match simulated rates and volumes with observed rates and volumes in the Separate Tank and Vertical Migration models. An example of a DFN that was used in the Middle Bakken member of the models can be seen in Figure 25.

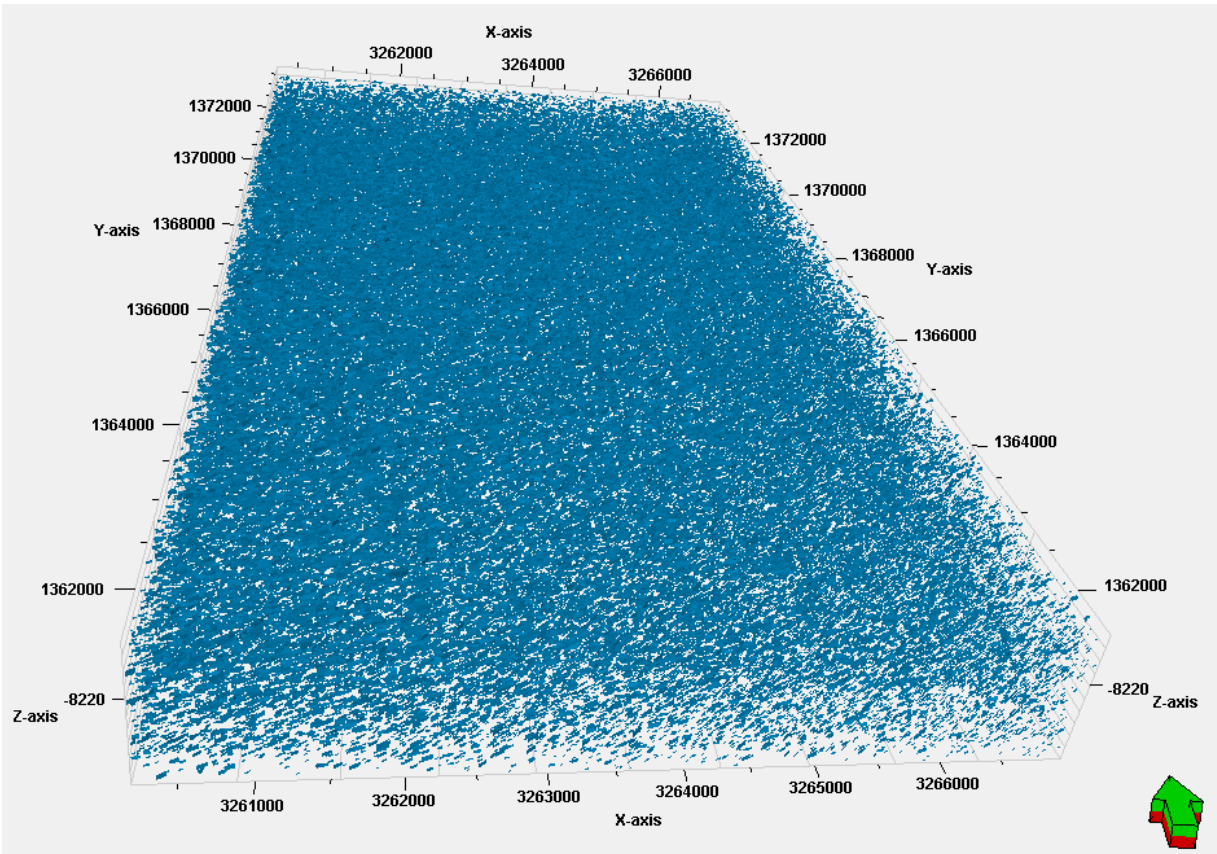


Figure 25: Example DFN of the Middle Bakken Member

The green and red arrow indicates North in Figure 25, and the blue rectangles represent fractures that have been explicitly modeled in the DFN for the Middle Bakken member. A total of 2 DFNs were used to model fracture properties of the stratigraphy in the model: one DFN for natural fractures in the Middle Bakken member in the Separate Tank model, and a second DFN for natural fractures in the Middle and Lower Bakken members in the Natural Fracture Vertical Migration model. Construction of the fracture networks for each interval required inputting information about fracture distribution, geometry, orientation, and aperture. The DFN properties for each interval were varied throughout the history matching process, so final DFN properties are discussed in the ‘History Matching’ section of the paper.

3.4.2.2. Fracture Relative Permeability Curves

Early work on the study of relative permeability curves for fluids located in natural fracture systems concluded that relative permeability is a linear function of saturation (Romm, 1966). Since Romm's work in 1966, there is some debate as to whether or not fluids within fractures should have linear relative permeability curves (Pieters and Graves, 1994). Linear relative permeability curves for fluids in natural fractures follow the idea that flow in a fracture is much more like tubular flow than Darcy's flow through a porous media. Since no relative permeability data for the project area was obtainable, a simplifying assumption was made to model the relative permeability curves for the natural fracture fluids in a linear fashion. The resulting linear relative permeability curves for the fracture fluids can be seen in Figure 26.

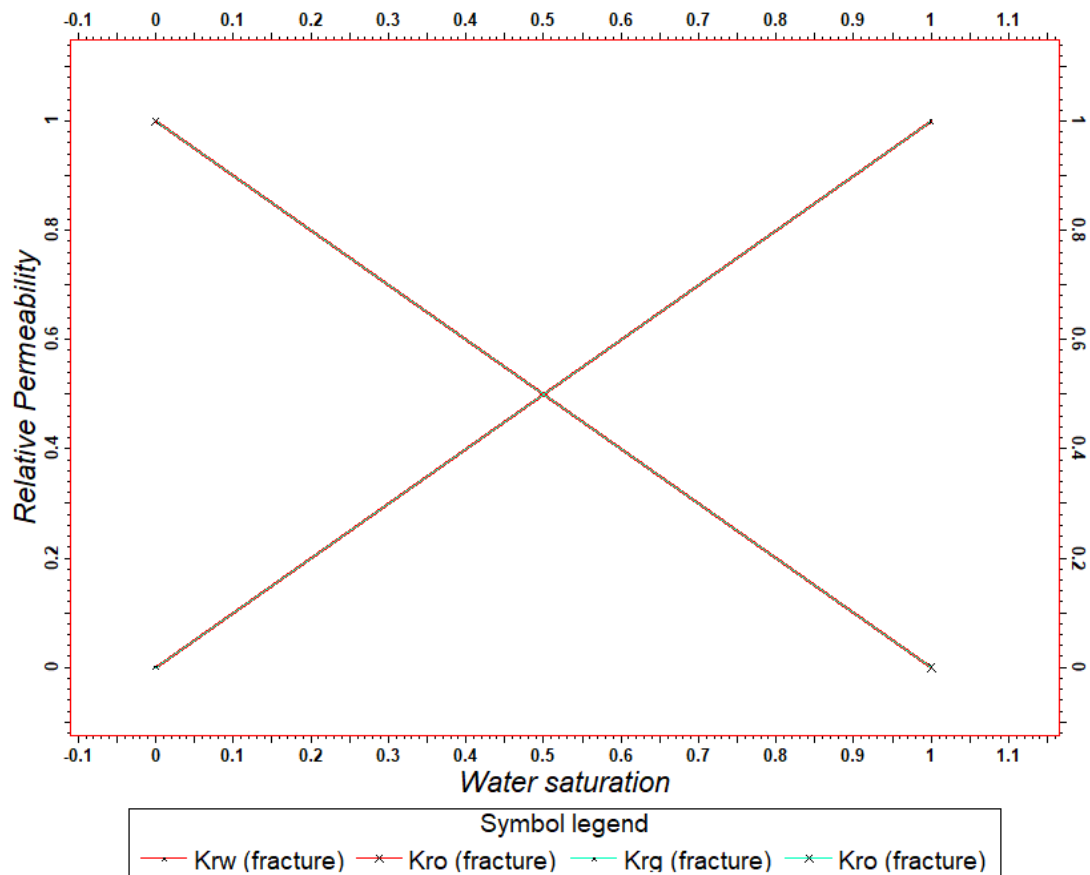


Figure 26: Linear Relative Permeability Curves for Fracture Fluids

3.5. Initialization

Initialization of the project models was completed to populate the grid blocks in each model with initial reservoir pressure and saturations for oil, water, and gas. Reservoir pressure for the NE Elm Coulee was determined through an estimation based on the formation pressure gradient for the area and formation depth. The pressure gradient in the NE Elm Coulee has been observed to be slightly overpressured at a value of approximately 0.53 psi per foot, and the depth of the target formations in the area range from 10,300 feet to 10,500 feet below the surface. The resulting reservoir pressure for the Middle Bakken member within the area was estimated to be 5,600 psi.

Fluid saturations for each stratigraphic member were obtained through PVT measurements and literature sources. Gas saturation was initialized at 0 percent in the models because the initial reservoir pressure was higher than the measured saturation pressure. The gas in the system existed within the fluid phase until pressure depletion past the saturation pressure; thus, the models were initialized as two-phase systems: oil and water. Water saturation of the Middle Bakken member ranges from 30 percent to 90 percent in the Elm Coulee Proper based on the map in Figure 27, and the Middle Bakken has an average water saturation of 68 percent across Elm Coulee Proper (Almanza, 2011). The water saturation of the Middle Bakken member in the NE Elm Coulee was estimated to be 50 percent or higher, so the model was initialized with a Middle Bakken water saturation of 50 percent.

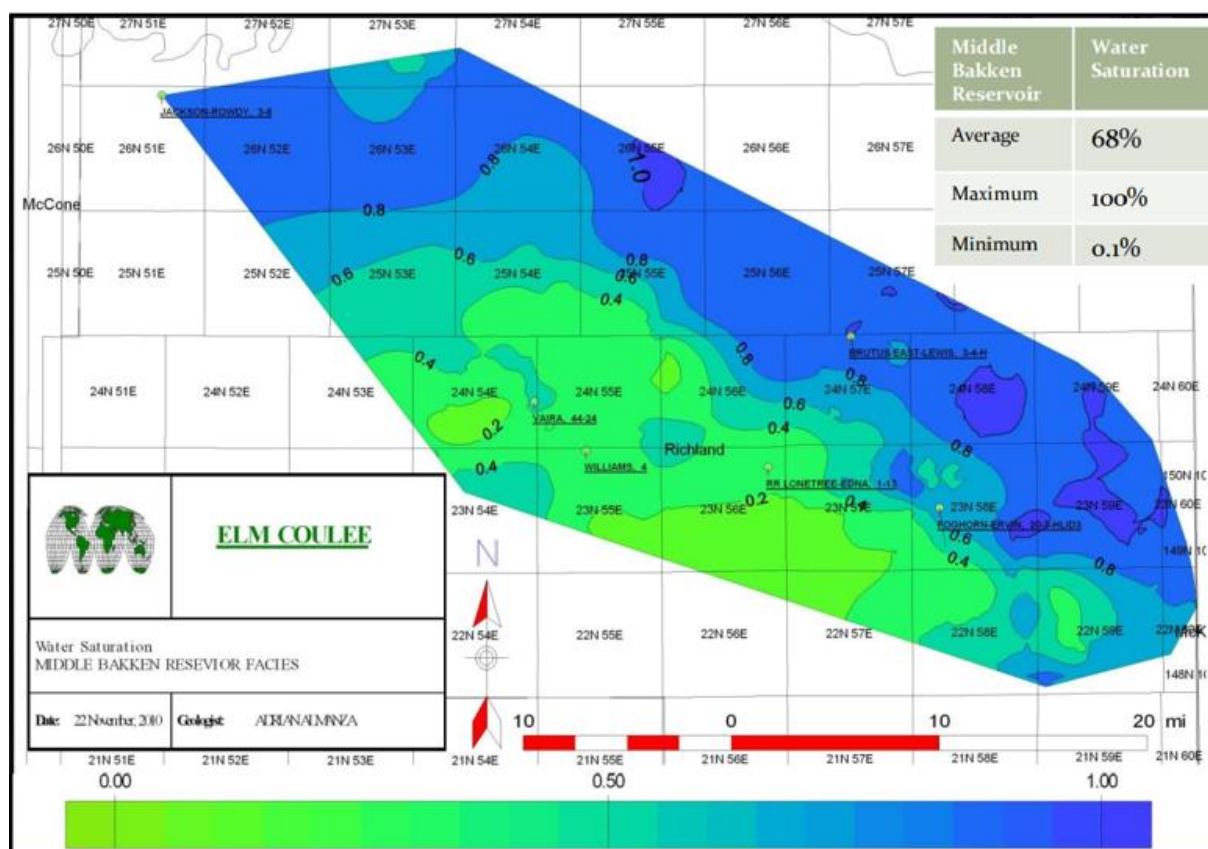


Figure 27: Average Middle Bakken Water Saturation in Elm Coulee Proper (Almanza, 2011)

The Three Forks formation was estimated to have a higher water saturation than the Middle Bakken member based on literature and published core reports. The Three Forks was assigned an initial water saturation value of 70 percent. Water saturation was used as one of the primary sources of history matching to determine the source of produced water in the NE Elm Coulee, and the sensitivity analysis performed during the history matching process to determine likely water saturations for the Middle Bakken member is located in the ‘History Matching’ section of the paper.

3.6. Well Construction

One of the final steps in constructing the flow simulations of the project area was to construct the Sundheim 21-27 well cluster in model space. The process of modeling the well cluster included modeling well trajectories and the hydraulic fracture completions for each of the wells.

3.6.1. Well Trajectories

The trajectories of the Sundheim 21-27 wells were modeled using a deviation survey for each wellbore. A deviation survey includes a list of measured depths, inclinations, and azimuths of the drilled wellbores. Before inputting the deviation surveys into Petrel for modeling, the surveys were converted to an ASCII file. A figure showing the resulting wellbore trajectories for each well can be seen in Figure 28, where the green arrow indicates North. The vertical and horizontal axes in Figure 28 show the dimensions of the model area in units of feet.

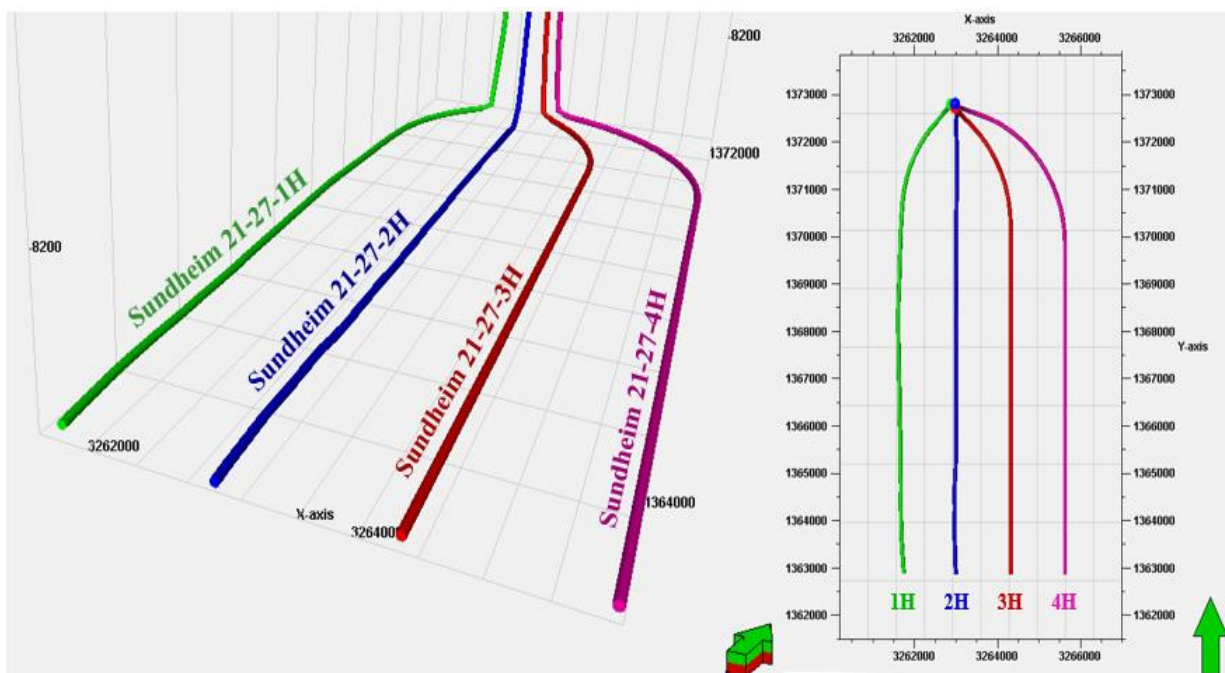


Figure 28: Sundheim 21-27 Well Cluster Trajectories

3.6.2. Hydraulic Fracture Completions

The Sundheim 21-27 wells were completed using perforated liners and multistage hydraulic fracturing. The hydraulic fracture completions for the Sundheim 21-27 wells were modeled using a discrete fracture network (DFN). The hydraulic fractures were modeled using a DFN instead of using Petrel's automated completion design function because a DFN more accurately accounts for the increased permeability and fluid flow from the hydraulic fractures. Petrel's simple completion technique for modeling hydraulic fractures averages the permeability of the fracture into the matrix grid, and it tends to overestimate flow contribution from the hydraulic fracture completion. The DFN technique for modeling hydraulic fractures upscales the fracture permeability into the fracture grid, and it more accurately accounts for increased permeability from the hydraulic fractures based on fracture volume and grid block volume. Modeling hydraulic fractures as a DFN also reduces simulation run times and produces a more realistic fracture distribution for the hydraulic fracture completions.

The completions were modeled as open-hole; thus, the completion modeling strategies only included the hydraulic fracture wings in the horizontal section. It was assumed that the flow contribution from the extremely low permeability matrix rock in areas along the open wellbore would be insignificant to the simulated flow rates. The hydraulic fractures were modeled using a 400 foot half-length, and the fractures were modeled with a vertical height equal to the thickness of the Middle Bakken member at approximately 25 feet. The geometry of the hydraulic fractures was altered to assess the possibility of fluid flow from the Three Forks formation during the history matching process, and the changes that were made to the hydraulic fracture geometry are outlined in the 'History Matching' section of the report.

3.6.2.1. Discrete Fracture Network (DFN) Completions

A DFN was used to model the hydraulic fracture completions along the lateral section of the Sundheim 21-27 wells. Modeling the completions as a DFN produces hydraulic fracture wings with variability in size and position and results in a heterogeneous distribution of fractures that are more representative of actual fracture geometry. Figure 29 shows the resulting horizontal section of Sundheim 21-27-1H after applying the DFN hydraulic fracture completion modeling technique. Additional figures showing the DFN modeled completions for the other wells, Sundheim 21-27-2H and Sundheim 21-27-3H, can be seen in Appendix A.

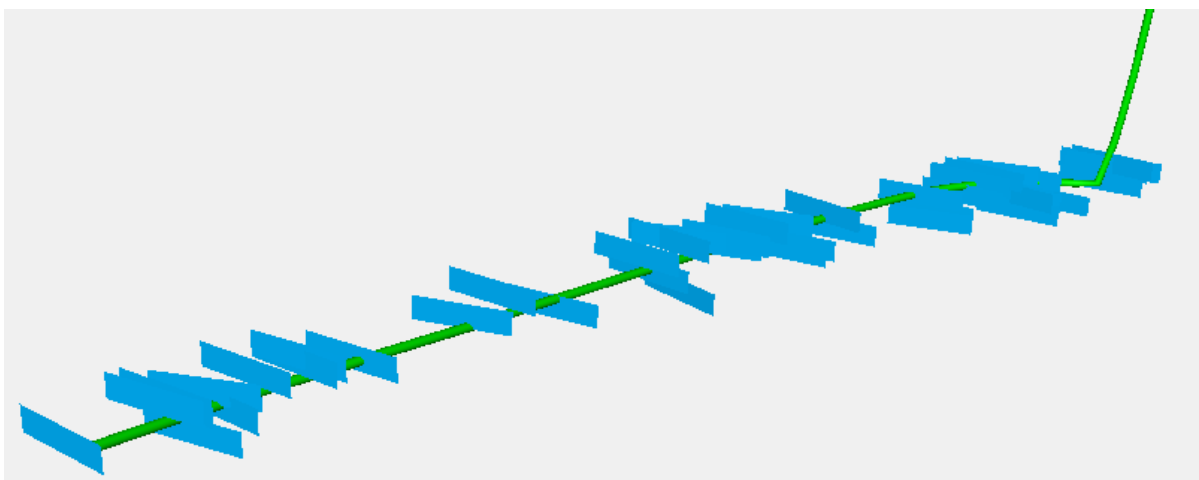


Figure 29: DFN Hydraulic Fracture Completion on Sundheim 21-27-1H

3.6.3. Well Production Constraints

Well production constraint data was not available for the project area; thus, the bottom hole flowing pressures (BHFP) for the wells were estimated based on an assumption that the fluid levels in the wellbores were mostly constant after the flowback period. The Sundheim 21-27 wells were constrained to a constant bottom hole flowing pressure of 1,000 psi for the duration of the modeling and history matching processes in all models.

4. History Matching

The goal of history matching in a flow simulation is to increase the prediction capabilities of the model. The reservoir models constructed of the project area were history matched to identify the source of produced water in the NE Elm Coulee. History matching the project area models was achieved by matching simulated results to observed results by changing fluid, rock, and well properties within an envelope of uncertainty.

Three models were history matched to determine the source of produced water in the NE Elm Coulee: the Separate Tank model and two Vertical Migration models. Reservoir production mechanisms were isolated in each model to identify the source of produced water in the NE Elm Coulee. The modeling cases are outlined in the sections below. In all cases, the Sundheim 21-27 wells were constrained to bottom hole flowing pressure and history matched to observed production rates and volumes.

Table IV separates the properties used in the models with less uncertainty from the properties with more uncertainty, and the properties with more uncertainty were altered within an uncertainty envelope during the history matching process to match simulated results with observed results. Well locations, reservoir pressure, porosity, and formation thicknesses remained constant throughout the history matching process. Matrix permeability, pressure dependent permeability, relative permeability curves, DFN properties, and water saturation were all properties that had the highest degree of uncertainty, and these properties were the main focus during the history matching process.

Table IV: Property Uncertainty Identification

Less Uncertainty	More Uncertainty
Well Locations	Matrix Permeability
Reservoir Pressure	Pressure Dependent Permeability
Porosity	Relative Permeability Curves
Formation Thickness	DFN Properties
	Water Saturation

4.1. Separate Tank Model

The Separate Tank model was constructed to determine if the source of produced water in the NE Elm Coulee was from matrix water saturation in the Middle Bakken member. The purpose of the Separate Tank model was to capture fluid production from the Middle Bakken member only. In the Separate Tank model, the Lower Bakken shale member was assigned a porosity of 0 percent and a permeability of 0 mD to effectively “shut-off” production influence from the Three Forks formation. The properties of the Middle Bakken member were altered to determine if a history match could be achieved for fluid production in the Separate Tank model. The history matching process for fluid production from the Middle Bakken member in the Separate Tank model is outlined below.

4.1.1. Separate Tank (ST) Base Case

The ST base case refers to the initial simulation run of the Separate Tank model before any influence from the history matching process. Figure 30 shows oil and water production rates for Sundheim 21-27-1H in the ST base case simulation run, where the blue/green circles represent observed rates and the blue/green lines represent simulated rates. The blue color represents water data and green represents oil data. Figure 31 shows the cumulative production volumes for oil and water for Sundheim 21-27-1H in the ST base case simulation run. In both figures, gas production has been left out to simplify the initial simulation results.

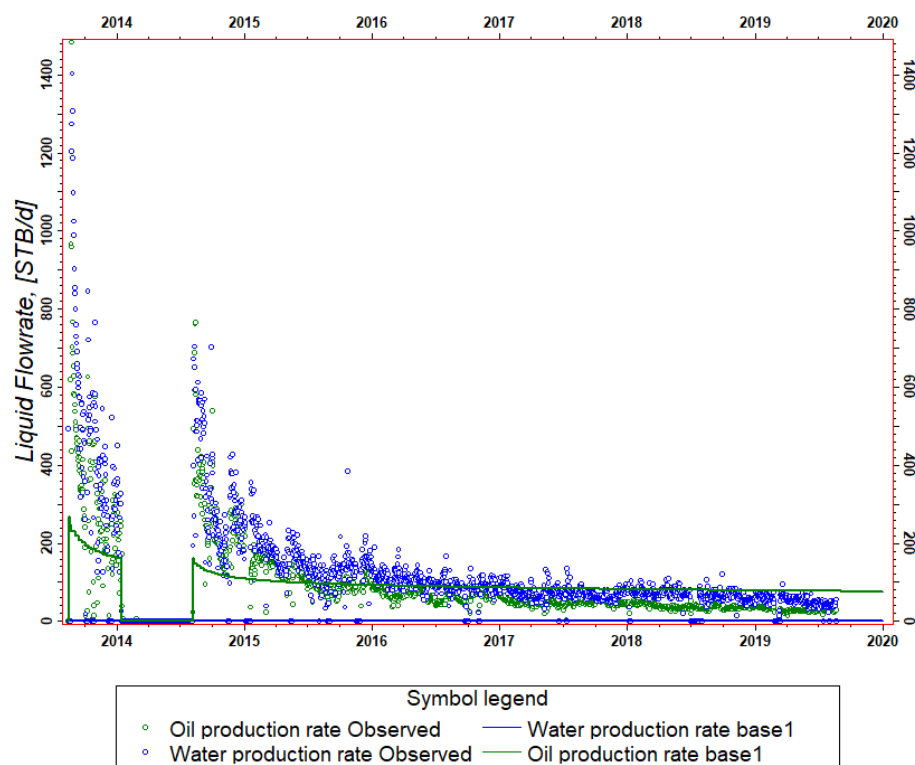


Figure 30: Separate Tank Base Case Rates

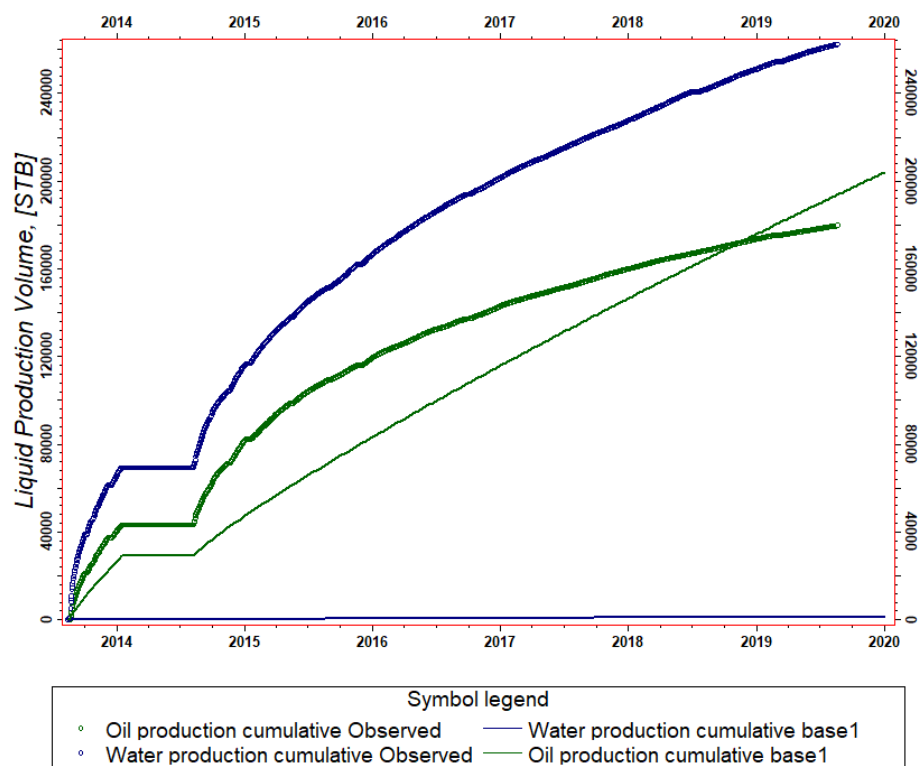


Figure 31: Separate Tank Base Case Volumes

The simulated ST base case results did not closely match observed oil or water rates and volumes. The simulated initial production rates for oil and water in the ST base case were significantly lower than the observed rates, with simulated water production rates and volumes being nearly zero. The initial simulated production rate for oil in the Separate Tank base case was significantly lower than observed rates, and late-time simulated oil production rates were higher than the observed data. The simulated cumulative water production volume in the ST base case was substantially lower than observed cumulative volumes, and the simulated cumulative oil volume started lower but ended up higher than the observed volume of oil recovered.

4.1.2. Matrix Permeability

The first property that was assessed in the history matching process of the Separate Tank model was matrix permeability. A sensitivity analysis was performed to determine the impact of increasing and decreasing the matrix permeability of the Middle Bakken member on observed rates and cumulative volumes in model space. The oil phase was the central focus of the sensitivity analysis. The Separate Tank base case matrix permeability value for the Middle Bakken was initialized at 0.02 mD, and permeability was increased to 0.04 mD and 0.08 mD to determine the impact of increased permeability on observed oil rates and volumes. Similarly, the matrix permeability of the Middle Bakken was decreased to 0.01 mD and 0.005 mD to determine the impact of a permeability reduction on observed oil rates and volumes in comparison to the Separate Tank base case. Figure 32 shows the resulting matrix permeability sensitivity analysis for oil rates on Sundheim 21-27-2H. Figure 33 shows the resulting matrix permeability sensitivity analysis for cumulative oil volumes on Sundheim 21-27-2H. Additional figures showing the matrix permeability sensitivity analysis for Sundheim 21-27-1H and Sundheim 21-27-3H on simulated oil rates are shown in Appendix A.

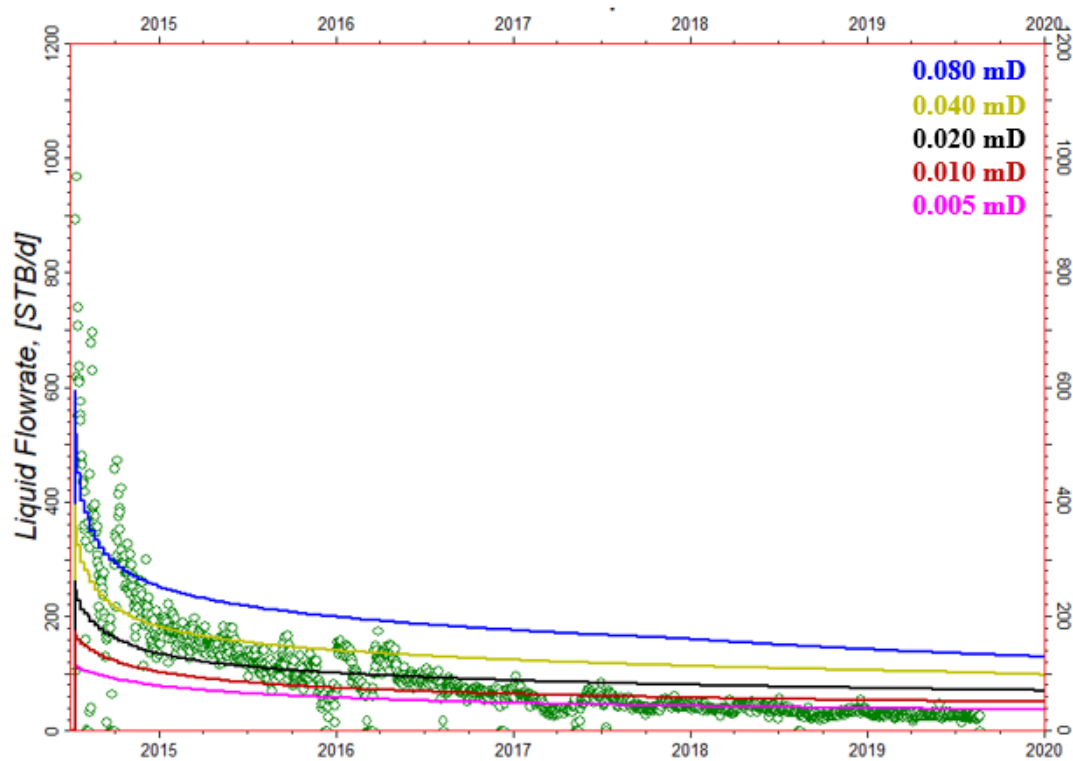


Figure 32: Matrix Permeability Sensitivity Analysis on Sundheim 21-27-2H Oil Rate

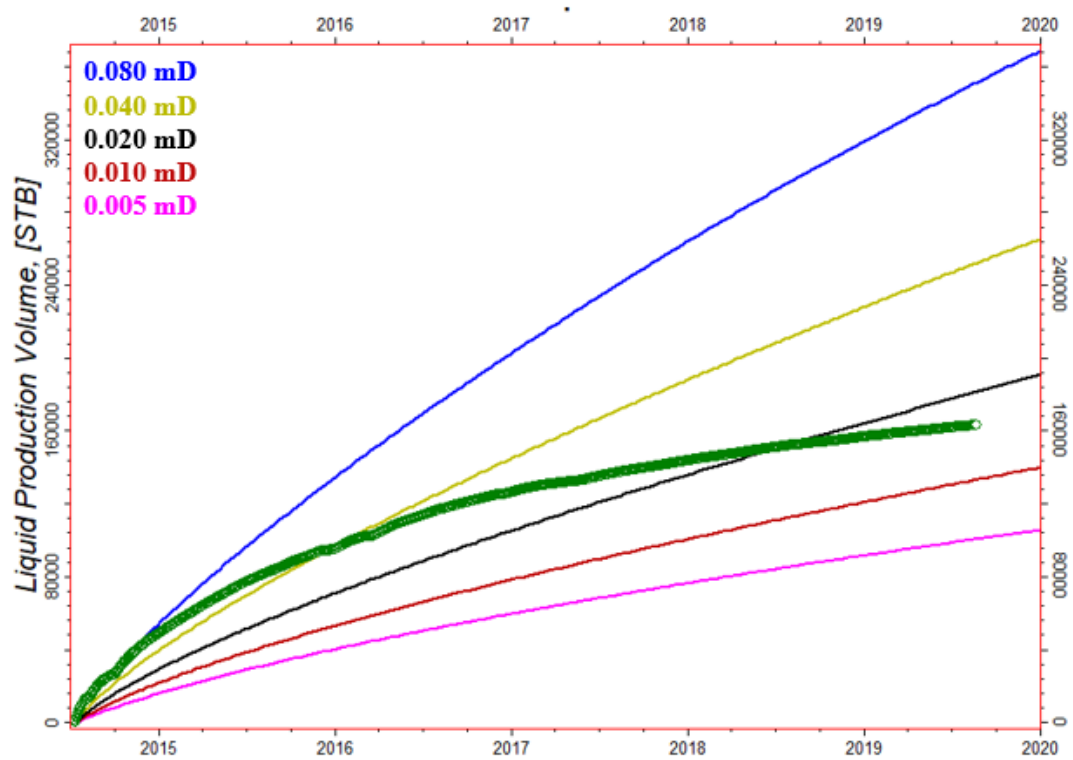


Figure 33: Matrix Permeability Sensitivity Analysis on Sundheim 21-27-2H Cumulative Oil Volume

The sensitivity analysis on matrix permeability identified several important observations in the early stages of history matching. The most notable observation from Figure 32 was that all of the simulation runs produced initial rates below the observed data, and all of the simulation runs produced late-time oil rates that were above the observed rate data. Figure 33 shows that none of the simulation runs that were completed for the matrix permeability sensitivity analysis for the Separate Tank model adequately captured the shape and magnitude of the cumulative oil volumes from the observed data. The simulated cumulative oil volume curves had a more linear shape than the observed cumulative curves for the wells. It was estimated that the matrix permeability for the project area in the NE Elm Coulee was between 0.010 mD and 0.020 mD based on the simulated cumulative oil volume curves in Figure 33.

4.1.3. Relative Permeability Curves

The ST base case produced a substantially lower volume of water than the observed data for all three Sundheim 21-27 wells. The initial oil-water relative permeability curves in the Separate Tank model, shown in Figure 23, allowed for almost no mobile water at an initial Middle Bakken matrix water saturation of 50 percent. The oil-water relative permeability curves for the Middle Bakken were used as a history matching parameter to produce more water in the Separate Tank model. The minimum water saturation endpoint of the water relative permeability curve (S_{wcr}) was decreased to allow for more mobile water at an initial water saturation of 50 percent. The S_{wcr} value in the relative permeability properties was adjusted from 0.30 to 0.20, and the change resulted in more mobile water at a water saturation of 50 percent. The primary adjustment made to the oil-water relative permeability curve is shown in Figure 34. The ST base case was ran using the adjusted oil-water relative permeability curve, and the resulting simulated oil and water rates for Sundheim 21-27-1H are shown in Figure 35.

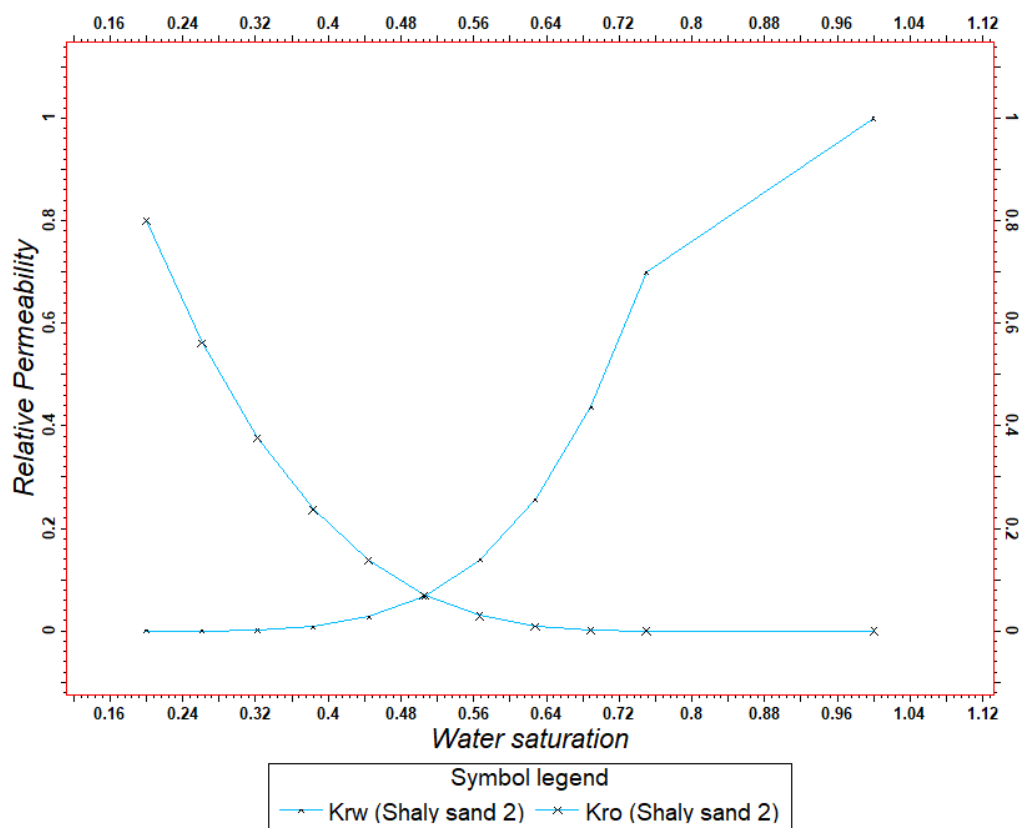


Figure 34: Initial Adjustment to the Oil-Water Relative Permeability Curve

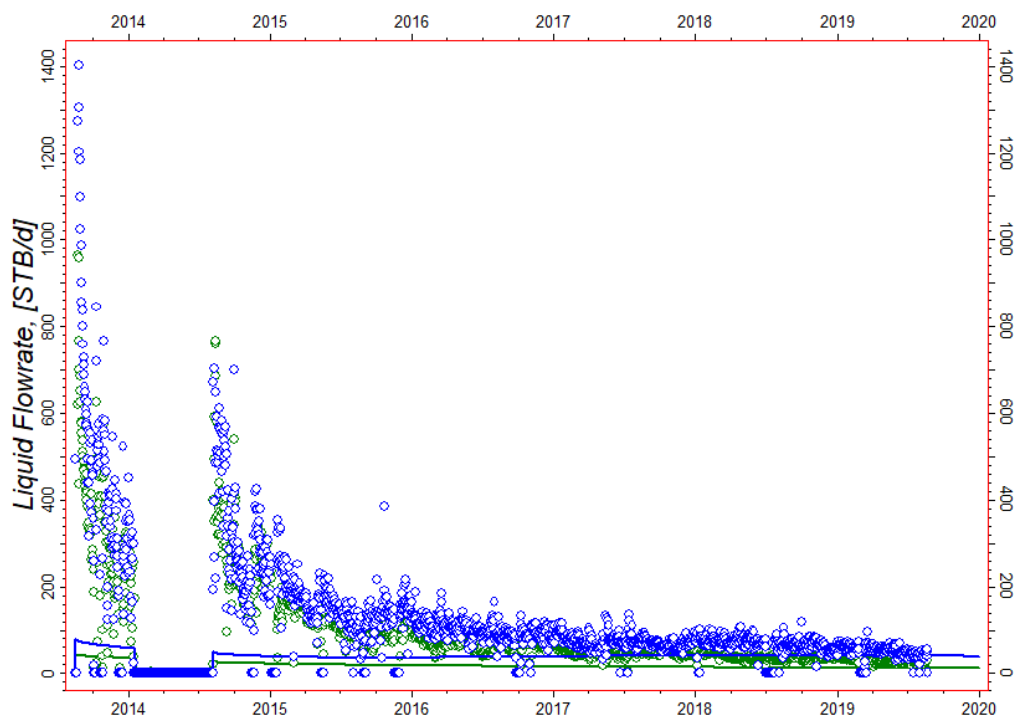


Figure 35: Oil and Water Rates for Sundheim 21-27-1H After Reducing S_{wcr}

The reduction of the S_{wcr} value resulted in increased water production for the Sundheim 21-27 wells at the initial water saturation; however, the change did not result in enough simulated water production to match observed rates and cumulative volumes. The simulated oil rates were also impacted from the changes to S_{wcr} in the relative permeability exponent. The simulated oil rates decreased significantly from the base case after reducing S_{wcr} . The Corey exponents for oil and water in the relative permeability model were altered to increase production throughout the saturation window for both oil and water. The Corey oil-water exponent was reduced from 3 to 1.95 to allow for more mobile oil in model space, and the Corey water exponent was reduced from 4 to 1.3 to increase water production in the model. The resulting changes to the relative permeability curves are shown in Figure 36. The simulated rate response to the changes in the Corey exponents in the relative permeability model are shown in Figure 37.

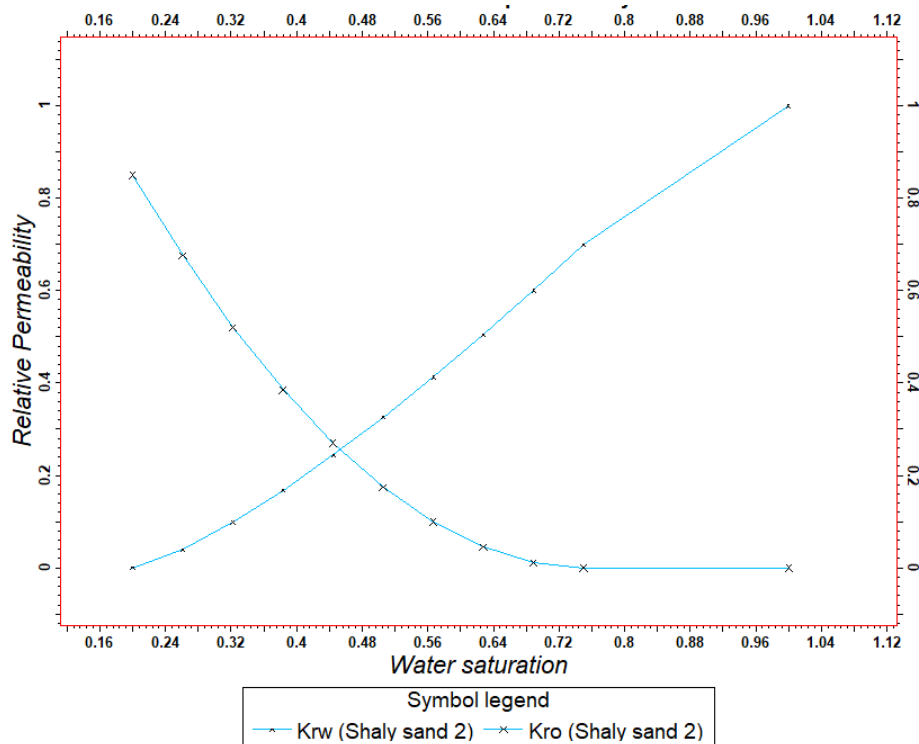


Figure 36: Relative Permeability Curves After Altering Corey Exponents

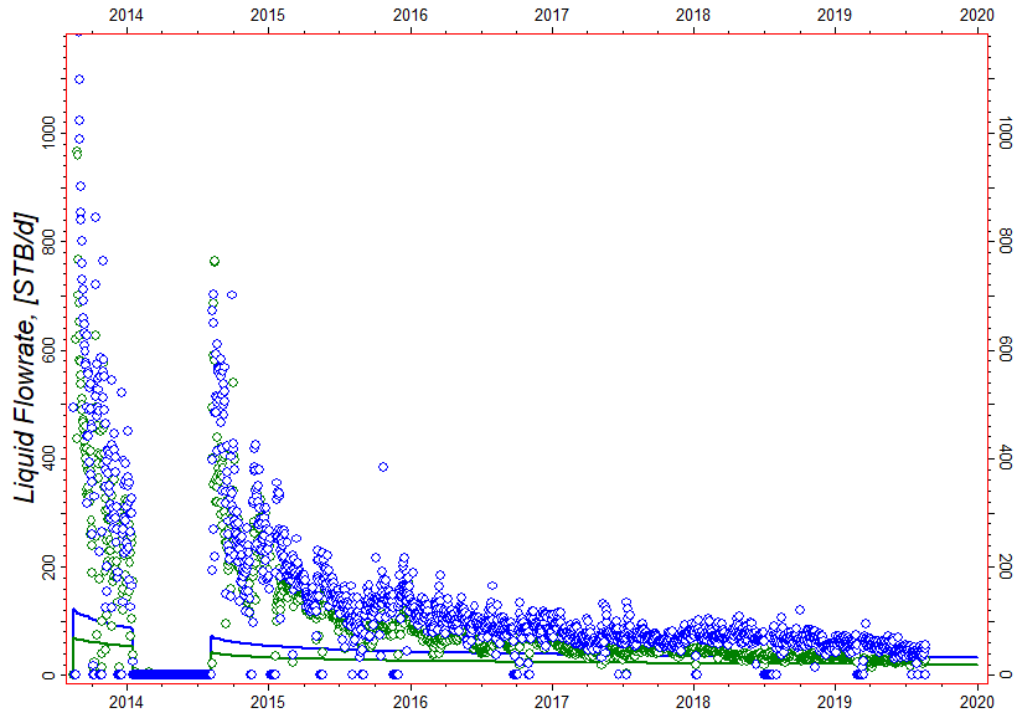


Figure 37: Oil and Water Rates for Sundheim 21-27-1H After Adjusting Corey Exponents

The adjustments to the Corey exponents in the matrix relative permeability curves resulted in increased fluid production for both oil and water in model space. A comparison between Figure 35 and Figure 37 shows that the adjustments to the Corey exponents increased initial production rates for both fluids types. The late-time simulated water production rates in Figure 37 are a result of the water relative permeability endpoint at the residual oil saturation, S_{orw} . The value for water relative permeability at S_{orw} was the final adjustment made to the relative permeability model to match late-time simulated and observed fluid rates in model space, and the value was reduced from 0.70 to 0.35. Figure 38 shows the resulting history matched relative permeability curves used in the Separate Tank model, and Figure 39 shows the simulated rate response to the relative permeability curves for both oil and water rates for Sundheim 21-27-1H. The change in S_{orw} did not result in significant changes to simulated water rates, but the change increased late-time simulated oil rates to more closely match observed data.

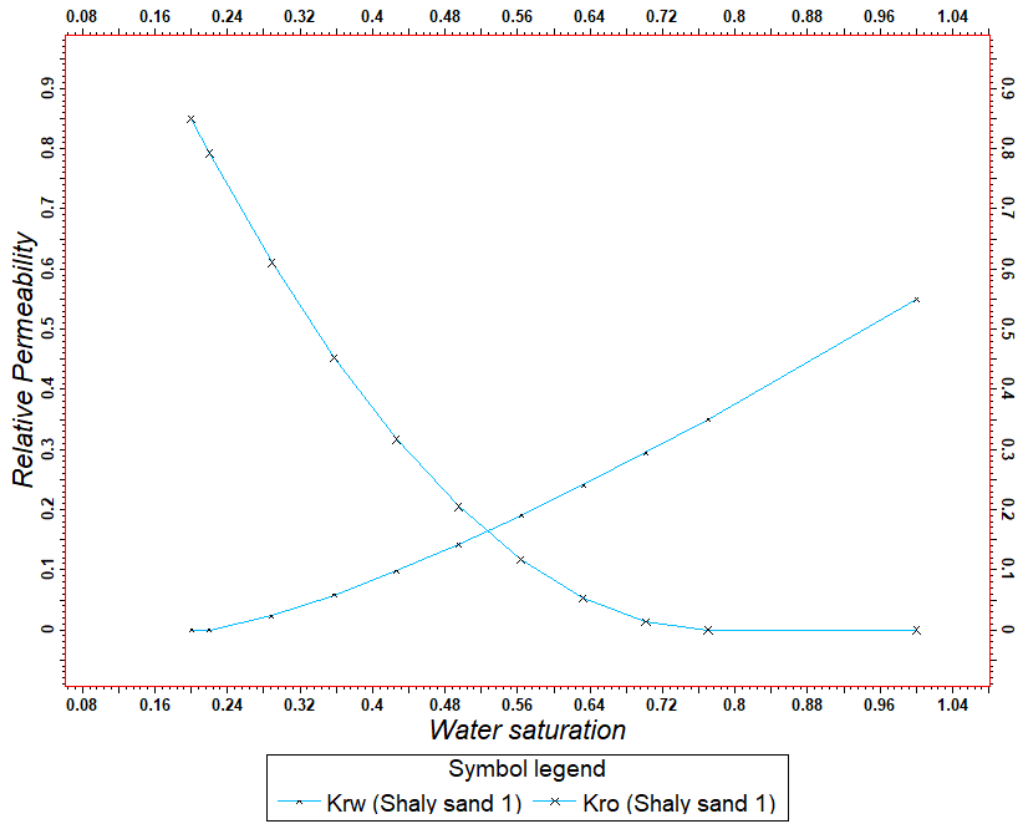


Figure 38: History Matched Oil-Water Relative Permeability Curves

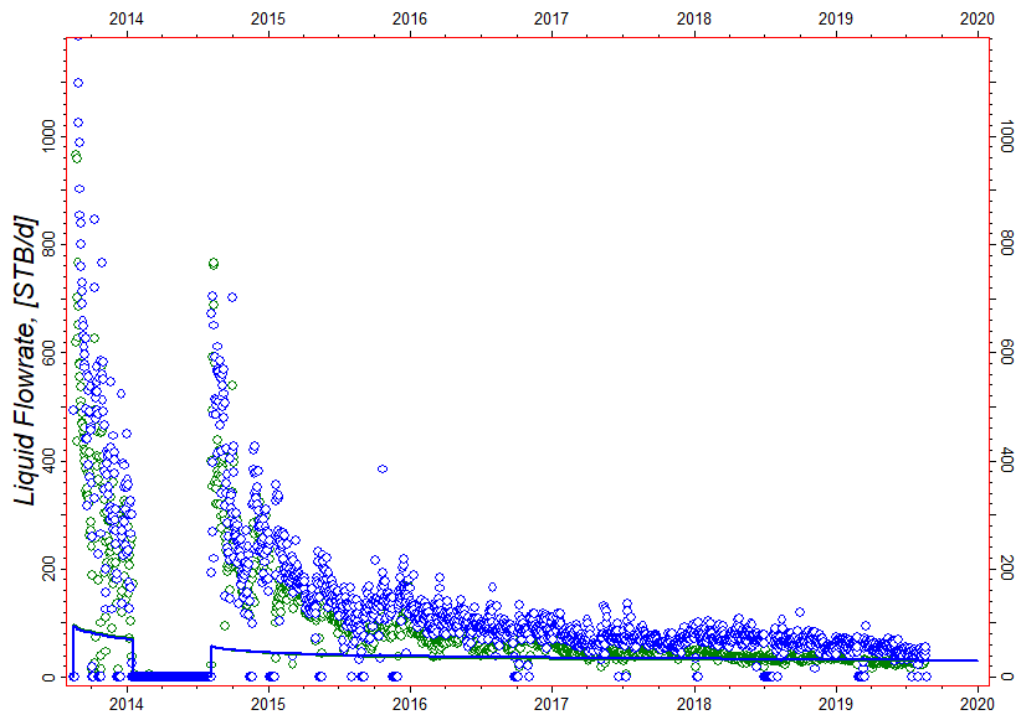


Figure 39: Oil and Water Rates for Sundheim 21-27-1H After Relative Permeability History Matching

The resulting history matched oil-water relative permeability curves, shown in Figure 38, represent a slightly water wet to an intermediate wet rock matrix, where the oil and water relative permeability curves cross at a S_w value of approximately 53 percent. A comparison between the initial relative permeability curves and the history matched relative permeability curves in the ST model is shown in Figure 94, located in Appendix A. The observed rate data for oil and water in the Sundheim 21-27 wells is characterized by a trend where oil and water rates closely follow the same pattern, and this data trend is indicative of an intermediate wet matrix rock. The simulated rate curves for oil and water, shown in Figure 39, overlap due to the intermediate wetting characteristics of the history matched relative permeability curves. It was hypothesized that the separation in observed oil and water rates for the Sundheim wells was a result of a matrix water saturation greater than 50 percent, and the process of history matching matrix water saturation is described below in the ‘Water Saturation’ subsection of the report.

4.1.4. Water Saturation

Separation in simulated oil and water rates was achieved by history matching the water saturation of the matrix rock in the Separate Tank model. Initial simulation runs were completed using a matrix water saturation of 50 percent, and a sensitivity analysis was performed to determine the impact of increasing the water saturation of the Middle Bakken member. Matrix water saturation in the Middle Bakken was increased to 55 percent and 60 percent, and simulated oil and water rates were analyzed to determine the most likely matrix water saturation value for the Middle Bakken member. Figure 40 shows the resulting matrix water saturation sensitivity analysis on the simulated oil and water rates for Sundheim 21-27-1H.

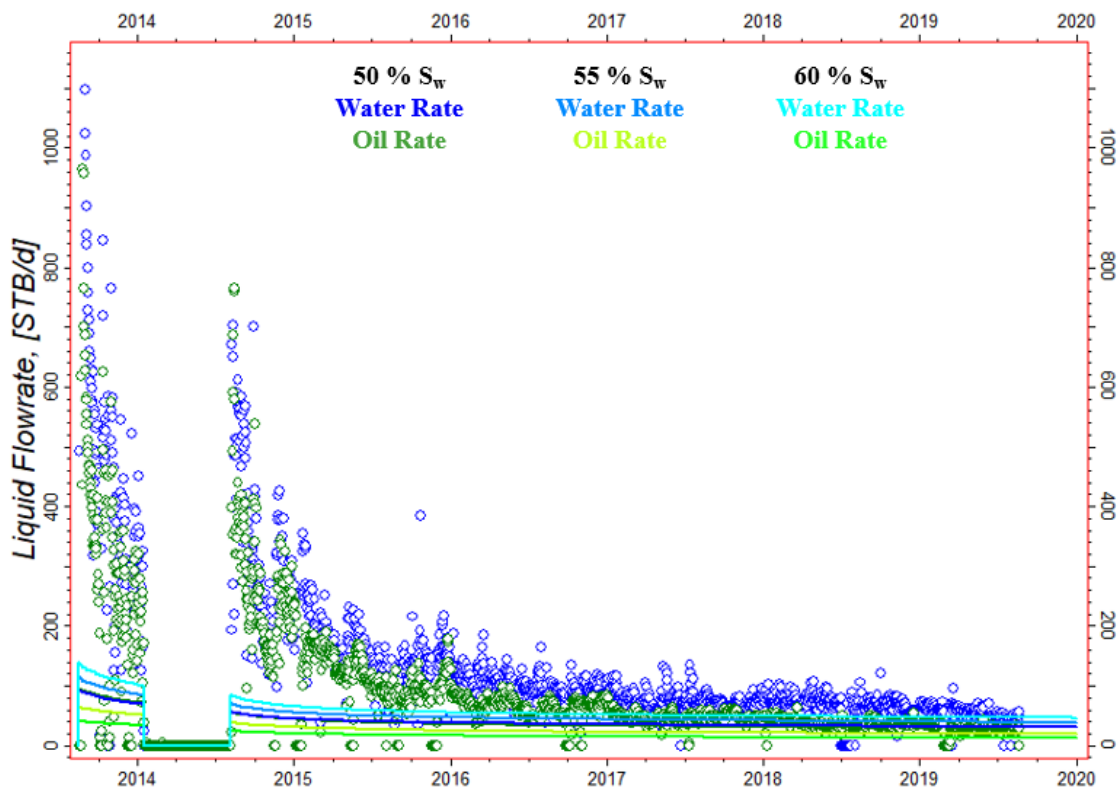


Figure 40: Separate Tank Matrix Water Saturation Sensitivity Analysis

Figure 40 shows the relationship between Middle Bakken matrix water saturation and simulated oil and water rates for Sundheim 21-27-1H. The reservoir exists in an undersaturated condition, so the oil saturation in model space is equal to one minus the matrix water saturation. The water saturation sensitivity analysis was performed to determine reasonable increases and decreases in simulated oil and water rates to determine the most likely water saturation for the Middle Bakken member. Increasing the matrix water saturation of the Middle Bakken to 55 percent resulted in a reasonable increase in simulated water rate and a reasonable decrease in simulated oil rate that matched the observed data; however, increasing the Middle Bakken matrix water saturation to 60 percent resulted in a drastic decrease in simulated oil rates. The resulting simulated oil rates in the 60 percent matrix water saturation case were much lower than the observed oil rates. Based on the simulated oil and water rates from the sensitivity analysis, it was determined that a likely matrix water saturation for the Middle Bakken was 55 percent.

4.1.5. Discrete Fracture Network (DFN) Optimization

A DFN representing the naturally fractured state of the Middle Bakken matrix was implemented into the Separate Tank model to account for fluid storage and flow contribution from the Middle Bakken natural fracture system. Observed fluid rate trends for the Sundheim 21-27 wells were characterized by initial production periods with high rates followed by periods of rapid rate decline, and it was hypothesized that the presence of natural fractures may contribute to the production rate trend that is observed in the wells.

The initial DFN for the Middle Bakken was modeled conservatively using a single fracture system with low fracture intensity to determine the impact of fracture presence on simulated rates and cumulative volumes. The initial DFN for the Middle Bakken was modeled using a fracture surface area per unit rock volume of $5\text{E-}6$. The fracture surface area per unit rock volume is a three-dimensional measurement of fracture intensity, and it is referred to as the P32 fracture intensity parameter in industry (Dershowitz & Herda, 1992). Natural fracture lengths in the DFN were assigned a constant value of 100 feet. The fractures were oriented with a mean dip azimuth of N60E to represent the principle stress direction in the reservoir (Almanza, 2011). The fracture permeability was determined using the default correlation within Petrel which is based on fracture aperture using the cubic law. The properties of the DFN were upscaled to the dual permeability fracture grid to account for the additional permeability of the Middle Bakken member due to the presence of the natural fractures. The process of upscaling the DFN properties to the fracture grid used the Oda corrected method. The Oda corrected method for upscaling DFN properties into the fracture grid accounts for connectivity of fracture networks to calculate fracture flow contribution. The initial DFN for the Middle Bakken is shown in Figure 41, and the simulated oil and water rate response to the initial DFN is shown in Figure 42.

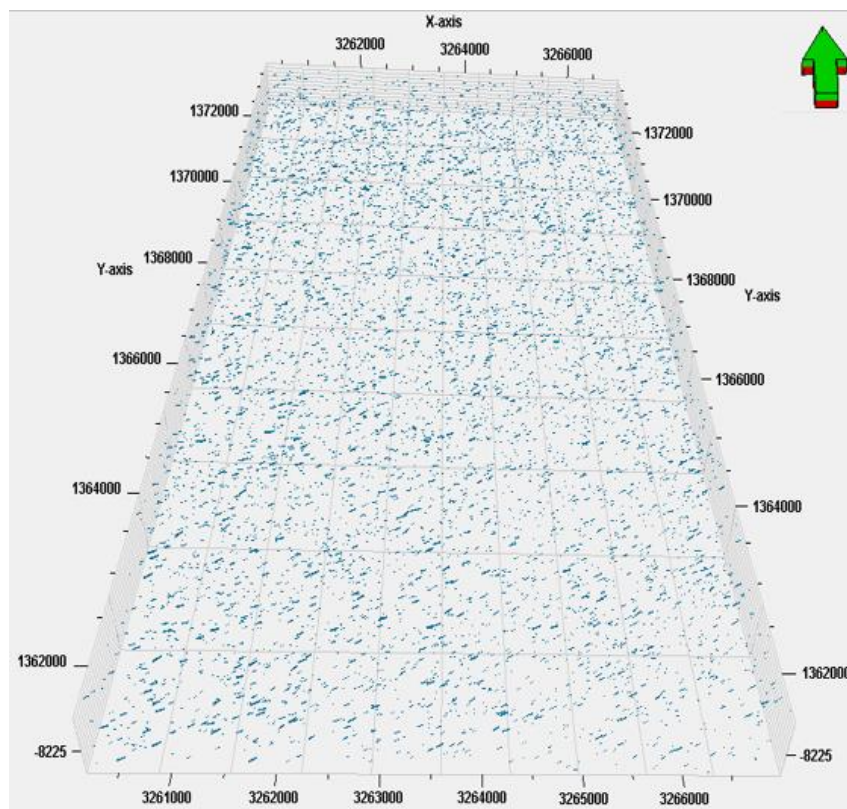


Figure 41: Initial Middle Bakken DFN

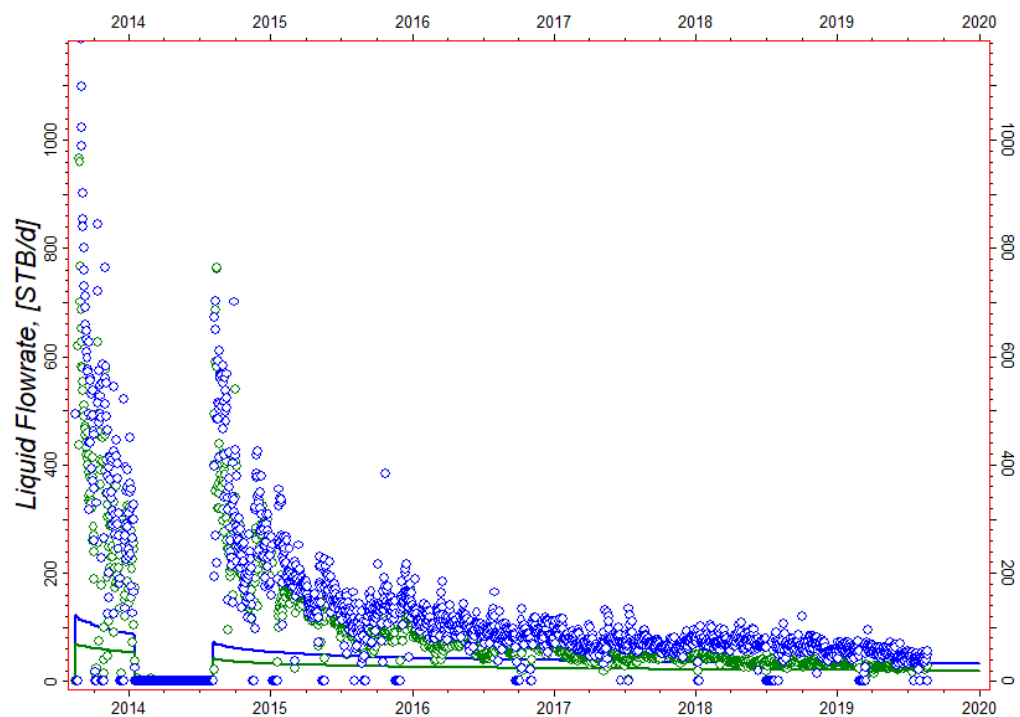


Figure 42: Sundheim 21-27-1H Oil and Water Rates using Initial DFN

The simulated oil and water production rates of the Sundheim 21-27 wells using the initial DFN were similar to the simulated rates before the initial DFN was implemented into model space. It was assumed that the DFN was modeled too conservatively in both fracture intensity and fracture permeability. Figure 43 shows the upscaled fracture grid that accounted for the increase in permeability from both the hydraulic fracture completions of the Sundheim 21-27 wells and the presence of the natural fracture DFN.

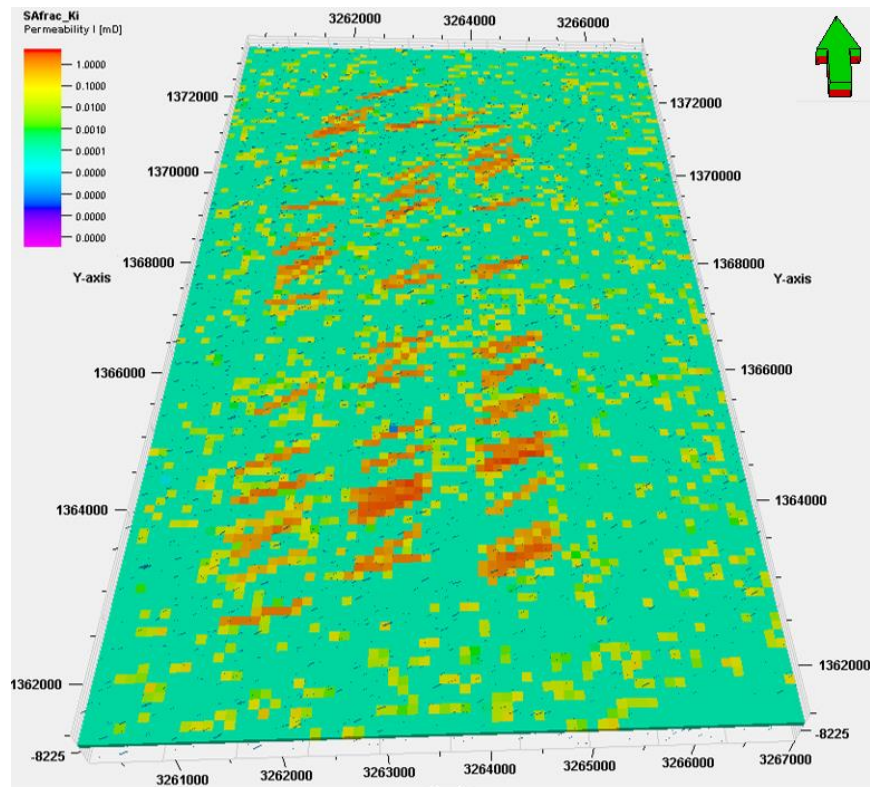


Figure 43: Permeability in the Middle Bakken Fracture Grid

The conservatively modeled initial DFN resulted in an average permeability of the fracture grid of 0.0001 mD. The DFN representing the hydraulic fractures of the Sundheim 21-27 wells can be seen in Figure 43. The permeability of the fracture grid in areas where hydraulic fractures existed was upwards of 1 mD, but the vast majority of the permeability in the fracture grid did not increase due to the presence of natural fractures in the Middle Bakken member. In

areas where fracture intensity was higher, the permeability of the fracture grid was 0.1 mD. The initial DFN properties did not adequately capture increases in flow from the fractures.

The DFN representing the natural fractures of the Middle Bakken member was subsequently altered to increase fracture intensity to increase the flow contribution of the fracture grid on the Sundheim 21-27 wells. Fracture intensity of the DFN was increased to $1\text{E-}4$ fractures per unit volume. Fracture permeability and aperture remained constant. An additional DFN was added to the Middle Bakken to represent the orthogonal fracture set in the Middle Bakken member, and orientation of the additional fracture DFN was modeled at N150E based on literature (Almanza, 2011). The orthogonal fracture set was assigned a fracture intensity of $5\text{E-}5$ fractures per unit volume. The resulting set of DFNs used to model the dual fracture system in the Middle Bakken member is shown in Figure 44.

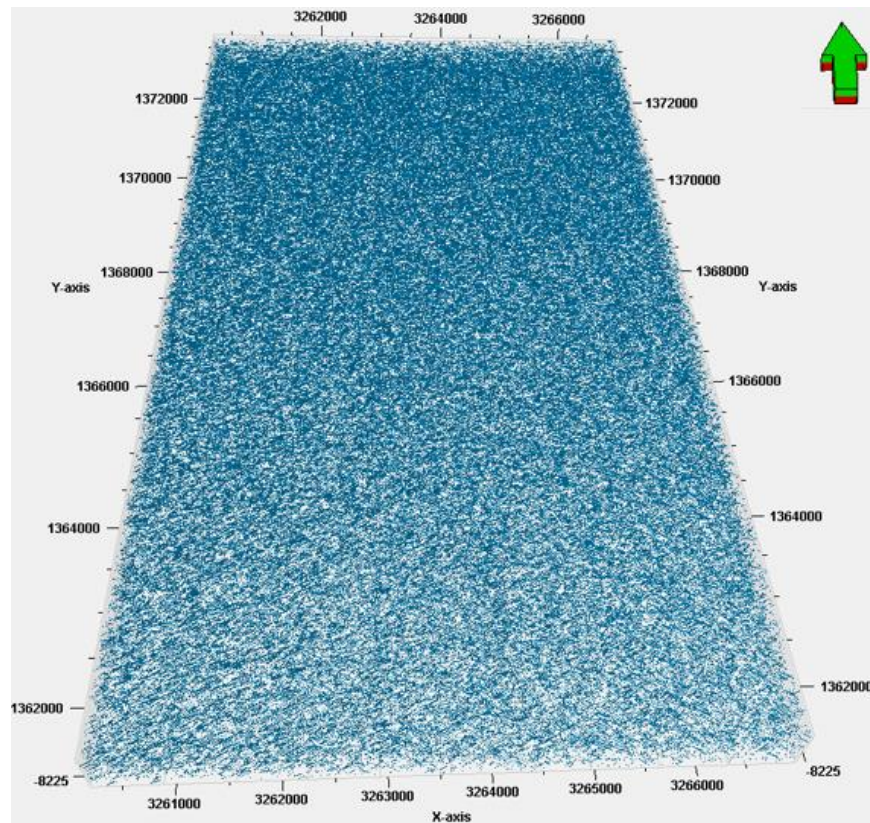


Figure 44: DFN Representing Dual Fracture Systems in the Middle Bakken Member

The altered properties of the Middle Bakken member DFN were upscaled into the fracture grid. The resulting fracture grid permeability is shown in Figure 45.

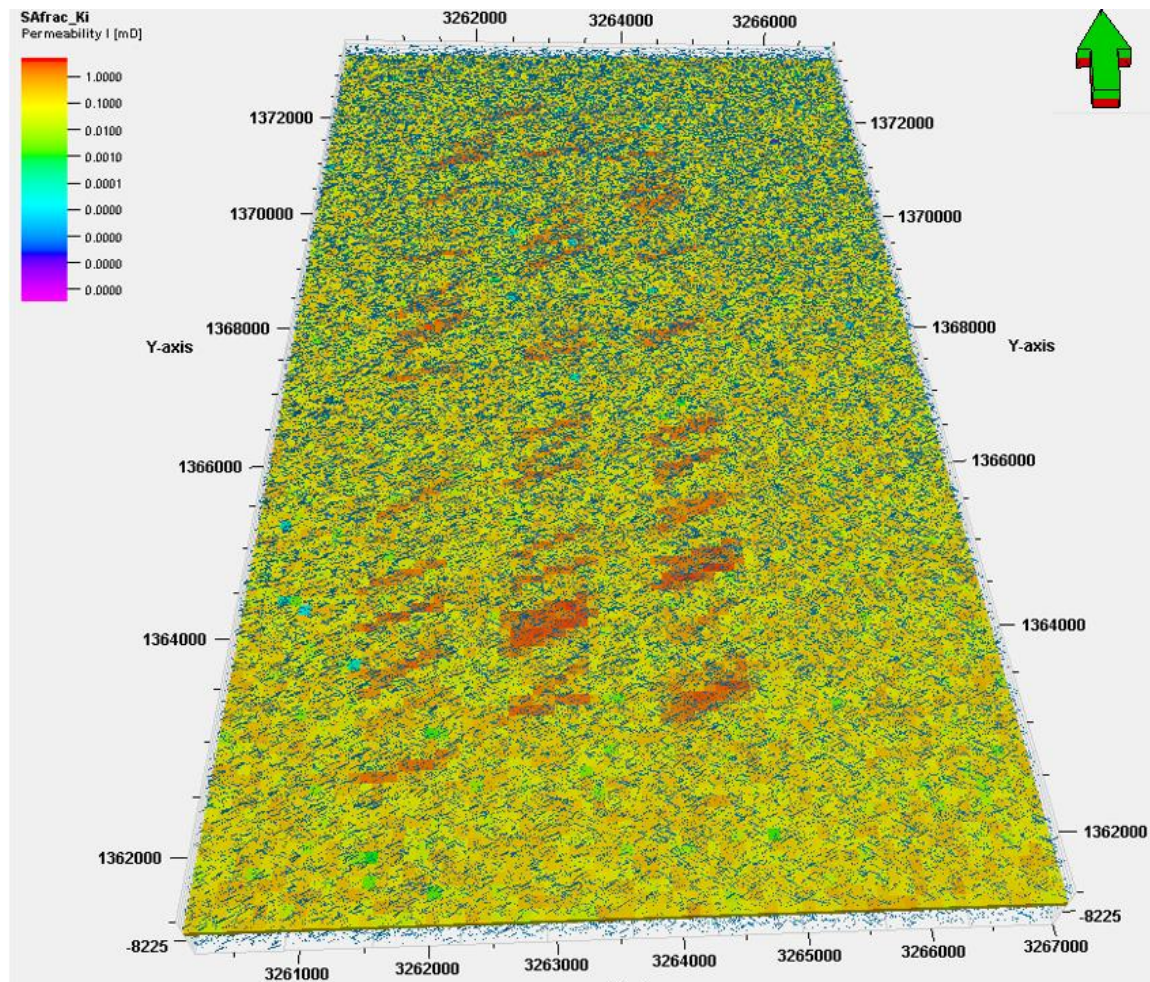


Figure 45: Initial Middle Bakken DFN

Average permeability in the fracture grid increased as a result of increasing fracture intensity in the principle stress DFN and from the introduction of the orthogonal fracture DFN. The majority of the fracture grid had permeability values of 0.1 mD, with areas within the fracture grid representing hydraulic fractures having a permeability of 1 mD. The resulting simulated oil and water rates for Sundheim 21-27-1H after increasing the permeability in the Middle Bakken fracture grid is shown in Figure 46.

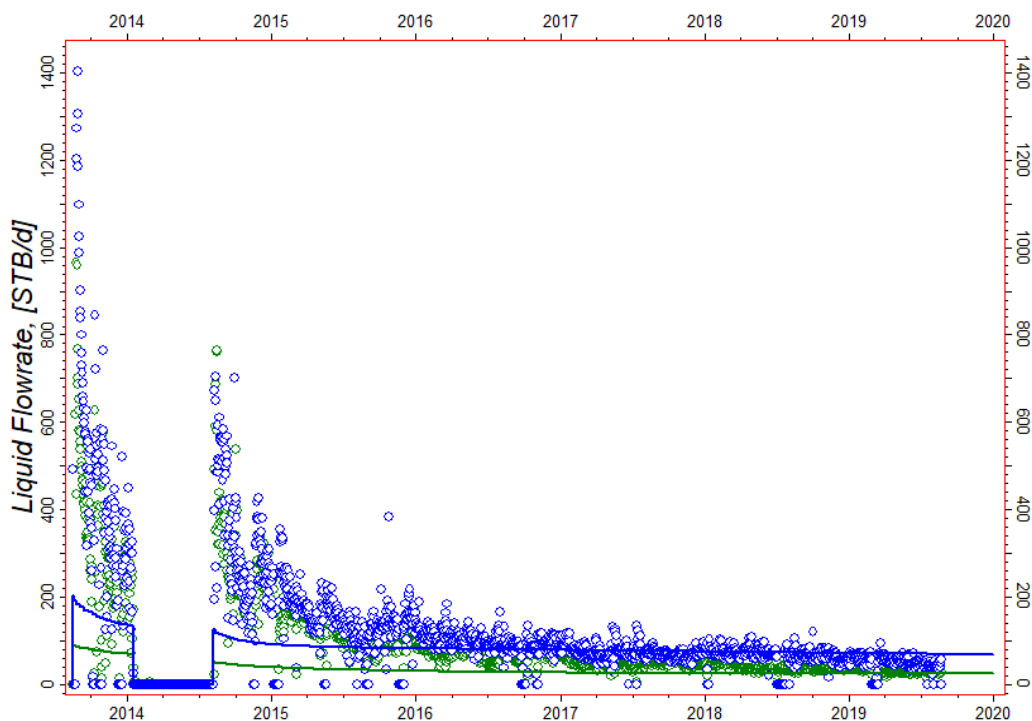


Figure 46: Sundheim 21-27-1H Oil and Water Rates Post DFN Modeling

The additional permeability in the fracture grid resulted in a slight increase to simulated oil and water production rates. Initial simulated oil rates increased by 30 barrels per day after increasing the intensity of the principle fracture field and after introducing the orthogonal DFN into model space. The initial simulated water rates increased by approximately 75 barrels per day after increasing natural fracture intensity in the DFN, and late-time simulated water rates were slightly increased after altering the DFN properties. The presence of the natural fractures had an observable influence on simulated fluid rates and cumulative volumes. The simulated rates and volumes are a function of both the matrix and fracture grid properties, and although the fracture grid added increased fluid storage and flow to the system, the contribution from the fracture grid was minimal when compared to flow contribution from the matrix grid. History matching of observed rates and cumulative volumes was ceased after observing the minimal increases to simulated results after increasing fracture frequency and intensity in the Middle Bakken DFN.

4.1.6. Pressure Dependent Permeability (T_m)

The final parameter that was used as a history matching tool in the Separate Tank model was the introduction of pressure dependent transmissibility (T_m) into model space. The pressure dependent transmissibility was used to model changes in matrix permeability as a result of decreasing pore pressure and increasing net confining stress in the Middle Bakken member. The history matching process, up until the introduction of pressure dependent permeability, did not adequately capture the initial rate trends observed in the Sundheim 21-27 wells. The goal behind the pressure dependent function was to match the initial production rates and the subsequent rapid rate decline that was observed in the Sundheim 21-27 wells.

Middle Bakken matrix permeability was reduced to 0.011 mD in the ST model to better match the observed data. Core reports for the Middle Bakken in the Elm Coulee field have measured permeability ranging from 0.010 mD to 0.040 mD; however, core measured permeability is not necessarily representative of the matrix permeability under reservoir conditions. Most unconventional reservoirs, including the Bakken, are initially over-pressured (pressure gradient is higher than hydrostatic). Matrix permeability therefore may be higher than measured core permeability because the high pore pressure at initial reservoir conditions is holding open small natural fractures and pore spaces that allow increased fluid flow.

The pressure dependent permeability was used as a history matching parameter to capture the dynamic nature of permeability in model space. It was hypothesized that reservoir permeability was greater than 0.011 mD at initial pressures due to open fracture networks and high pore pressure. Reservoir permeability may have eventually dropped below the initial value when pore pressure depletion and net confining stress began to act on the matrix rock, closing fracture networks and pore throats due to long-term fluid production. Table V shows the initial pressure dependent transmissibility table before the history matching process.

Table V: Initial Pressure Dependent Transmissibility Table

Pressure (psi)	T_m
3,000	1.00
3,400	1.00
3,800	1.00
3,990	1.00
4,200	1.00
5,000	1.00
5,600	1.00

The initial pressure dependent transmissibility values were set at 1.00 at all pressure intervals to represent a static permeability value for the Middle Bakken member, and these values were used in all of the previously shown model results. The T_m values were subsequently altered to capture the dynamic nature of permeability in the Middle Bakken member. Initial T_m values were increased to model increased reservoir permeability at initial reservoir pressures. The initial changes to the pressure dependent transmissibility are shown in Table VI.

Table VI: Modified Pressure Dependent Transmissibility Table

Pressure (psi)	T_m
3,000	1.00
3,400	1.50
3,800	2.00
3,990	3.00
4,200	3.00
5,000	3.00
5,600	3.00

The pressure values in the table were altered to create more intervals within the realistic pressure envelope for the reservoir. The T_m values for pressures above 5,600 psi did not affect simulated results because they existed above reservoir pressure for the Middle Bakken member. The T_m values at pressures above 3,900 psi were raised to 3.00 to represent increased permeability in the Middle Bakken at higher reservoir pressure. The T_m values at 3,800 psi and 3,400 psi were set to 2.00 and 1.50, respectively, to model reductions in permeability due to pore

pressure depletion and increasing net confining stress. The simulated rate response to the initial changes to the pressure transmissibility table are shown in Figure 47 for Sundheim 21-27-1H.

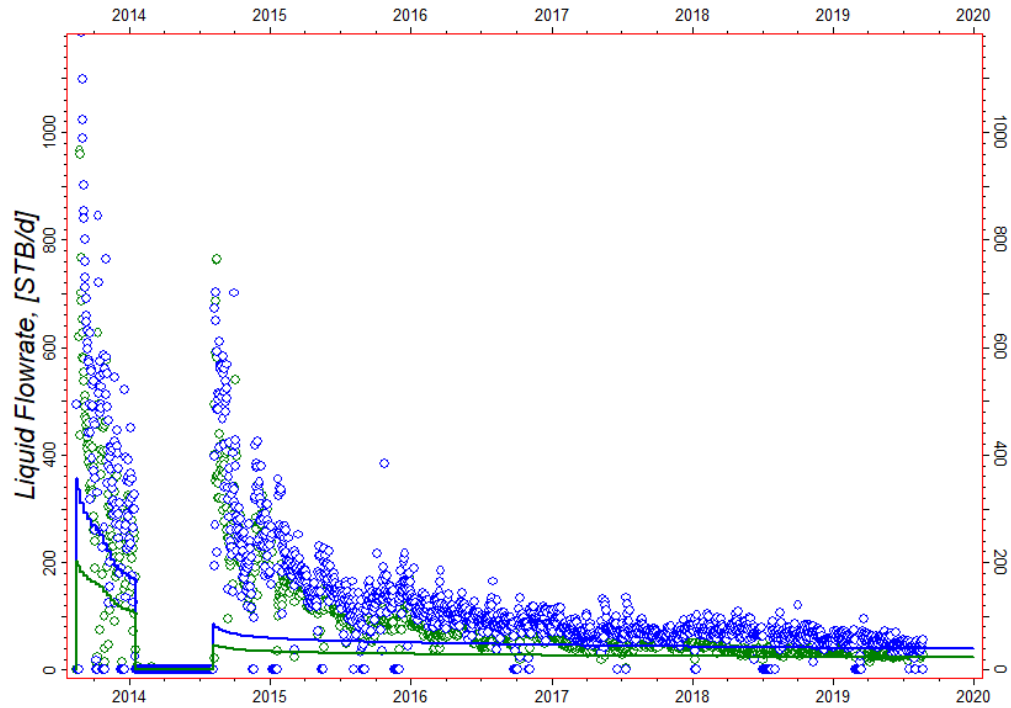


Figure 47: Sundheim 21-27-1H Oil and Water Rates with Initial T_m Modification

The initial changes in the pressure dependent transmissibility table resulted in an increase of simulated initial oil and water rates, but the magnitude of the initial production rates was still lower than the observed data. Additional changes were made to the pressure dependent function in the Separate Tank model to further increase the magnitude of the simulated initial production rates to match the observed data. The additional changes to the T_m table are shown in Table VII.

Table VII: History Matched Pressure Dependent Transmissibility Table

Pressure (psi)	T_m
3,000	1.00
3,400	1.00
3,800	1.35
3,990	4.00
4,200	10.00
5,000	10.00
5,600	10.00

The T_m values for initial reservoir pressure were increased to 10.00 to represent an initial permeability value of approximately 0.11 mD for the Middle Bakken member at higher reservoir pressures. The initial permeability was estimated to be a magnitude higher than the previously defined matrix permeability value of 0.011 mD because of flow contribution from the small open micro fractures and pore spaces. The hydraulic fracture completion of the Sundheim 21-27 wells interacted with the natural fracture system in the Middle Bakken member to provide a high initial permeability. The observed production data trend of high initial oil and water rates is a result of the high permeability natural fracture system being drained, and the subsequent rapid decline in observed rates was a product of the fractures closing and overall permeability of the near-wellbore region declining. Figure 48 shows the simulated oil and water rates for Sundheim 21-27-1H using the history matched pressure dependent permeability system in the Separate Tank model.

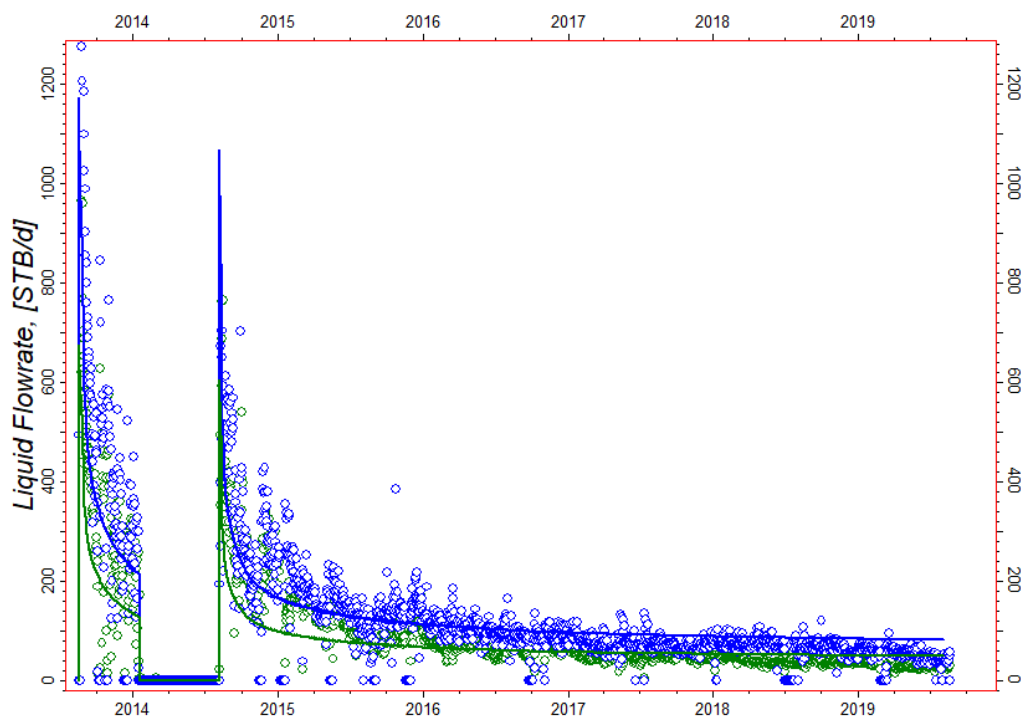


Figure 48: Sundheim 21-27-1H Oil and Water Rates with History Matched T_m

4.2. Vertical Migration Models

The Vertical Migration models were constructed to determine if the source of produced water in the Middle Bakken member of the NE Elm Coulee is due to migration from the heavily water saturated Three Forks formation. The purpose of the Vertical Migration models was to capture water production in the Middle Bakken member that was a direct result of Vertical Migration from the Three Forks formation. Vertical Migration from the Three Forks formation into the Middle Bakken was hypothesized to come from two sources: migration through hydraulic fractures that may have penetrated into the Three Forks from the Middle Bakken completions, and migration through a natural fracture network in the Lower Bakken shale member. Separate scenarios were constructed in model space to test each theory individually.

The Vertical Migration models used some parameters from the history matching process of the Separate Tank model. The history matched relative permeability curves and the Middle Bakken DFN from the Separate Tank model were used in the initial runs of both Vertical Migration models. Similar to the Separate Tank model, the Sundheim 21-27 wells were constrained to a constant bottom hole flowing pressure and history matched using rates and cumulative volumes. The history matching process for water production in the Middle Bakken from Three Forks fluid migration is outlined below.

4.2.1. Hydraulic Fracture Vertical Migration (HFVM) Base Case

The HFVM base case refers to the initial simulation run that was completed to test the theory that water production in the Middle Bakken member is a result of water that has migrated into the Middle Bakken from the Three Forks formation via hydraulic fracture completions. Some properties were altered in model space to configure the HFVM model before running the base case, and the changes are outlined in the subsequent section of the report.

4.2.1.1. Hydraulic Fracture Vertical Migration Initial Changes

The main changes to the model before running the base case were fracture geometry, water saturation, and some rock properties. The hydraulic fracture geometry was altered in the HFVM model to create taller hydraulic fractures that penetrated into the upper bench of the Three Forks formation. The adjusted hydraulic fracture geometry is shown in Figure 49, where the hydraulic fractures for the Sundheim 21-27 wells have been increased in vertical height to penetrate into the Three Forks as compared to the fracture geometry shown in Figure 29, which only penetrates through the thickness of the Middle Bakken member. Fracture half-length remained constant at 400 feet

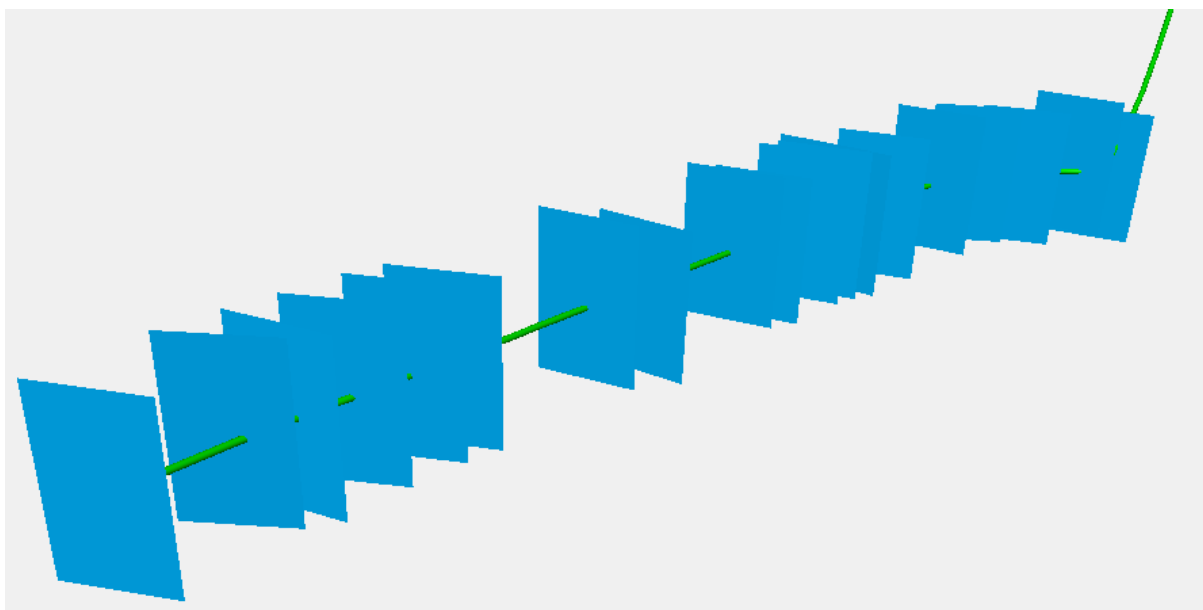


Figure 49: Tall Hydraulic Fractures Penetrating into the Three Forks Formation

The Middle Bakken was assigned a water saturation value 20 percent. A 20 percent water saturation value represents irreducible water saturation, S_{wir} , to effectively “shut-off” mobile water from the Middle Bakken matrix in the HFVM base case. The Three Forks formation was assigned a water saturation of 75 percent. Water saturation was set to S_{wir} in the Lower Bakken to isolate water production solely from the Three Forks formation. The resulting produced water

in model space was a result of water migration from the Three Forks formation via the hydraulic fractures. The initial simulated oil and water rates for Sundheim 21-27-1H are shown for the HFVM base case in Figure 50.

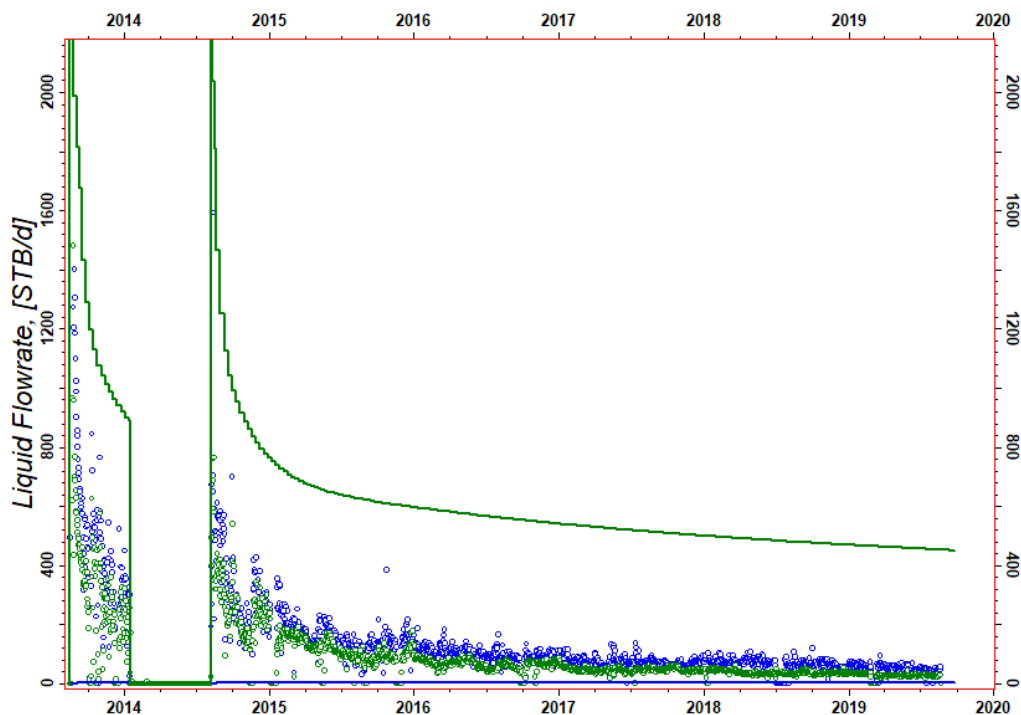


Figure 50: Sundheim 21-27-1H Hydraulic Fracture Vertical Migration Model Base Case Rates

The oil and water rates in the HFVM base case simulation run did not match the observed data. The simulated water rate was zero in the HFVM base case, and the simulated oil rates were much higher than the observed oil rates for all of the Sundheim 21-27 wells. The low water saturation in the Middle Bakken resulted in too much oil in place for the HFVM base case. The hydraulic fracture permeability was too low in the HFVM base case, preventing water from being able to migrate from the Three Forks into the Middle Bakken. Changes were made to the properties in the HFVM model to encourage water production from the Three Forks into the Middle Bakken via hydraulic fractures.

4.2.1.2. Hydraulic Fracture Permeability

The permeability of the hydraulic fractures was increased to promote water migration from the Three Forks into the Middle Bakken. The HFVM base case used hydraulic fracture permeabilities that were generated in Petrel by correlating permeability to fracture aperture. The initial hydraulic fracture permeabilities were upscaled into the fracture grid of the Middle Bakken, Lower Bakken, and Three Forks members, and the permeability in the initial fracture grid for the Lower Bakken is shown in Figure 51.

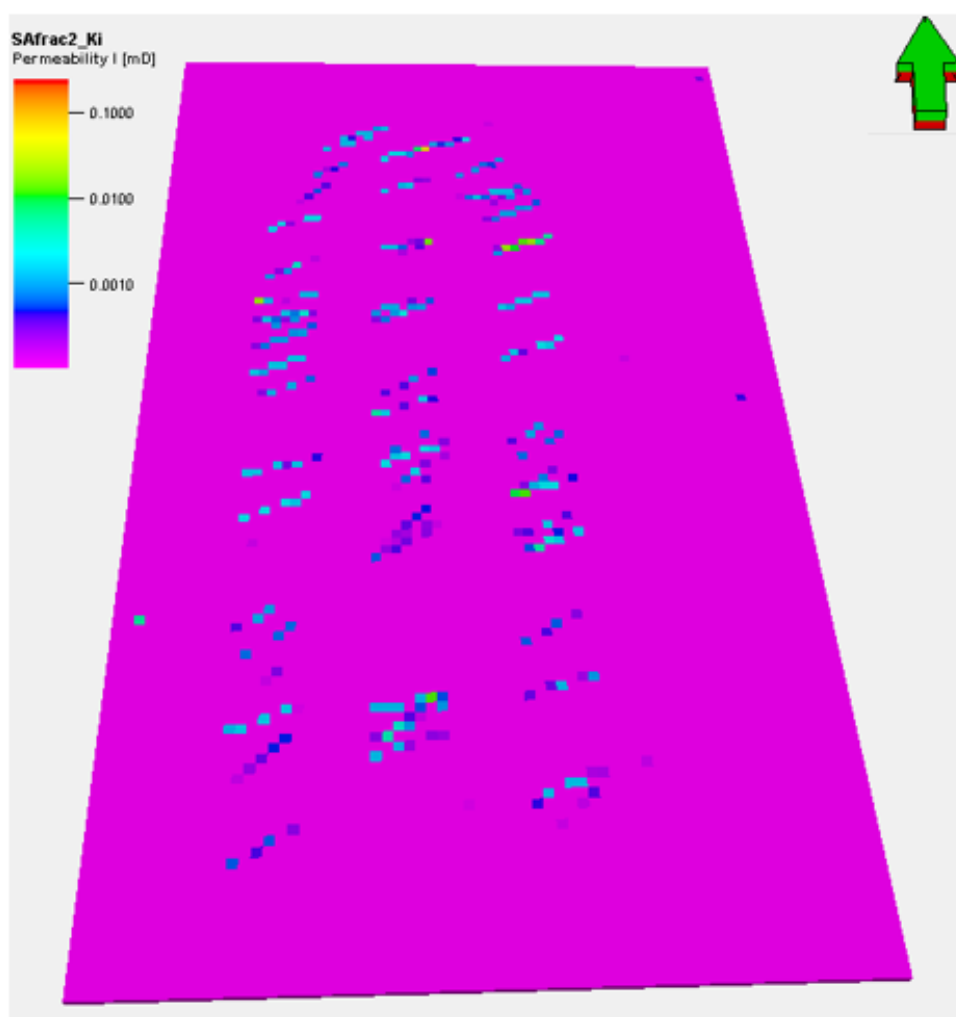


Figure 51: Lower Bakken Initial Fracture Grid Permeability

The upscaled fracture grid of the Lower Bakken member, reflecting the initial permeability values of the hydraulic fractures, shows that the hydraulic fractures only increased

the fracture grid permeability to approximately 0.001 mD. It was estimated that the initial permeability value assigned to the hydraulic fractures was too low. Hydraulic fracture permeability was increased so that the fracture grid permeability more accurately reflected the flow potential of the hydraulic fractures. The goal in increasing fracture permeability was to increase the upscaled permeability in the fracture grid so that water could migrate from the Three Forks into the Middle Bakken through high permeability hydraulic fracture channels. Figure 52 shows the Lower Bakken fracture grid after increasing hydraulic fracture permeability.

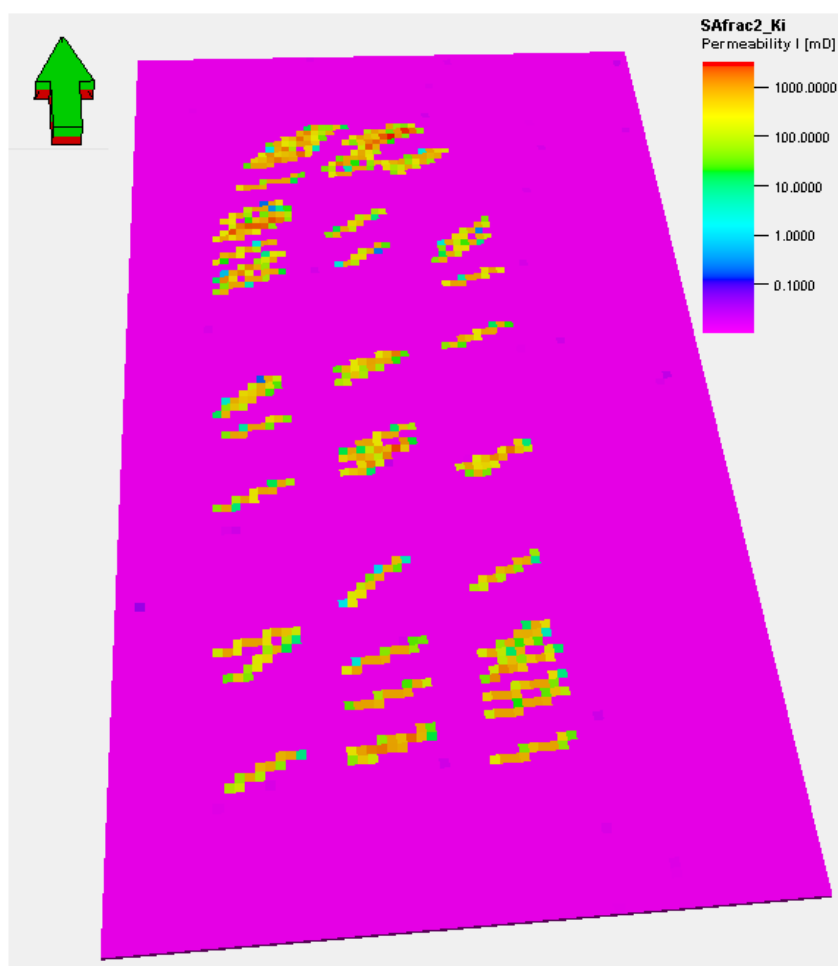


Figure 52: Lower Bakken Fracture Grid Permeability After Increasing Hydraulic Fracture Permeability

Figure 52 shows that increasing the hydraulic fracture permeability values resulted in an increase to the permeability of the Lower Bakken in the fracture grid. The hydraulic fracture

permeability increased from an average value of 0.001 mD to 100.0 mD. The HFVM model was ran after increasing the permeability of the hydraulic fractures to encourage water migration from the Three Forks to the Middle Bakken via the hydraulic fractures. Figure 53 shows the simulated oil and water rates for Sundheim 21-27-1H after increasing the hydraulic fracture permeability to promote water migration from the Three Forks into the Middle Bakken via hydraulic fractures.

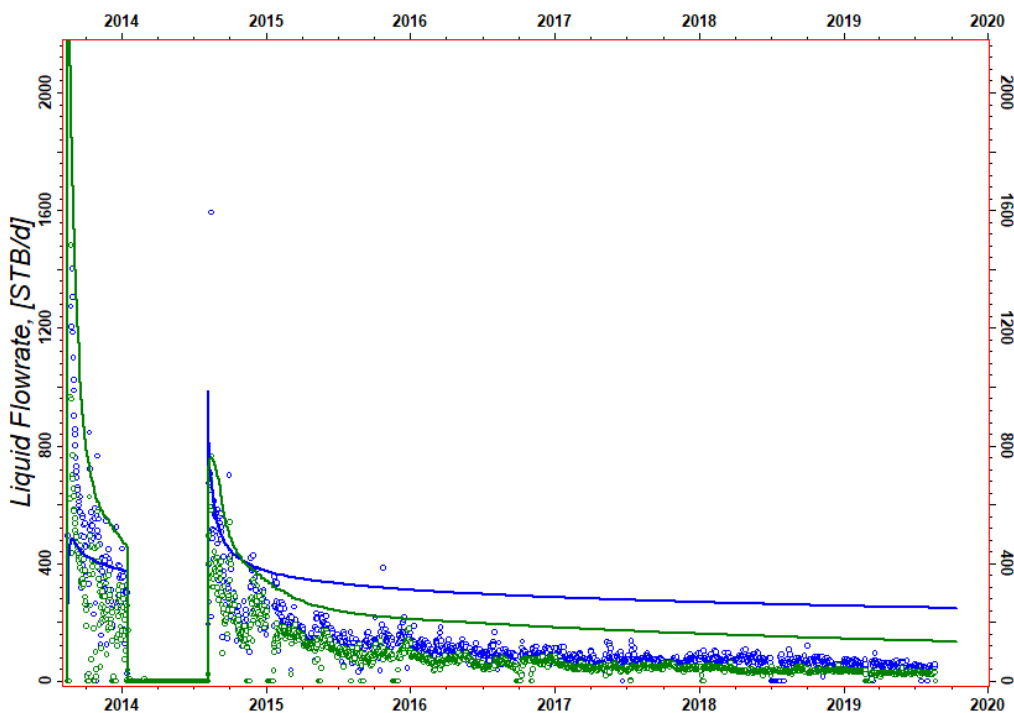


Figure 53: Sundheim 21-27-1H Oil and Water Rates After Increasing Hydraulic Fracture Permeability

Increasing hydraulic fracture permeability resulted in simulated water migration from the Three Forks to the Middle Bakken via hydraulic fracture. Simulated water production due to migration from hydraulic fractures began as soon as the Sundheim 21-27 wells came online due to the high permeability flow channel connecting the Three Forks to the Middle Bakken member. The magnitude of oil production after increasing the hydraulic fracture permeability is too high, and the high oil production is a result of the low matrix water saturation in the Middle Bakken.

The low water saturation results in too much oil in place for the Middle Bakken. The simulated water production due to hydraulic fracture migration from the Three Forks is also too high after initial increases in hydraulic fracture permeability.

4.2.1.3. Matrix Permeability

Matrix permeability was used as a history matching parameter in the HFVM model to match simulated and observed oil and water rates in the Sundheim 21-27 wells. Initial permeability in the Middle Bakken was set to 0.020 mD for previous model runs in the Hydraulic Fracture Vertical Migration model. The permeability of the Middle Bakken was reduced to better match simulated results to the observed data. Matrix permeability was reduced in intervals to achieve a history match of the simulated results to the observed data. After reducing the matrix permeability to 0.005 mD, the simulated oil rate magnitude was much closer to the observed data; however, the simulated water rates remained similar to the rates after increasing the hydraulic fracture permeability in Figure 53. Figure 54 shows the resulting simulated oil and water rates for Sundheim 21-27-1H after reducing matrix permeability in the Middle Bakken member from 0.020 mD to 0.005 mD.

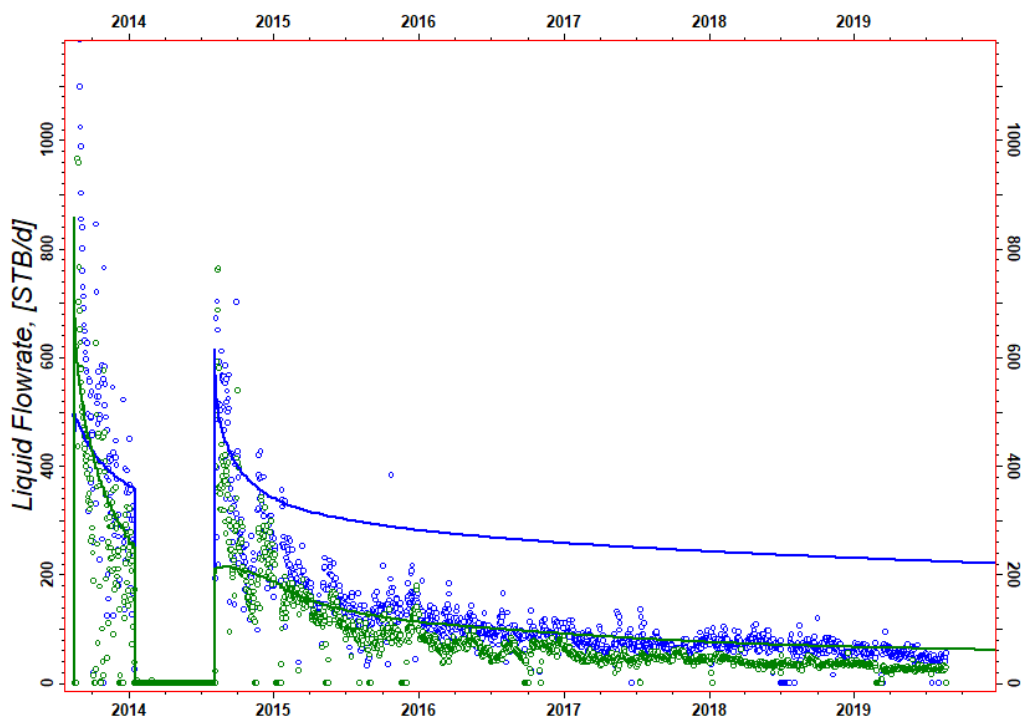


Figure 54: Sundheim 21-27-1H Oil and Water Rates After Reducing Middle Bakken Permeability

The reduction in matrix permeability for the Middle Bakken helped to reduce simulated oil rates for the Sundheim 21-27 wells. While the simulated oil production much more closely matched the observed data, simulated water production was still higher than the observed data. The magnitude of water migrating into the Middle Bakken from the Three Forks via hydraulic fractures resulted in too much water production in the Sundheim 21-27 wells after reducing Middle Bakken matrix permeability. The driving production mechanism for water production in the HFVM model was hydraulic fracture permeability.

Final adjustments to the HFVM model were made to match simulated and observed oil and water rates. The permeability of the hydraulic fractures was decreased to limit the volume of water migrating from the Three Forks to the Middle Bakken. The reductions to the permeability of the hydraulic fractures reduced the average permeability in the Lower Bakken fracture grid to approximately 50 mD. Matrix permeability in the Middle Bakken was reduced to 0.0015 mD to

further limit the volume of oil being produced in the Sundheim 21-27 wells. The changes to the hydraulic fracture permeability and Middle Bakken matrix permeability reduced the magnitudes of the simulated oil and water rates to more closely match the oil and water rates from the observed data. Figure 55 shows the permeability in the Lower Bakken fracture grid after reducing hydraulic fracture permeability. Figure 56 shows the resulting simulated oil and water rates for Sundheim 21-27-1H after the final adjustments. A discussion highlighting the reasons for discontinuing the history matching process of the HFVM model are discussed in the ‘Results’ section of the report.

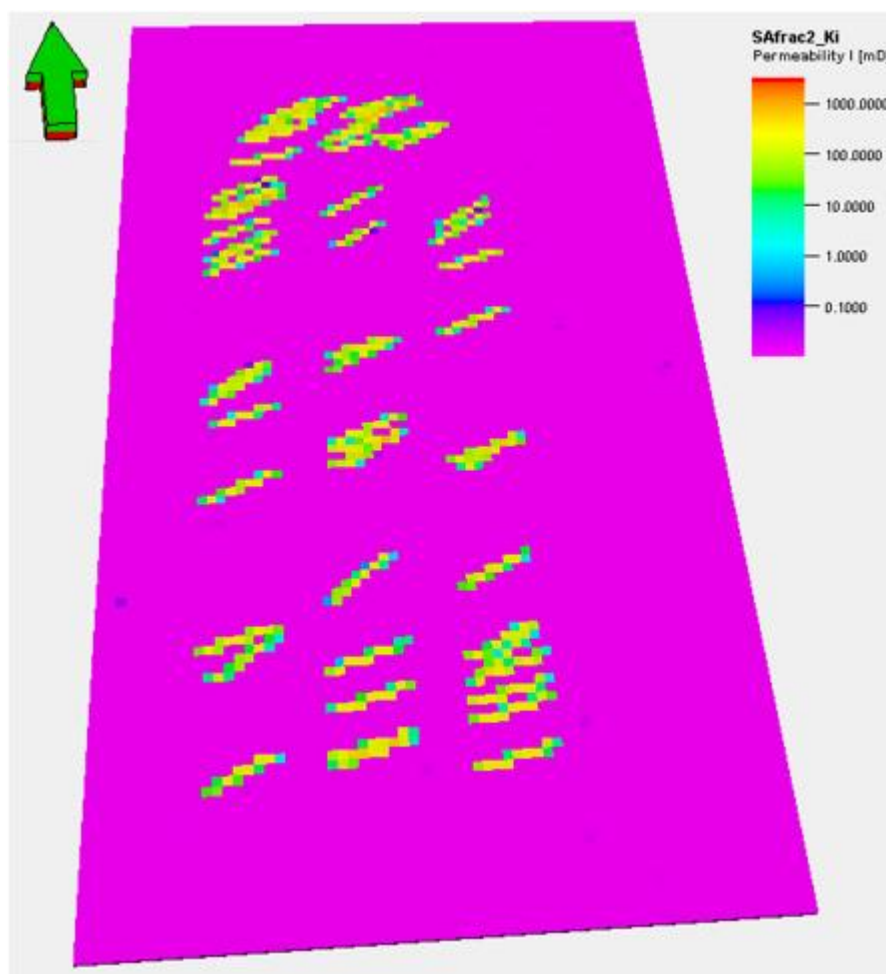


Figure 55: Final Lower Bakken Fracture Grid Permeability

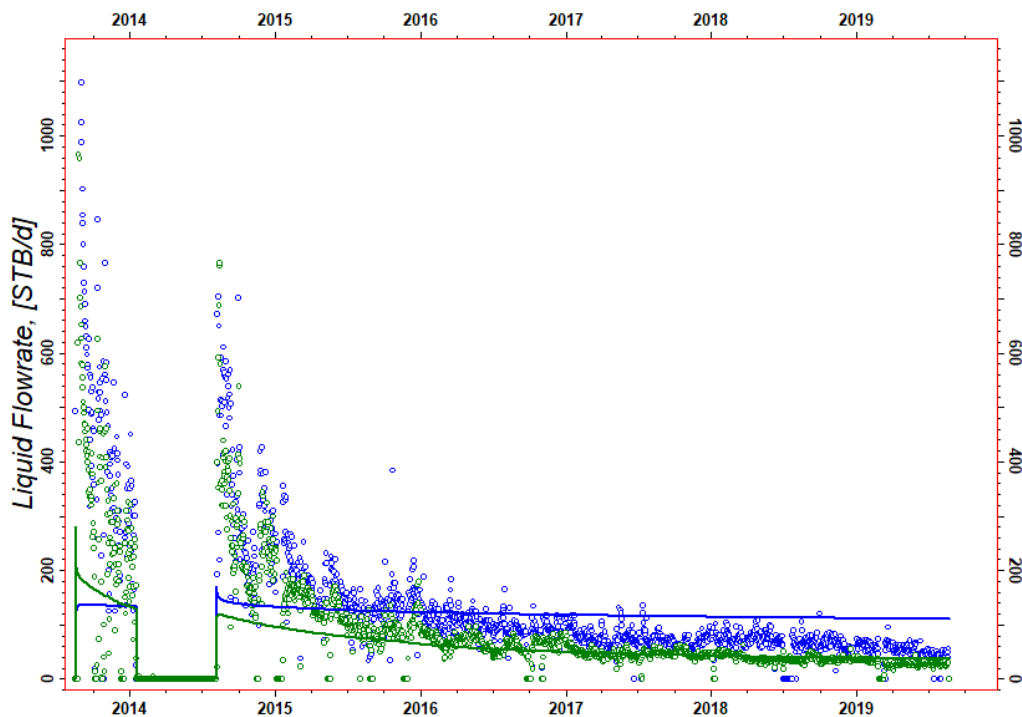


Figure 56: Final Simulated Oil and Water Rates for Hydraulic Fracture Vertical Migration Case

4.2.2. Natural Fracture Vertical Migration (NFVM) Base Case

The NFVM base case refers to the initial simulation run that was completed to test the theory that water production in the Middle Bakken member is a result of water that has migrated into the Middle Bakken from the Three Forks formation via natural fracture networks in the Lower Bakken shale member. Some properties were altered in model space to configure the NFVM model before running the base case, and the changes are outlined in the subsequent section of the report.

4.2.2.1. Natural Fracture Vertical Migration Initial Changes

The hydraulic fracture geometry was changed in the NFVM model as compared to the HFVM model. The hydraulic fracture vertical height was reduced so that the fractures only propagated within the Middle Bakken member. The resulting hydraulic fracture height in the NFVM model was approximately 25 feet. The reduction in hydraulic fracture height prevented

water migration from the Three Forks into the Middle Bakken via hydraulic fractures in model space.

Two DFNs were added to the Lower Bakken shale member to create a natural fracture network. The properties of the DFN closely matched the properties of the DFN that were used in the Middle Bakken for the Separate Tank model. Two fracture sets were created in the DFN for the Lower Bakken shale member: a principle natural fracture system and an orthogonal natural fracture system. Fracture intensity of the principle DFN was set to $1\text{E-}4$ fractures per unit volume with an orientation of N60E. Orientation of the orthogonal fracture DFN was modeled at N150E. The orthogonal fracture set was assigned a P32 fracture intensity of $5\text{E-}5$. The resulting set of DFNs used to model the dual fracture system in the Lower Bakken member are shown in Figure 57.

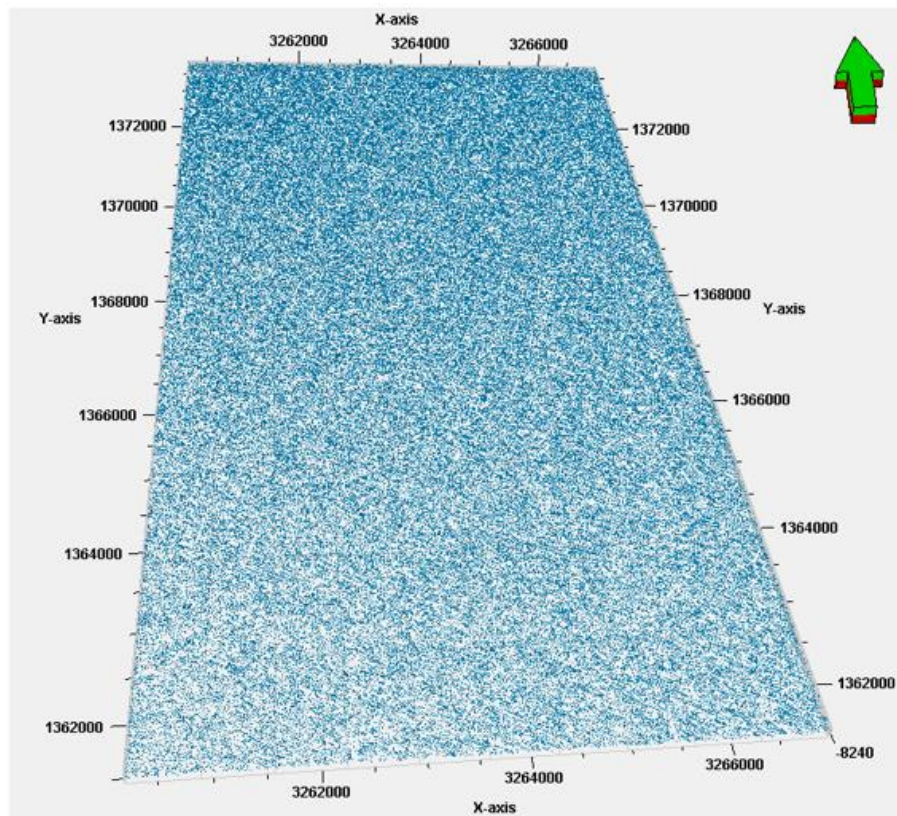


Figure 57: Initial DFN for the Lower Bakken Shale Member

The properties of the DFN were upscaled into the fracture grid to account for the increased permeability of the Lower Bakken shale member due to the presence of natural fractures. Figure 58 shows the fracture grid for the Lower Bakken shale member after upscaling the DFN fracture properties into the fracture grid.

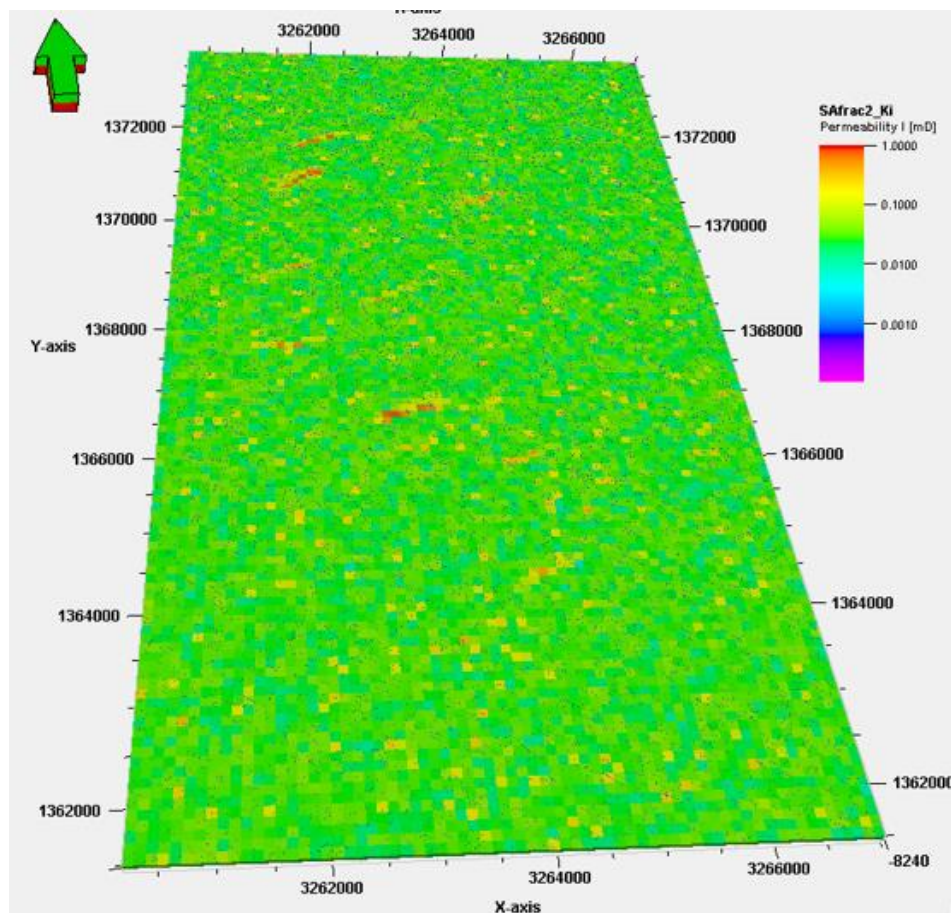


Figure 58: Fracture Grid of the Lower Bakken After Upscaling DFN Properties

The fracture grid for the Lower Bakken had an average permeability of approximately 0.05 mD after upscaling the DFN properties. The Middle and Lower Bakken members were assigned a water saturation representative of the irreducible water saturation, S_{wir} , of 20 percent to simulate water production that was a direct result of vertical migration from the Three Forks formation through the Lower Bakken shale natural fracture systems. The irreducible water saturation value prevented simulated production influence from mobile water in the Middle and

Lower Bakken members. Water saturation in the Three Forks was set to 75 percent. Matrix permeability in the Middle Bakken was set to 0.020 mD. The initial simulated oil and water rates for Sundheim 21-27-1H in the NFVM base case are shown in Figure 59.

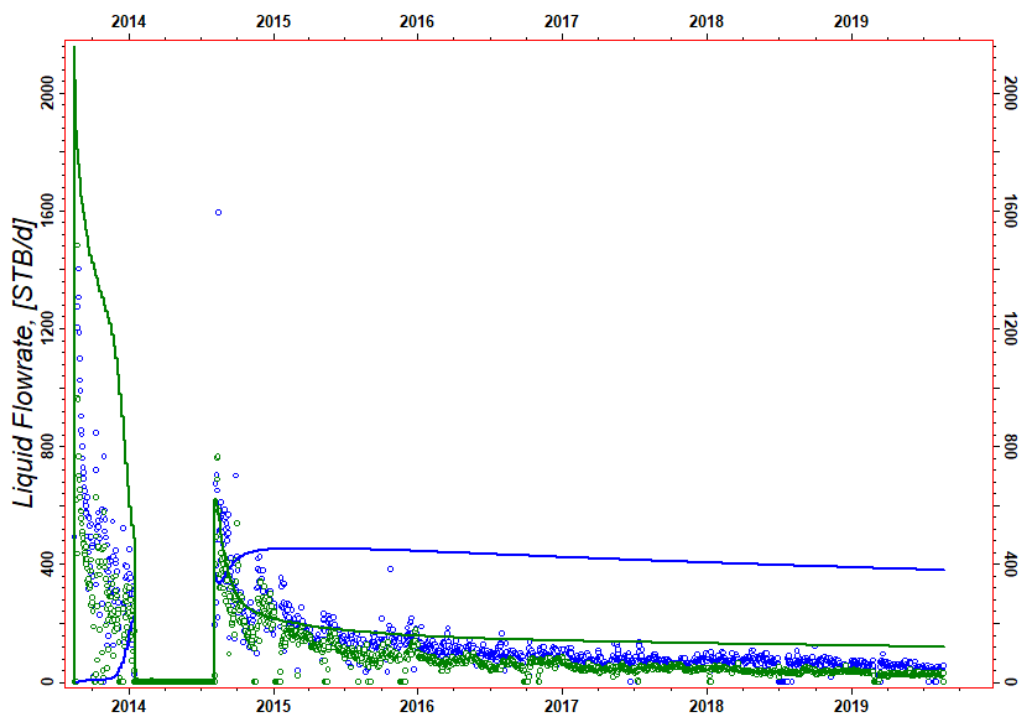


Figure 59: Natural Fracture Base Case Sundheim 21-27-1H Oil and Water Rates

Initial simulated oil production rates in NFVM base case were higher than the observed data. The long-term oil production rates in the NFVM base case were higher than the observed data, indicating that the irreducible water saturation in the Middle Bakken caused the Middle Bakken to have too much oil in place. Simulated water production in the natural fracture base case started in November of 2013 because the migration of water through the Lower Bakken shale member took approximately 3 months to reach the Middle Bakken member. The magnitude of water production in the NFVM base case was significantly higher than the observed data, with simulated rates being 200 barrels per day to 400 barrels per day higher than the observed water production rates for Sundheim 21-27-1H.

4.2.2.2. Lower Bakken DFN Adjustments

The properties of the DFN in the Lower Bakken member were adjusted to reduce the permeability of the fracture grid. The fracture intensities of the DFNs in the Lower Bakken shale were each reduced by a magnitude of 100 to reduce the overall permeability of the fracture grid in the Lower Bakken shale member. The purpose of lowering the fracture intensity and overall fracture grid permeability was to limit the volume of water migrating into the Middle Bakken from the Three Forks through the natural fractures in the Lower Bakken shale member to more closely match observed and simulated water production data. The reduced fracture intensities were upscaled into the fracture grid of the Lower Bakken member, and Figure 60 shows the permeability of the updated Lower Bakken fracture grid.

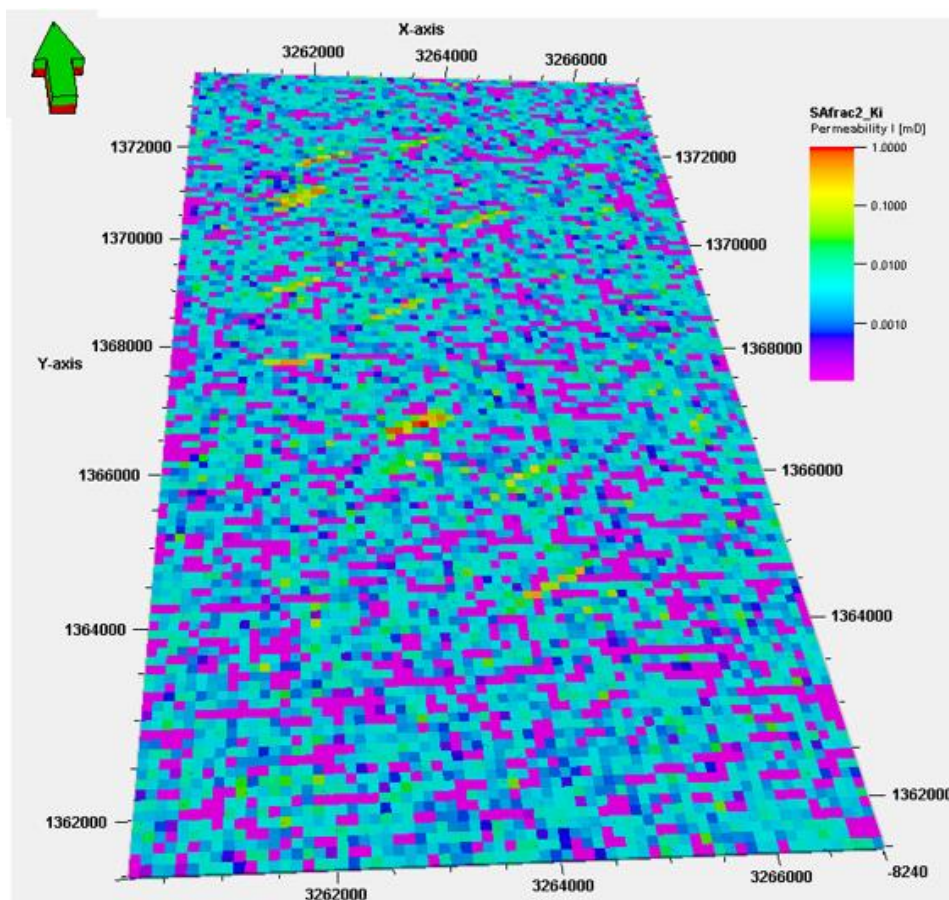


Figure 60: Fracture Grid of the Lower Bakken After Reducing DFN Intensity

The reductions in the DFN intensity of the Lower Bakken member resulted in an average permeability of 0.005 mD in the fracture grid of the Lower Bakken. Simulated oil and water rates for Sundheim 21-27-1H after reducing the DFN fracture intensities are shown in Figure 61.

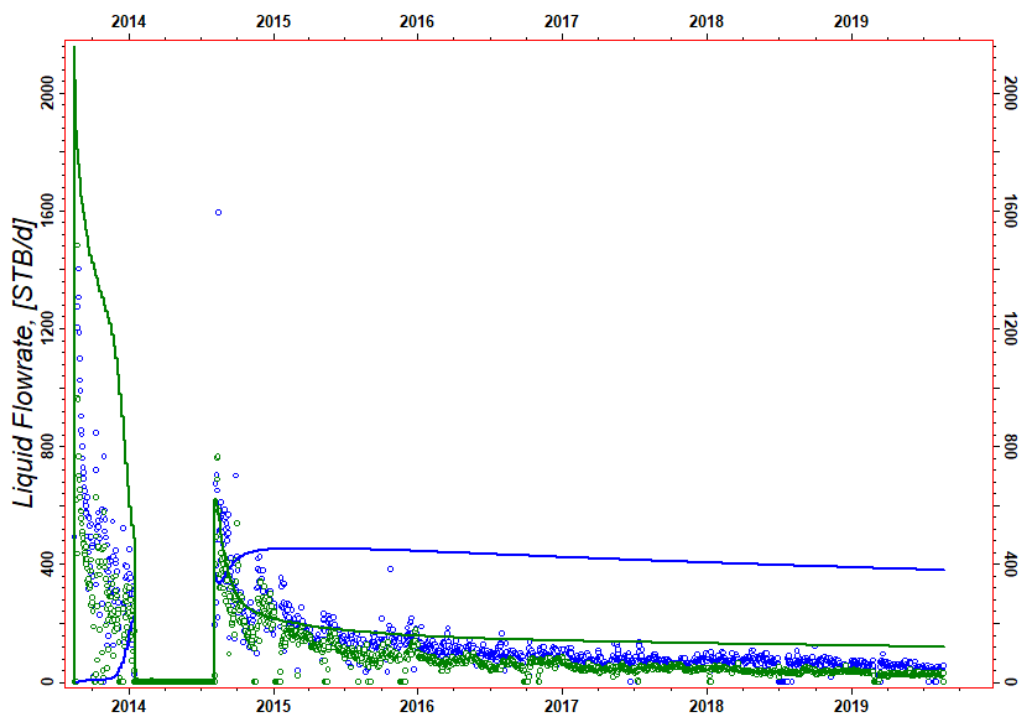


Figure 61: Water Migration for Natural Fracture Vertical Migration Model in Sundheim 21-27-1H

The reduction in the natural fracture intensity of the Lower Bakken DFN did not adequately capture the trend of the observed production data in the Sundheim 21-27 wells. The simulated oil production rates were still much higher than the observed data due to the low water saturation of the Middle Bakken. The low water saturation in the Middle Bakken resulted in too much oil in place for the Middle Bakken member. Simulated water rates were still much higher than the observed data, indicating that the volume of water that was migrating from the Three Forks into the Middle Bakken was higher in model space than in reality.

Final adjustments were made in the NFVM model to reduce the simulated oil and water rates to better match the observed data. Matrix permeability in the Middle Bakken was reduced

to 0.005 mD to reduce the simulated oil rates and cumulative volumes. The hydraulic fracture intensities of both fracture systems in the Lower Bakken were reduced by a magnitude of 10 to reduce the permeability of the Lower Bakken fracture grid. The resulting permeability in the fracture grid is shown in Figure 62, and the final simulated results of the history matched NFVM model for Sundheim 21-27-1H are shown in Figure 63.

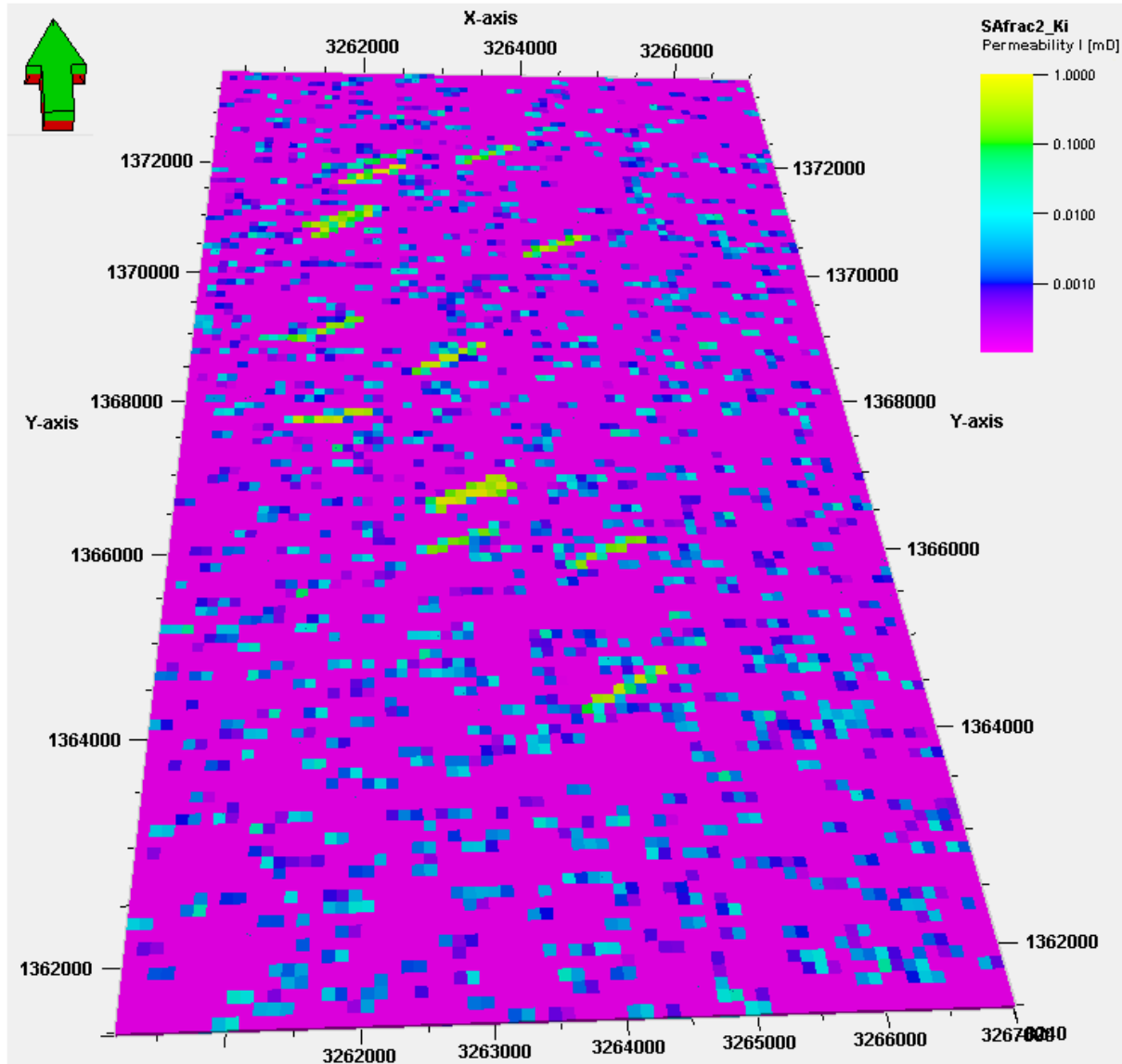


Figure 62: History Matched Lower Bakken Fracture Grid Permeability

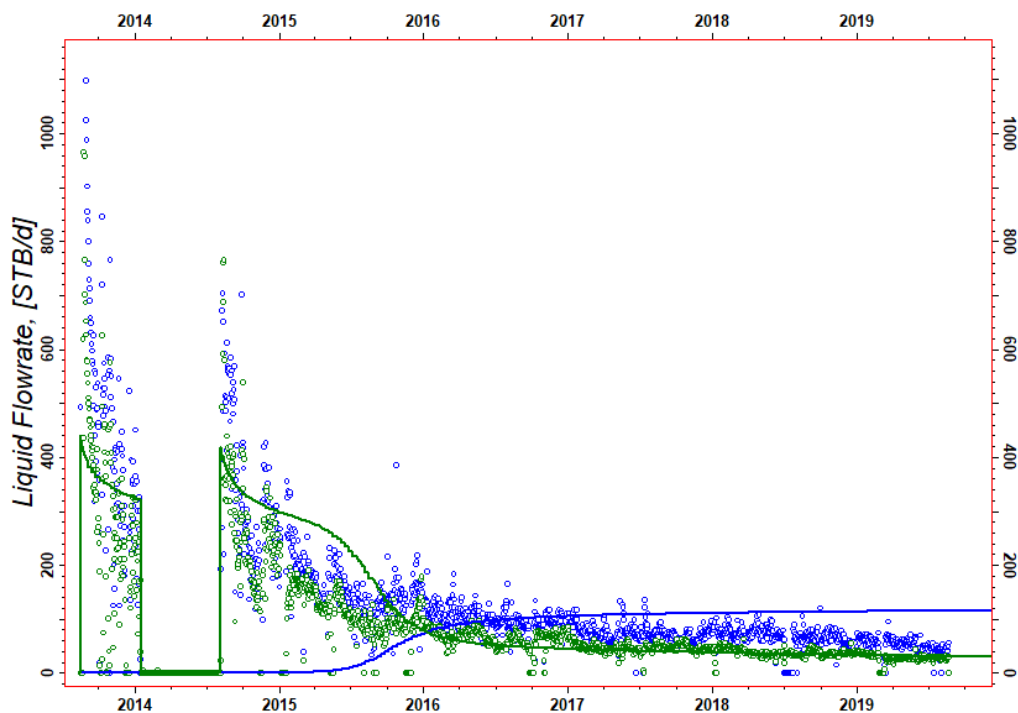


Figure 63: Sundheim 21-27-1H History Matched NFVM Simulated Oil and Water Rates

The reduction in natural fracture intensity of the Lower Bakken member resulted in a reduction of the average permeability of the Lower Bakken fracture grid. Most of the fracture grid had a permeability of 0 mD. Areas of higher fracture intensity in the Lower Bakken had an average permeability of 0.005 mD. The reduction to the permeability in the fracture grid of the Lower Bakken resulted in a lower simulated water production rate in the Sundheim 21-27 wells, and the fracture grid permeability reduction delayed water production in the NFVM model until mid-2015. Middle Bakken matrix permeability was reduced in the final run of the NFVM model to limit the simulated oil rates. The simulated oil rates using a Middle Bakken matrix permeability of 0.005 mD matched the late-time rates of the observed data. A discussion highlighting the reasons for discontinuing the history matching process of the NFVM model are discussed in the ‘Results’ section of the report.

5. Results

Final simulation results from the Separate Tank model and the Vertical Migration models are outlined in the sections below. The results include a discussion of the properties that were changed during the history matching process, and the simulated results for each case are shown.

5.1. Separate Tank Model

The Separate Tank model was constructed to determine if the source of the produced water in the NE Elm Coulee was from Middle Bakken matrix water saturation. Simulated fluid rates and cumulative volumes were matched to observed data for the Sundheim 21-27 wells in the Separate Tank model. The final history matching results are a combination of changing matrix permeability, oil-water relative permeability curves, Middle Bakken matrix water saturation, and Middle Bakken DFN properties. A pressure dependent function was added to the Separate Tank model to capture the dynamic nature of permeability in the model as reservoir pore pressure decreased and net confining stress on the Middle Bakken member increased.

5.1.1. Separate Tank Results

Figures 64 and 65 show the resulting history matched production rates and cumulative volumes for Sundheim 21-27-1H in the Separate Tank model (gas results are shown in red). Additional figures showing simulated rates and volumes compared to the observed data for the other Sundheim 21-27 wells in the Separate Tank model are shown in Appendix A. High initial production rates were captured in the Separate Tank model using the pressure dependent function. Mid-time simulated production rates were slightly lower than the observed data, and late-time simulated production rates in the wells were slightly higher than the observed data in the Separate Tank Model. The simulated cumulative volumes in the Separate Tank model were close to the observed cumulative volumes recovered in the Sundheim 21-27 wells.

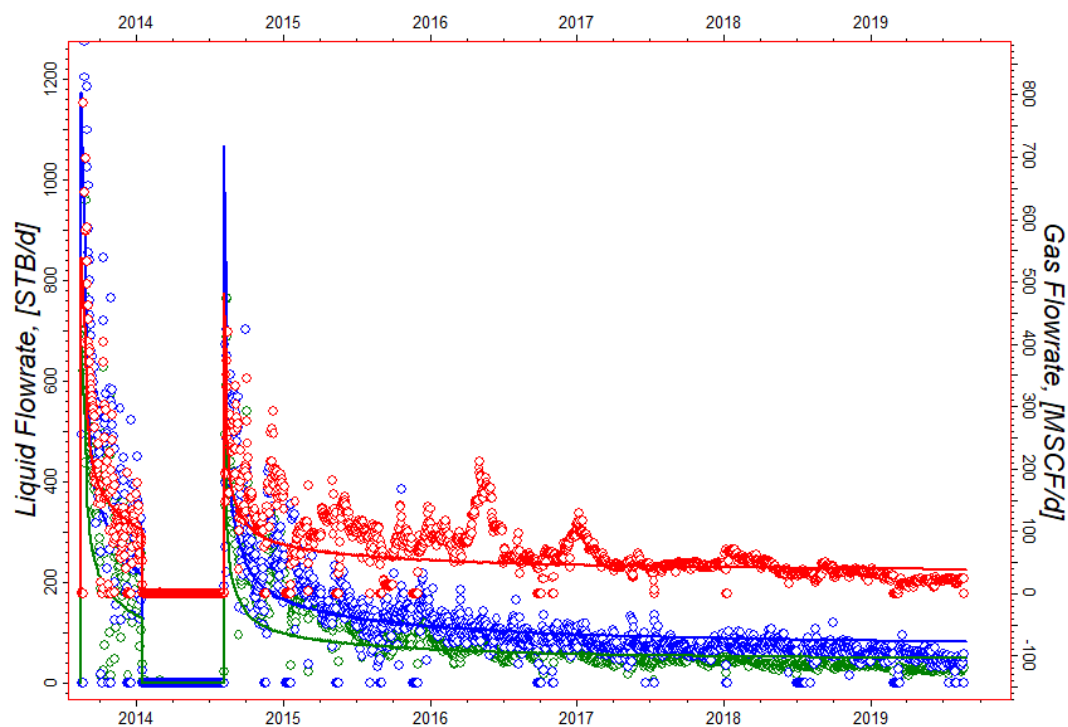


Figure 64: Sundheim 21-27-1H Separate Tank History Matched Rates

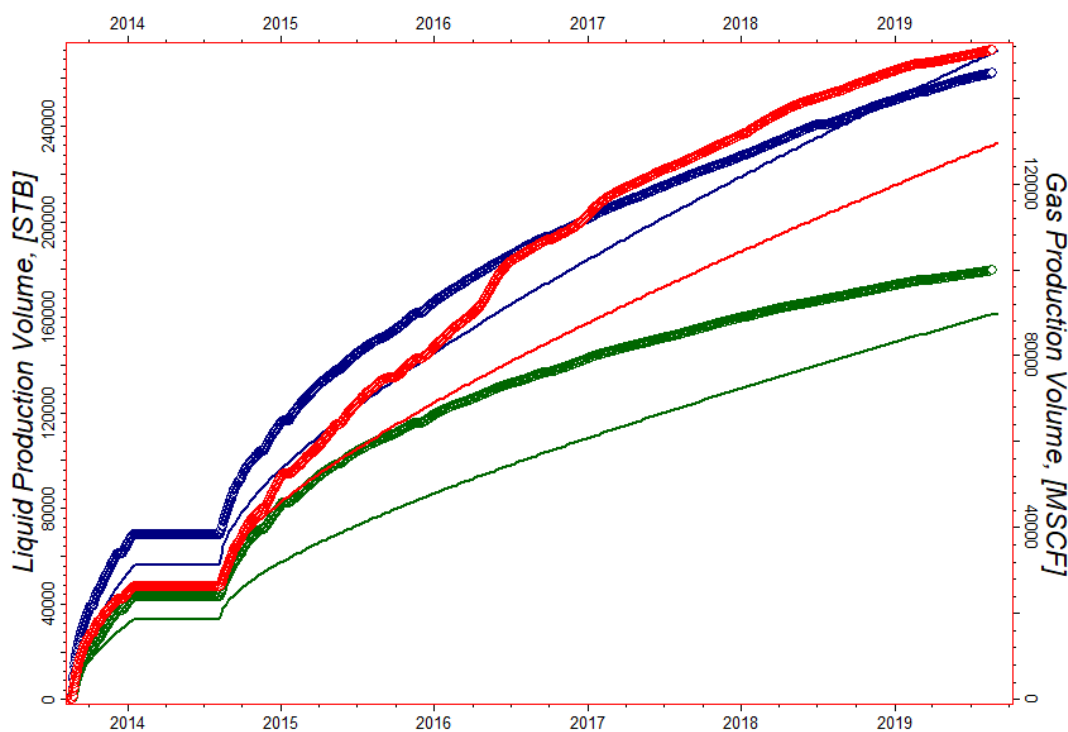


Figure 65: Sundheim 21-27-1H Separate Tank History Matched Cumulative Volumes

5.2. Vertical Migration Models

The Vertical Migration models were constructed to determine if the source of produced water in the NE Elm Coulee was from vertical migration into the Middle Bakken from the Three Forks formation. Two cases were constructed and history matched in the Vertical Migration models: the Hydraulic Fracture Vertical Migration case and the Natural Fracture Vertical Migration case. Final simulation results from each model are outlined in the sections below. Each section contains final simulated results after the history matching process with a discussion of the properties that were changed during the history matching process.

5.2.1. Hydraulic Fracture Vertical Migration (HFVM) Model

The HFVM model was constructed to determine if the source of the produced water in the NE Elm Coulee was from vertical migration of water from the Three Forks into the Middle Bakken via hydraulic fractures. Simulated late-term oil rate was matched in the HFVM model; however, initial oil rates and water rates were not successfully matched in the HFVM model. The final history matching results are a combination of changing Middle Bakken matrix permeability and hydraulic fracture permeability.

5.2.1.1. Hydraulic Fracture Vertical Migration Results

Figures 66 and 67 show the comparison between simulated and observed data in the HFVM model for Sundheim 21-27-1H. Additional figures comparing simulated and observed results for the other Sundheim 21-27 wells in the HFVM model are shown in Appendix A. The late-time oil production rates in the HFVM model matched the observed data; however, initial simulated rates for both oil and water did not match the observed data. Simulated water production rates did not match the observed data in the HFVM model. The simulated water rates were higher than the observed rates and the data did not fit the trend of the observed water

production. Simulated cumulative volumes for all phases were not able to be matched in the HFVM model.

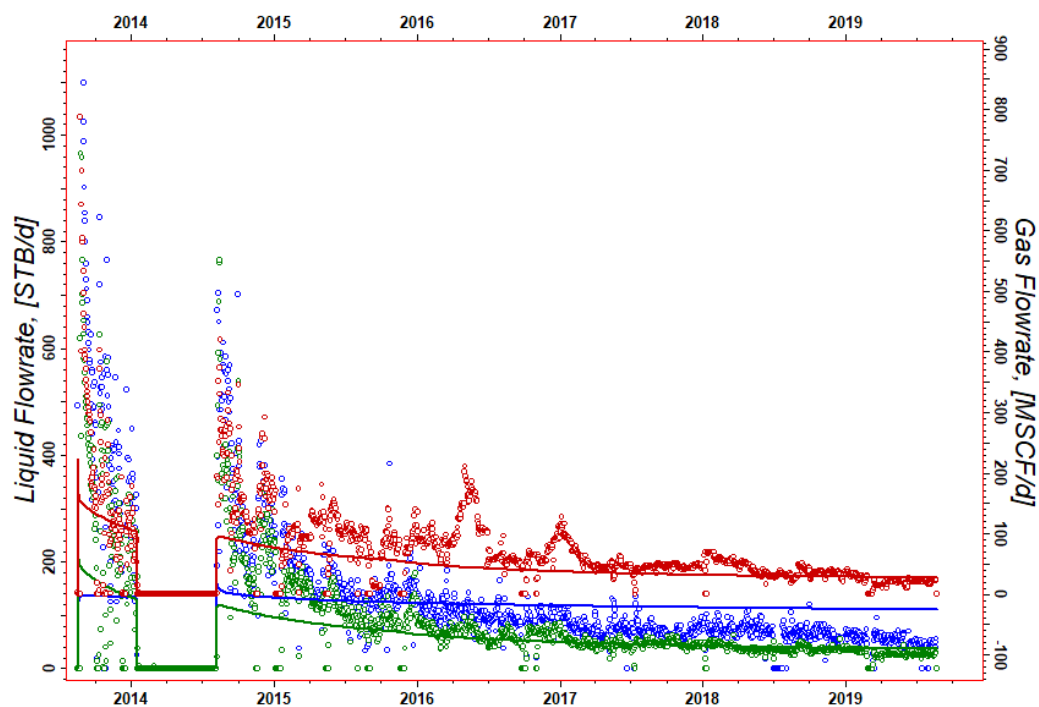


Figure 66: Sundheim 21-27-1H HFVM History Matched Rates

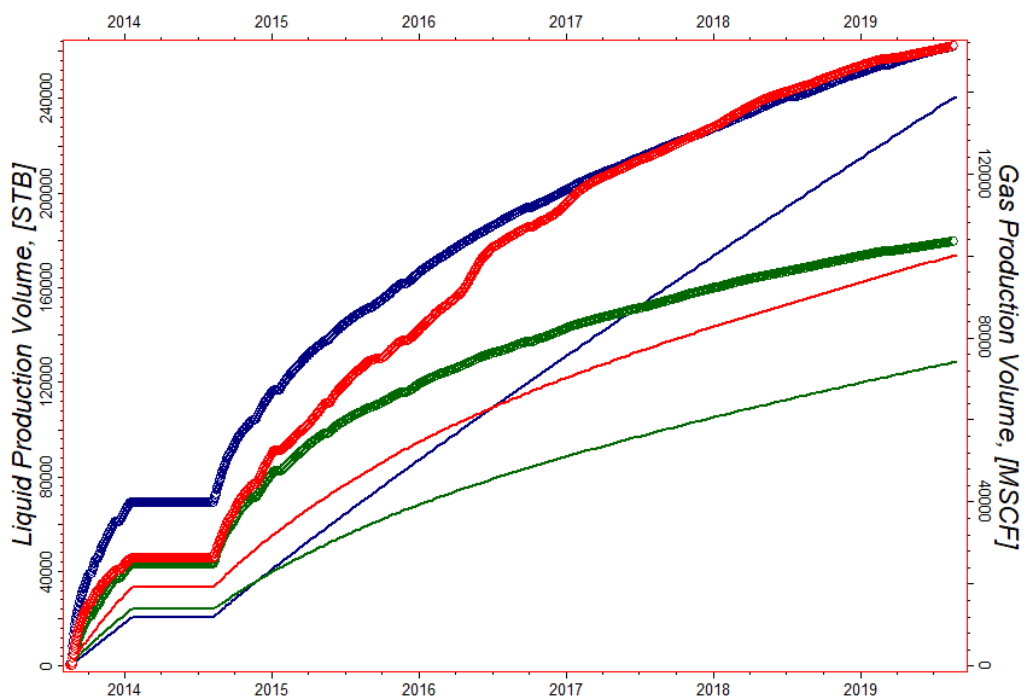


Figure 67: Sundheim 21-27-1H HFVM History Matched Cumulative Volumes

5.2.2. Natural Fracture Vertical Migration (NFVM) Model

The NFVM model was constructed to determine if the source of the produced water in the NE Elm Coulee was from vertical migration of water from the Three Forks into the Middle Bakken via natural fracture networks in the Lower Bakken shale member. Simulated initial oil rates and late-term rates were loosely matched in the NFVM model; however, water rates were not successfully matched in the NFVM model. The final history matching results are a combination of changing Middle Bakken matrix permeability and Lower Bakken DFN properties.

5.2.2.1. Natural Fracture Vertical Migration Results

Figures 68 and 69 show the comparison between simulated and observed data in the NFVM model for Sundheim 21-27-1H. Additional figures comparing simulated and observed results for the other Sundheim 21-27 wells in the NFVM model are shown in Appendix A. Simulated oil production rates in the NFVM model loosely matched the observed oil rates for the Sundheim 21-27 wells. The observed decline in the oil rates after the wells initially began production was unable to be matched in the NFVM model; however, initial magnitude and late-time oil production rates closely matched the observed data. The simulated water production in the NFVM model did not adequately capture the magnitude or trend of the observed water production. The simulated water production in the NFVM model was delayed, indicating that the water migration through the Lower Bakken shale member took over a year to migrate into the Middle Bakken. The observed data shows that water production began immediately in all of the Sundheim 21-27 wells. Once the simulated water rates began to increase in the model, the magnitude of the simulated water production did not match the observed data. The NFVM

simulated water production overestimated the observed rate of water production in the wells.

Simulated cumulative volumes for all phases were not able to be matched in the NFVM model.

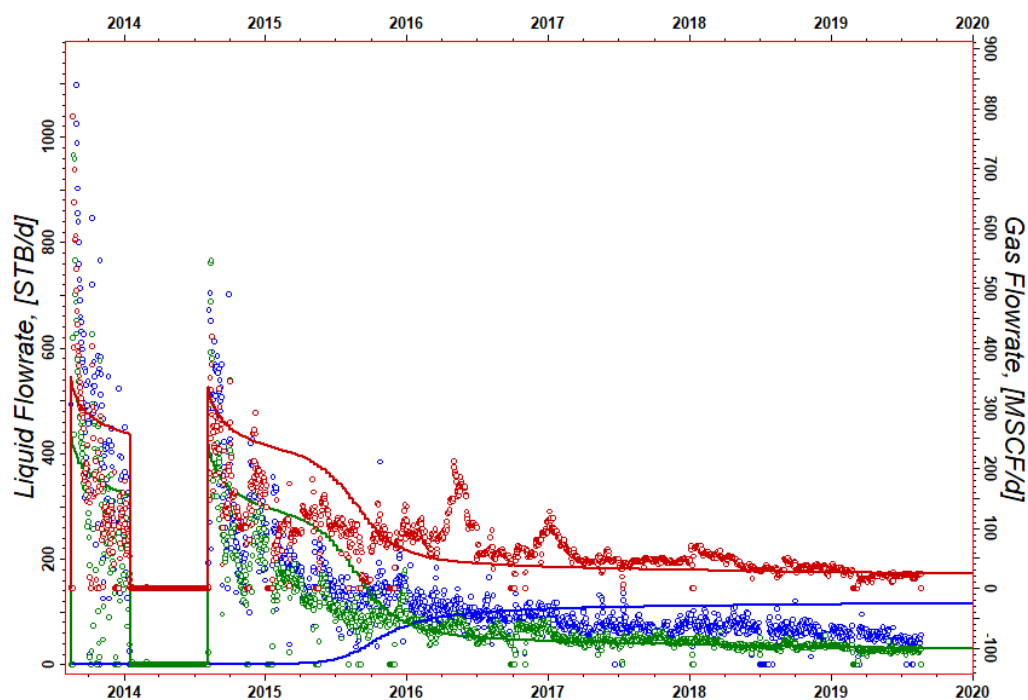


Figure 68: Sundheim 21-27-1H NFVM History Matched Rates

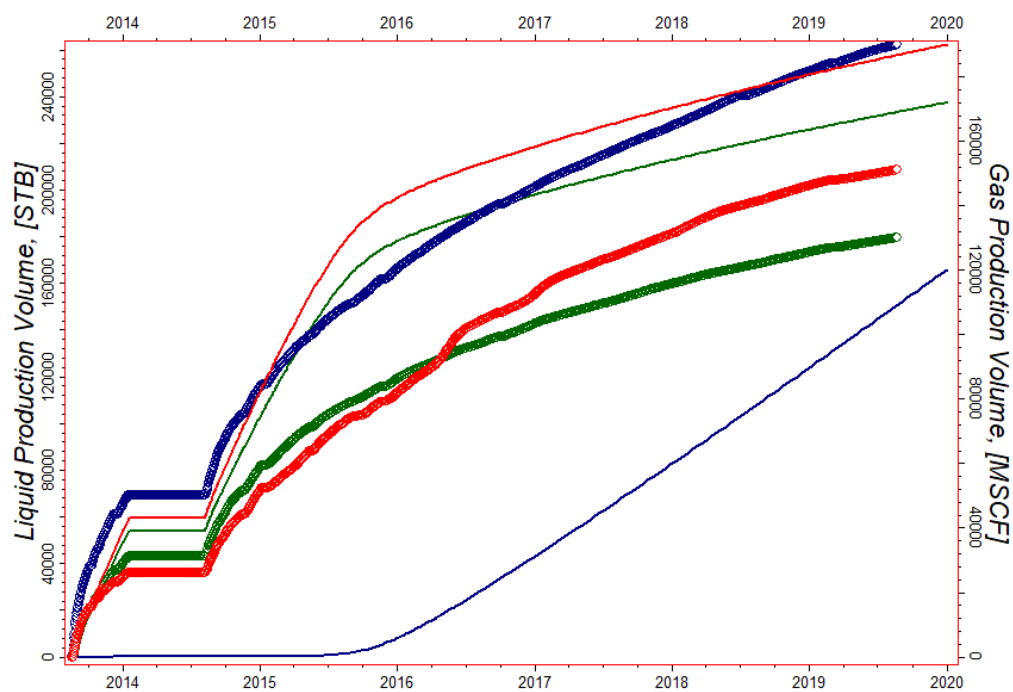


Figure 69: Sundheim 21-27-1H NFVM History Matched Cumulative Volumes

5.3. Discussion

The Separate Tank model and both Vertical Migration Models were constructed to determine the source of produced water in the NE Elm Coulee. All three models underwent the history matching process to match simulated and observed fluid rates and cumulative volumes. In all three cases, the history matching process was able to better reconcile differences between simulated results and observed data; however, some of the parameters that were changed to achieve a history match for the Vertical Migration models were unrealistic. The following subsections answer the study questions for the project with a discussion and summary of evidence from all three models of the project area.

5.3.1. Study Question 1

The primary study question for the project was to determine the source of produced water in the NE Elm Coulee. After history matching the Separate Tank model and both Vertical Migration Models, it was determined that the most likely source for the produced water in the NE Elm Coulee is Middle Bakken matrix water saturation.

5.3.1.1. Separate Tank Evidence

The Separate Tank model was able to adequately reproduce observed fluid rates and cumulative volumes using a realistic set of history matching parameters. Reservoir permeability values range from 0.010 mD to 0.040 mD in the NE Elm Coulee based on literature, and the history matched Separate Tank model used a Middle Bakken matrix permeability of 0.011 mD. The Middle Bakken matrix water saturation for the NE Elm Coulee was predicted to be 50 percent or higher from previous studies. The Separate Tank model used a Middle Bakken matrix water saturation of 55 percent to capture the magnitude and trend of observed fluid production. Other parameters that were used to history match the Separate Tank model, including oil-water

relative permeability curves, DFN properties, and a pressure dependent transmissibility function, all fell within a realistic envelope of uncertainty. The Middle Bakken's high matrix water saturation in the NE Elm Coulee may be a result of leftover water that was not consumed during the hydrocarbon generation process.

5.3.1.2. Vertical Migration Evidence

The Vertical Migration models were unable to adequately reproduce observed fluid rates and cumulative volumes using a realistic set of history matching parameters. The Middle Bakken matrix permeability used to match simulated and observed oil rates was 0.0015 mD in the HFVM model and 0.005 mD in the NFVM model. The Middle Bakken matrix permeability has been observed to be an order of magnitude higher than these values within the NE Elm Coulee. The matrix permeability for the Middle Bakken had to be reduced past the point of reality to achieve a history match in the Vertical Migration models to limit the amount of oil production due to the excessive volume of oil in place in both the HFVM model and the NFVM model based on the low Middle Bakken matrix water saturation.

In order to match simulated and observed water rates in the HFVM model, the water saturation for the Middle Bakken had to be set to 20 percent. Water saturation for the Elm Coulee Proper has been observed to increase towards the location of the study area, and literature for the NE Elm Coulee identifies a likely water saturation for the NE Elm Coulee to be at least 50 percent. The combination of water migration from the Three Forks into the Middle Bakken via hydraulic fracture and Middle Bakken water saturation of at least 50 percent results in simulated water production that is much too high to match the observed data. Figure 70 shows the simulated cumulative water volumes when a realistic Middle Bakken water saturation of 50 percent is modeled in combination with hydraulic fracture water migration from the Three Forks.

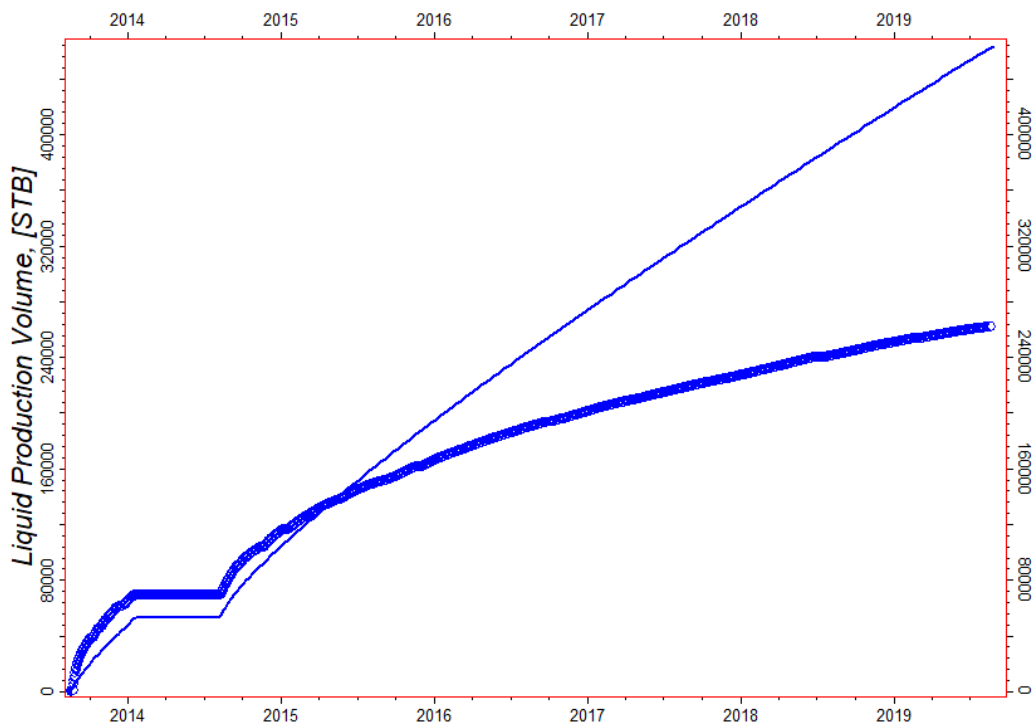


Figure 70: Sundheim 21-27-1H Simulated Cumulative Water Recovery in HFVM Model with 50 Percent Middle Bakken Matrix Water Saturation

The history matching process to isolate water production in the Middle Bakken due to vertical migration of water from the Three Forks into the Middle Bakken via natural fracturing in the Lower Bakken resulted in unrealistic results that did not reproduce the observed data in the Sundheim 21-27 wells. The simulated water production trend in the NFVM model did not match the trend of the observed water production data in the Sundheim 21-27 wells. The observed water production in the Sundheim 21-27 wells was characterized by a trend where initial water rates were of the highest magnitude, followed by a period of water rate decline. The simulated water production rates in the NFVM model started very low and took several months to one year to reach the Middle Bakken and match the magnitude of the observed data. The observed data indicates that the water is being produced immediately, and the simulated delay in water production due to migration times from the Three Forks into the Middle Bakken is unrepresentative of the observed water production data.

Middle Bakken matrix water saturation in the NFVM model was also set to an unrealistically low value of 20 percent to match simulated and observed water production. The combination of a realistic Middle Bakken water saturation and migration of water from the Three Forks into the Middle Bakken via natural fracture systems produces a volume of water that is much higher than the observed data.

5.3.2. Study Question 2

Study question 2 for the project was to determine the impact of natural fracture presence on fluid production in the NE Elm Coulee. The impact of natural fracture presence was analyzed by removing the DFN fracture networks from the Middle Bakken member of the ST model, and simulated oil rates were compared between the two scenarios. Figure 71 shows the simulated oil rates for Sundheim 21-27-1H with and without the Middle Bakken DFN fracture network. Figure 72 shows simulated cumulative fluid volumes with and without the Middle Bakken DFN.

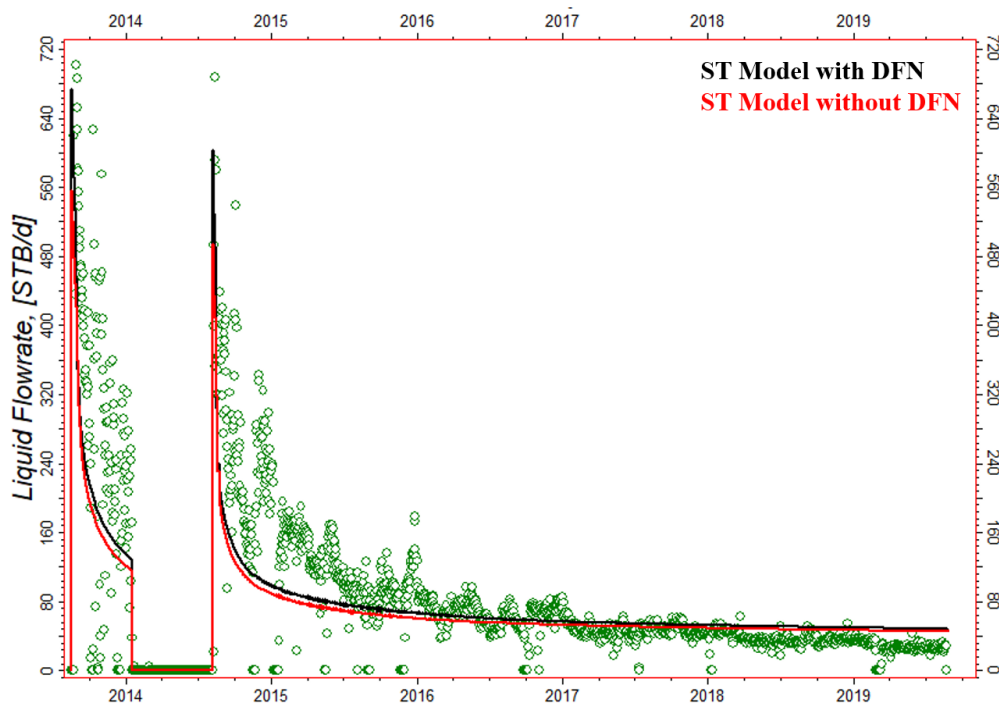


Figure 71: Sundheim 21-27-1H Simulated Oil Rates in the ST Model with and without Middle Bakken DFN

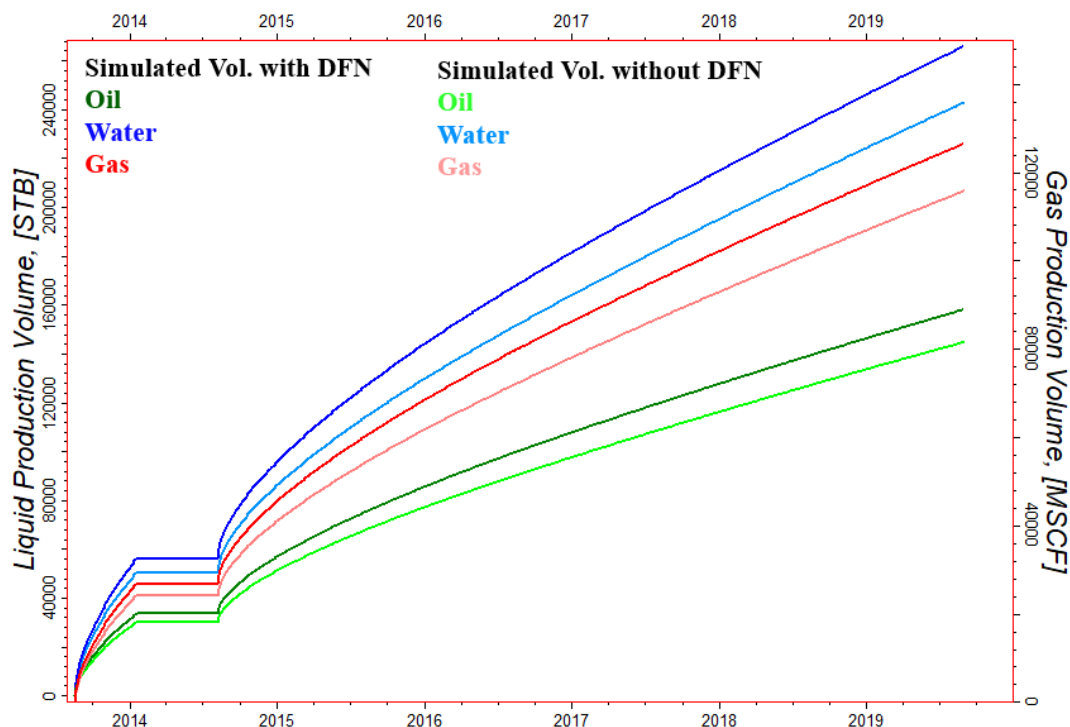


Figure 72: Sundheim 21-27-1H Simulated Cumulative Volumes in the ST Model with and without Middle Bakken DFN

The presence of natural fractures slightly increased initial production rates in the model; however, the long-term impact of natural fracturing is minimal on simulated fluid production rates and volumes. Initial simulated oil rates in the two scenarios differ by almost 100 BOPD, but the long-term simulated production rates differ by only approximately 3 BOPD. The absence of fracture networks in the Middle Bakken resulted in a decrease of only 7 percent to 8 percent in simulated cumulative fluid volumes in the ST model over the production period for the Sundheim 21-27 wells. Tables 8-10 show the difference in simulated cumulative fluid volumes for the ST model with and without the Middle Bakken fracture networks. The tables are located in Appendix A.

Initial production is impacted the most by hydraulic fracture flow channels and wellbore interaction with open natural fractures. The hydraulic fracture networks created during the

completion process are the leading source of fluid production in unconventional reservoirs. The natural fractures that intersect with hydraulic fracture completions are immediately drained during flowback and the initial production period, leading to an increase in initial production rates. Natural fracture influence on fluid production is minimized after the initial natural fractures that are contacted by hydraulic fractures have been depleted. Natural fractures that do not intersect with hydraulic fractures have minimal impacts on production because of isolation from direct flow into the wellbore.

5.3.3. Study Question 3

Study question 3 for the project was to determine whether or not operators within the NE Elm Coulee can minimize expenses related to excessive water production. The increased water production in the NE Elm Coulee is likely a result of matrix water saturation in the Middle Bakken; thus, there are no effective drilling strategies or completion methods that can eliminate water production-related expenses in the NE Elm Coulee. The observed water and oil production rates in the NE Elm Coulee are a direct result of fluid saturations in the Middle Bakken, so production in the NE Elm Coulee cannot be altered through reservoir or drilling engineering-based mitigation strategies.

There are, however, operational strategies for decreasing expenses in the NE Elm Coulee that are a result of high water production. Operators in the field should look to dispose of the produced water via waste-water injection wells rather than other methods, such as trucking or pipelining. There are a number of wells within the NE Elm Coulee that have been shut-in for various reasons, and these wells could allow operators to inject waste water from nearby producing wells in an attempt to reduce water production related expenses.

6. Conclusions

A study area was selected within Township 25N, Range 58E of eastern Montana for numerical flow simulation to determine the source of produced water in the NE Elm Coulee. The study area within the NE Elm Coulee was composed of three hydraulically fractured, horizontal wells that were drilled and completed within the Middle Bakken. A total of three reservoir models were constructed of the area by isolating production mechanisms in model space to determine the source of produced water in the area.

The Separate Tank (ST) model was constructed to determine if the source of the produced water was from matrix water saturation in the Middle Bakken member. Two vertical migration models, the Hydraulic Fracture Vertical Migration (HFVM) model and the Natural Fracture Vertical Migration (NFVM) model, were constructed to determine if the source of the produced water was from vertical migration from the Three Forks formation into the Middle Bakken via hydraulic fracture flow paths or natural fracture networks in the Lower Bakken shale. The conclusions from the reservoir models are listed below:

1. The source of the produced water in the NE Elm Coulee is likely high matrix water saturation in the Middle Bakken member. The Vertical Migration models required unrealistic reservoir parameters to achieve a history match of simulated and observed rates and cumulative volumes. History matching parameters in the ST model fell within the realistic envelope of uncertainty and reasonably reproduced observed rates and cumulative volumes.
2. The produced water in the NE Elm Coulee is not likely migrating from the Three Forks into the Middle Bakken via hydraulic fracture flow paths. Vertical water migration from the Three Forks into the Middle Bakken through hydraulic

fractures, in combination with a likely Middle Bakken matrix water saturation value, caused wells in the NE Elm Coulee to produce larger simulated volumes of water than observed.

3. The produced water in the NE Elm Coulee is not likely migrating from the Three Forks into the Middle Bakken via natural fracture networks in the Lower Bakken shale. The fracture networks in the Bakken are mostly discontinuous, limiting the amount of water that can travel vertically from the Three Forks into the Middle Bakken. The trend of the observed water production data did not match the simulated scenario of water migration via natural fracture networks in the Lower Bakken shale.
4. Natural fracture presence in the Middle Bakken increased both initial and long-term simulated fluid production rates in hydraulically fractured, horizontal wells. Most of the increase in fluid production due to natural fracture presence was observed during the initial production period from interaction with hydraulic fracture networks and natural fracture drainage. Simulated long-term production rates were minimally impacted by natural fracture presence because of natural fracture closure due to decreasing pore pressure and increasing net confining stress.
5. The water production volumes in the NE Elm Coulee cannot be reduced by optimizing drilling or completion methods. Operators in the NE Elm Coulee may be able to reduce water production related expenses in the area by injecting produced water into disposal wells rather than relying on trucking methods or pipeline infrastructure.

7. References

- Almanza, A. (2011). Integrated Three Dimensional Geological Model of the Devonian Bakken Formation Elm Coulee Field, Williston Basin: Richland County Montana. Master's Thesis. Colorado School of Mines, Golden, Colorado.
- Borglum, S. J., & Todd, B. J. (2012). An Investigation of Ancient Geological Events and Localized Fracturing on Current Bakken Production Trends. Society of Petroleum Engineers. doi:10.2118/161331-MS
- Burke, R. B. (1996). Lodgepole Formation Buildups (Waulsortian-like), Williston Basin, North Dakota. Society of Exploration Geophysicists.
- Cox, S. A., Cook, D., Dunek, K., Daniels, G. R., Jump, C. J., & Barree, R. D. (2008). Unconventional Resource Play Evaluation: A Look at the Bakken Shale Play of North Dakota. Society of Petroleum Engineers. doi:10.2118/114171-MS
- Dershowitz, W. S., & Herda, H. H. (1992). Interpretation of fracture spacing and intensity. American Rock Mechanics Association.
- Hamlin, H. S., Smye, K., Dommissie, R., Eastwood, R., Lemons, C. R., & McDaid, G. (2017). Geology and Petrophysics of the Bakken Unconventional Petroleum System. Unconventional Resources Technology Conference. doi:10.15530/URTEC-2017-2670679
- Jin, H., Sonnenberg, S. A., & Sarg, J. F. (2015). Source Rock Potential and Sequence Stratigraphy of Bakken Shales in the Williston Basin. Unconventional Resources Technology Conference. doi:10.15530/URTEC-2015-2169797
- Khatri, S. (2017). Controls on Fracture Network Characteristics of the Middle Member of the Bakken Formation, Elm Coulee Field, Williston Basin, USA. Master's Thesis. University of Nebraska-Lincoln, Lincoln, Nebraska.
- Kurtoglu, B., Cox, S. A., & Kazemi, H. (2011). Evaluation of Long-Term Performance of Oil Wells in Elm Coulee Field. Society of Petroleum Engineers. doi:10.2118/149273-MS
- LeFever, J. A., LeFever, R. D., & Nordeng, S. H. (2013). Reservoirs of the Bakken Petroleum System: A Core-Based Perspective: North Dakota Geological Survey, Bismark, North Dakota. https://www.dmr.nd.gov/ndgs/documents/Publication_List/pdf/geoinv/GI-171_1.pdf

- Meissner, F. (1978). Petroleum geology of the Bakken Formation, Williston basin, North Dakota and Montana, In D. Rehrig, The economic geology of the Williston basin: Proceedings of the Montana Geological Society, 24th Annual Conference. p. 207-227.
- Montana Board of Oil and Gas. (2018). [Image of Elm Coulee Water Cut Distribution].
- Nordeng, S. H. (2009). The Bakken Petroleum System: An Example of a Continuous Petroleum Accumulation. North Dakota Department of Mineral Resources Newsletter, 36, p. 21-24.
- Pieters, D. A., & Graves, R. M. (1994, January 1). Fracture Relative Permeability: Linear or Non-Linear Function of Saturation. Society of Petroleum Engineers. doi:10.2118/28701-MS
- Price, L. C. (1999). Origins and Characteristics of the Basin-Centered Continuous Reservoir Unconventional Oil-Resource Base of the Bakken Source System, Williston Basin. unpublished. <http://www.undeerc.org/Price/>
- Romm, E. S. (1996). *Fluid Flow in Fractures*. Nedra Publishing House, Moscow.
- Sonnenberg, S. A., & Pramudito, A. (2009). Petroleum geology of the giant Elm Coulee field, Williston Basin. *AAPG Bulletin*, 93(9), 1127–1153. <https://doi.org/10.1306/052809090006>
- Sonnenberg, S. A. (2014). The Upper Bakken Shale Resource Play, Williston Basin. Unconventional Resources Technology Conference. doi:10.15530/URTEC-2014-1918895
- Sonnenberg, S. A. (2015). Keys to Production, Three Forks Formation, Williston Basin. Unconventional Resources Technology Conference. doi:10.15530/URTEC-2015-2148989
- Sonnenberg, S. A., Theloy, C., & Jin, H. (2017). The giant continuous oil accumulation in the bakken petroleum system, U.S. williston basin. *AAPG Memoir*. 113(1), p. 91-119. American Association of Petroleum Geologists. <https://doi.org/10.1306/13572002M113508>
- Steptoe, A. (2012). Petrofacies and Depositional Systems of the Bakken Formation in the Williston Basin, North Dakota. Master's Thesis. West Virginia University.
- Stroud, J. (2010). The role of the lower Lodgepole Formation in the Bakken Petroleum System, Billings Nose, North Dakota: Master's Thesis. Colorado School of Mines, Golden, Colorado.

- Stroud, J., & Sonnenberg, S. A. (2011). The Role of the Lower Lodgepole Formation in the Bakken Petroleum System, Billings Nose, North Dakota. The Bakken-Three Forks Petroleum System in the Williston Basin. p. 332-364.
- The Bakken Formation: A basic explanation. *Bakken Oil Business Journal*. (n.d.). Retrieved June 10, 2018, from <https://bakkenoilbiz.com/oil-news/thebakkenformation/>
- Theloy, C., & Sonnenberg, S. A. (2013). Integrating Geology and Engineering: Implications for Production in the Bakken Play, Williston Basin. Unconventional Resources Technology Conference. doi:10.1190/urtec2013-100
- Todd, B. J., Reichhardt, D. K., & Heath, L. A. (2017). An Evaluation of EOR Potential in the Elm Coulee Bakken Formation, Richland County, Montana. Society of Petroleum Engineers. doi:10.2118/185028-MS
- Tran, T., Sinurat, P. D., & Wattenbarger, B. A. (2011). Production Characteristics of the Bakken Shale Oil. Society of Petroleum Engineers. doi:10.2118/145684-MS
- Webster, R. L. (1984). Petroleum Source Rocks and Stratigraphy of the Bakken Formation in North Dakota. *Hydrocarbon Source Rocks of the Greater Rocky Mountain Region*.

8. Appendix A: Additional Tables and Figures

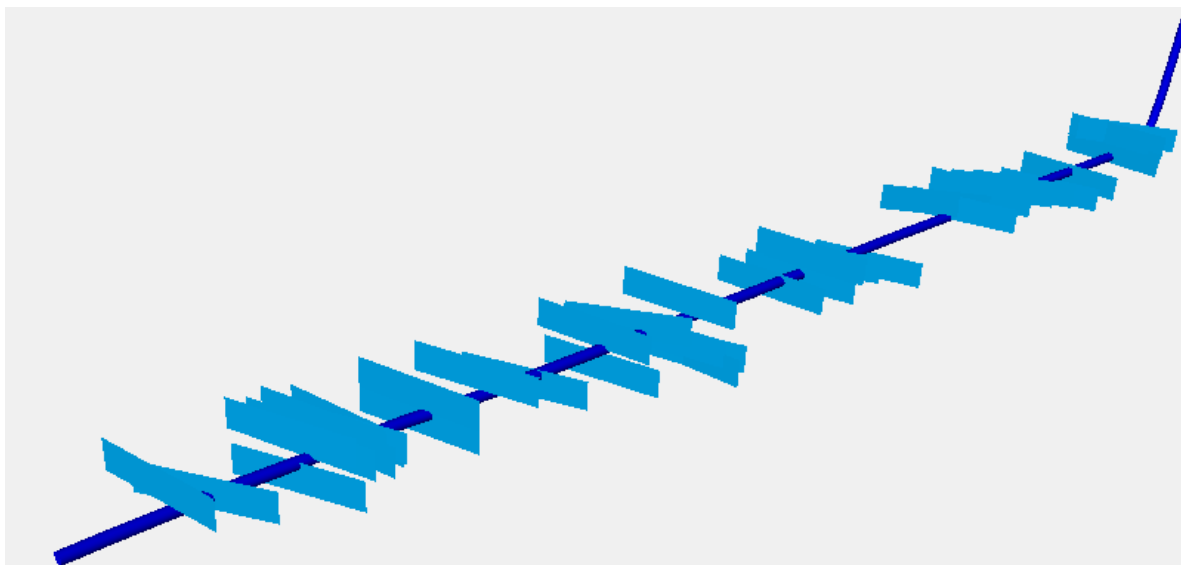


Figure 73: DFN Hydraulic Fracture Completion on Sundheim 21-27-2H

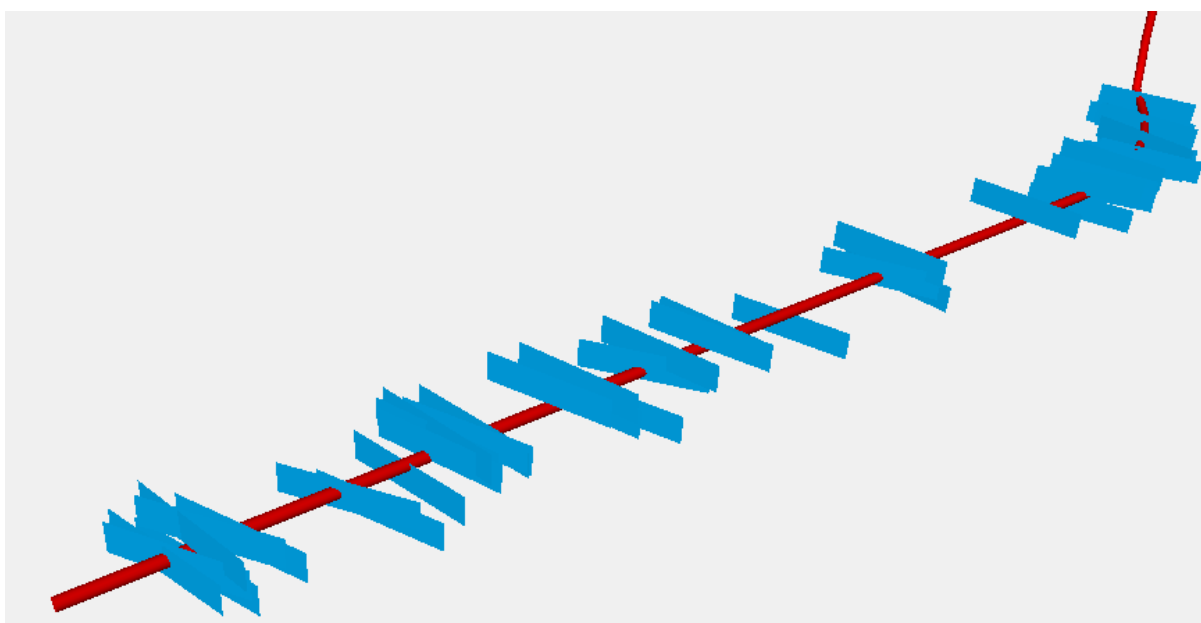


Figure 74: DFN Hydraulic Fracture Completion on Sundheim 21-27-3H

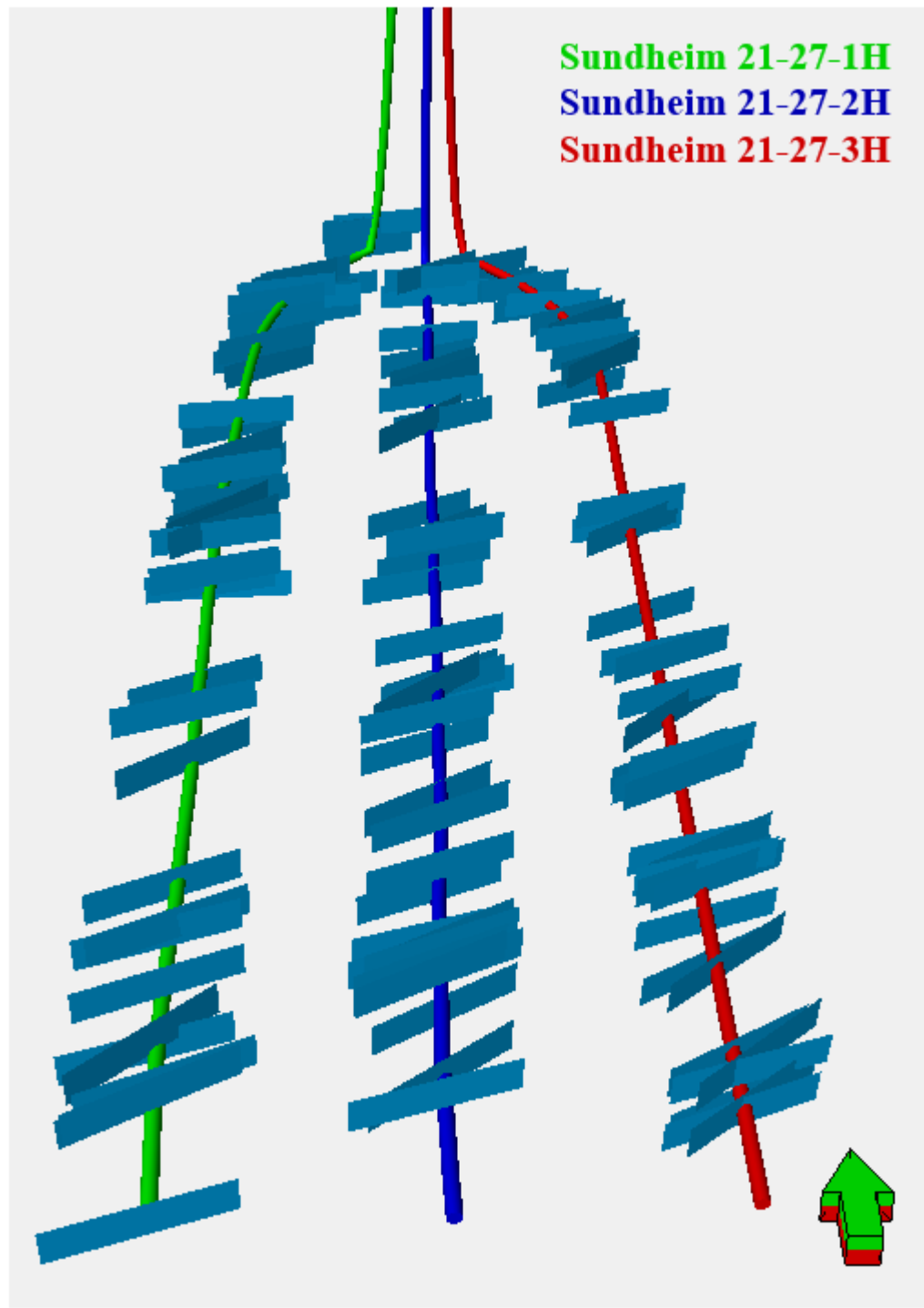


Figure 75: DFN Completions on Sundheim 21-27 Wells

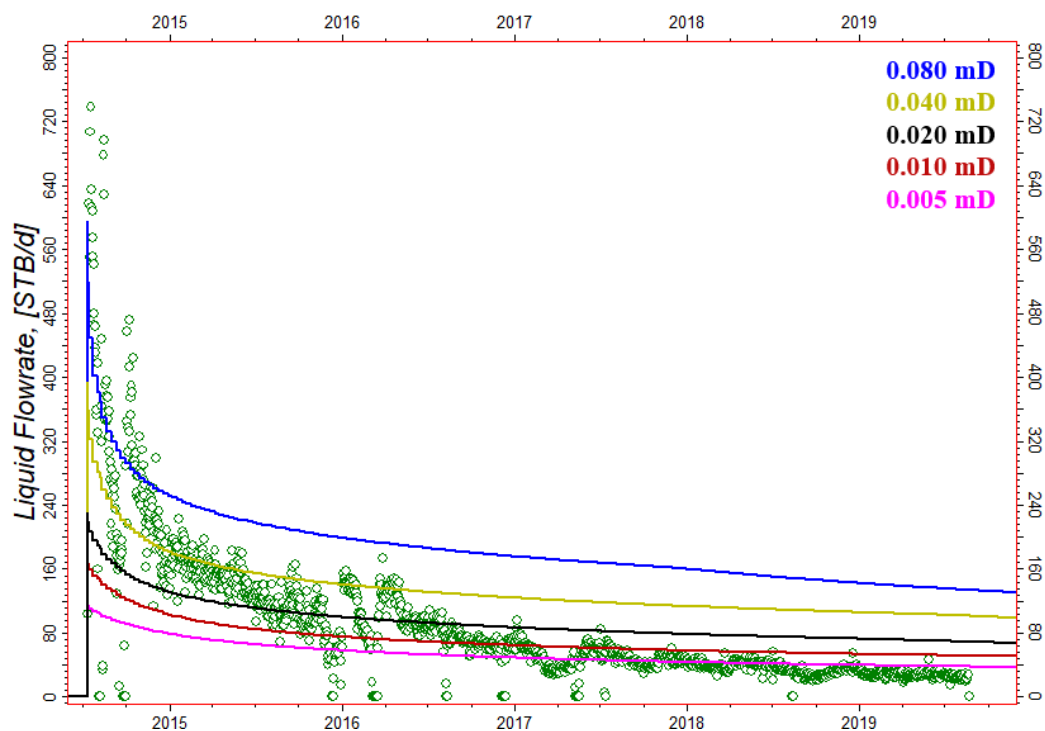


Figure 76: Middle Bakken Matrix Permeability Sensitivity Analysis on Sundheim 21-27-2H Oil Rates

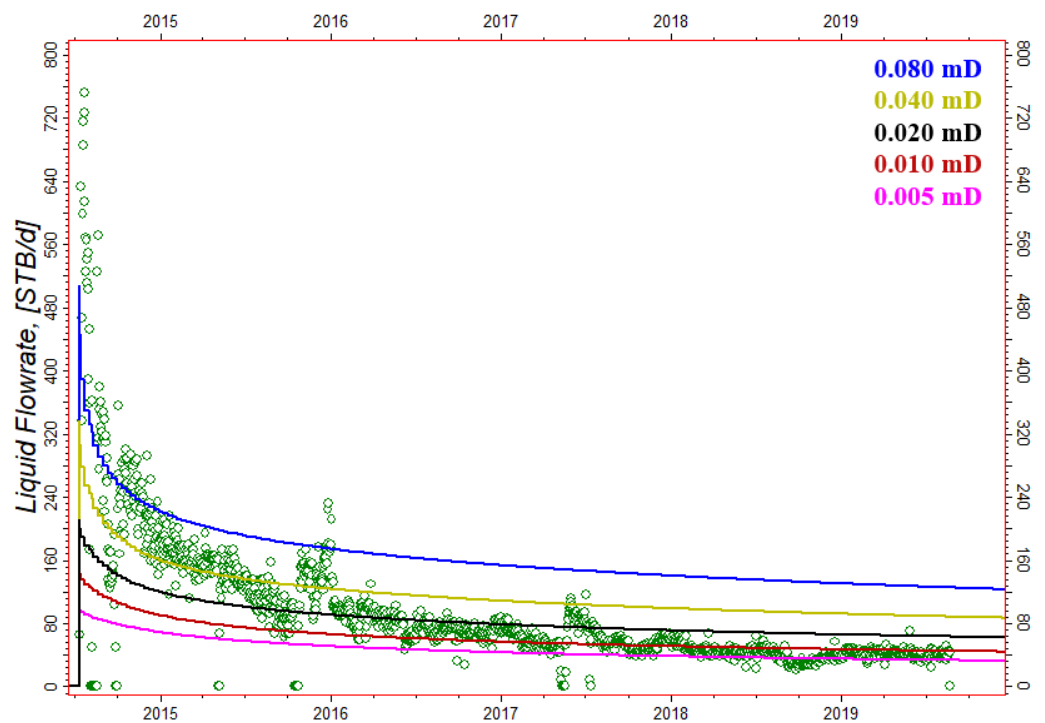


Figure 77: Middle Bakken Matrix Permeability Sensitivity Analysis on Sundheim 21-27-3H Oil Rates

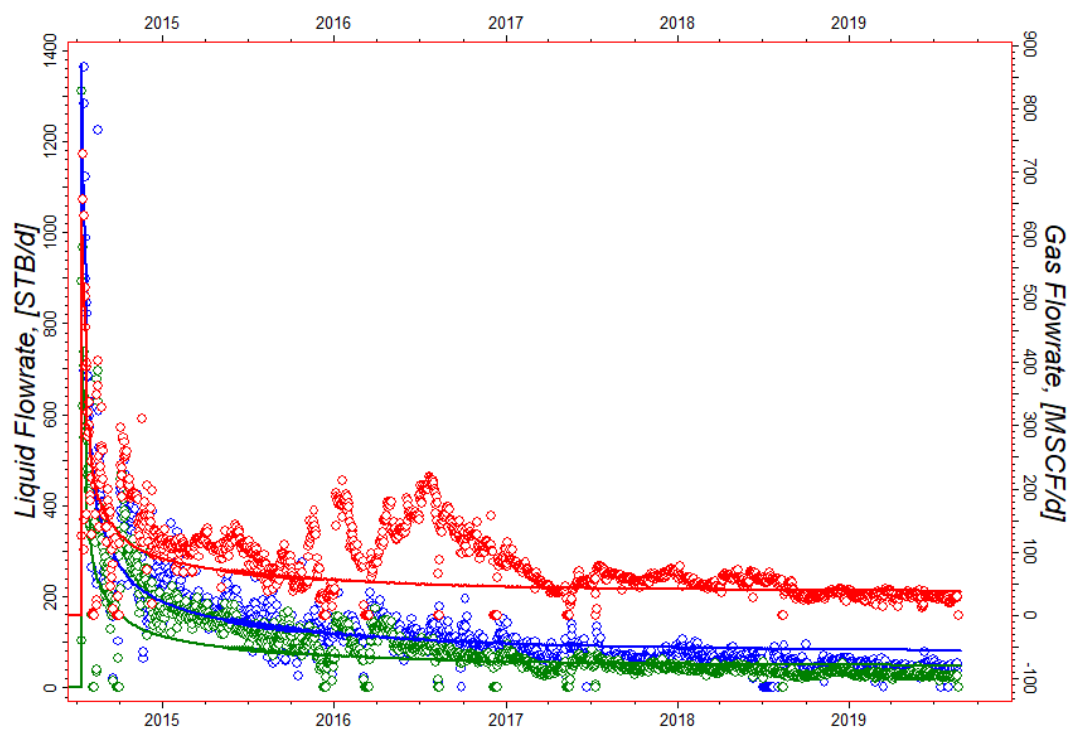


Figure 78: Sundheim 21-27-2H Separate Tank History Matched Cumulative Volumes

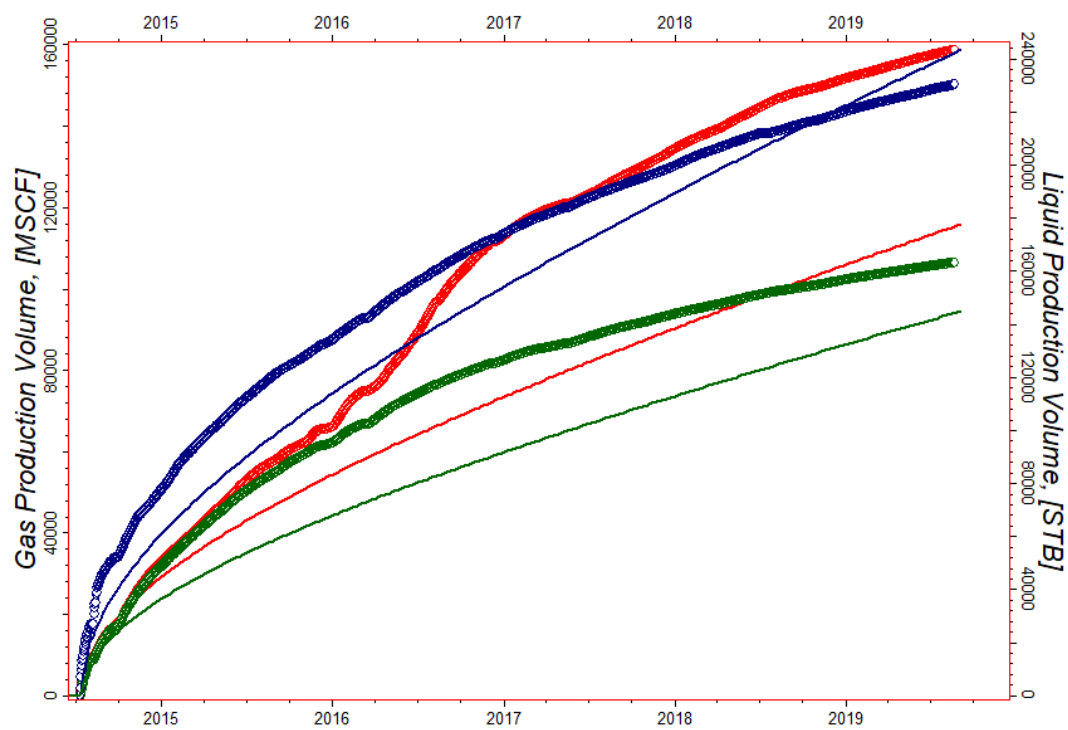


Figure 79: Sundheim 21-27-2H Separate Tank History Matched Cumulative Volumes

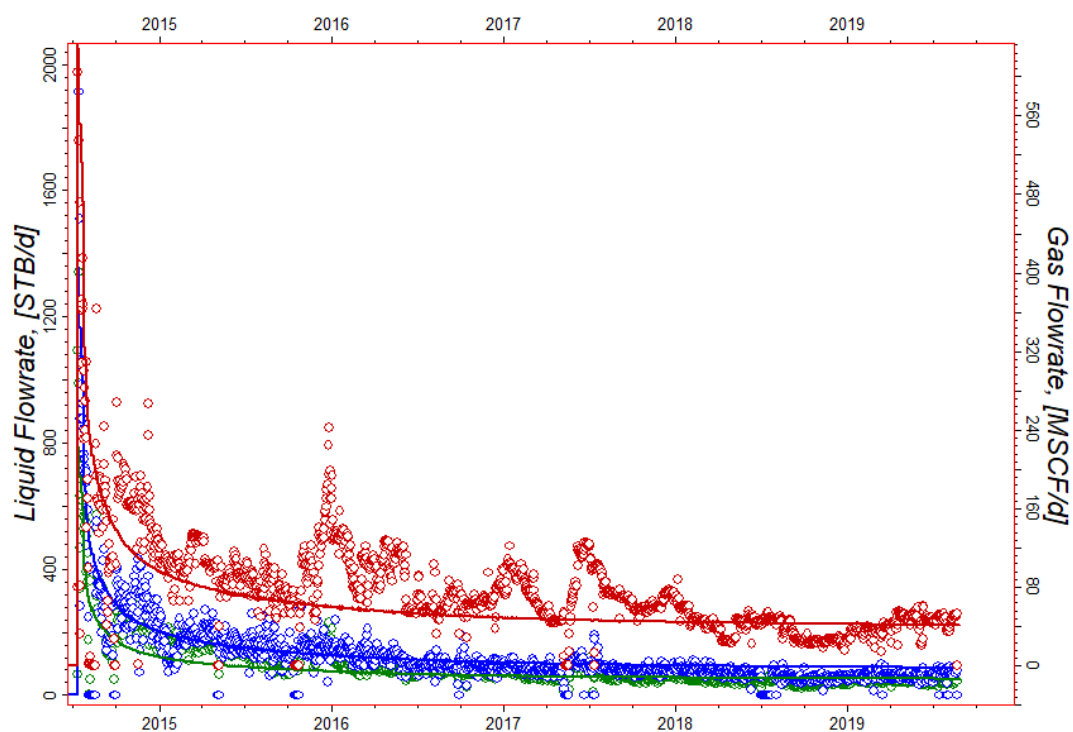


Figure 80: Sundheim 21-27-3H Separate Tank History Matched Rates

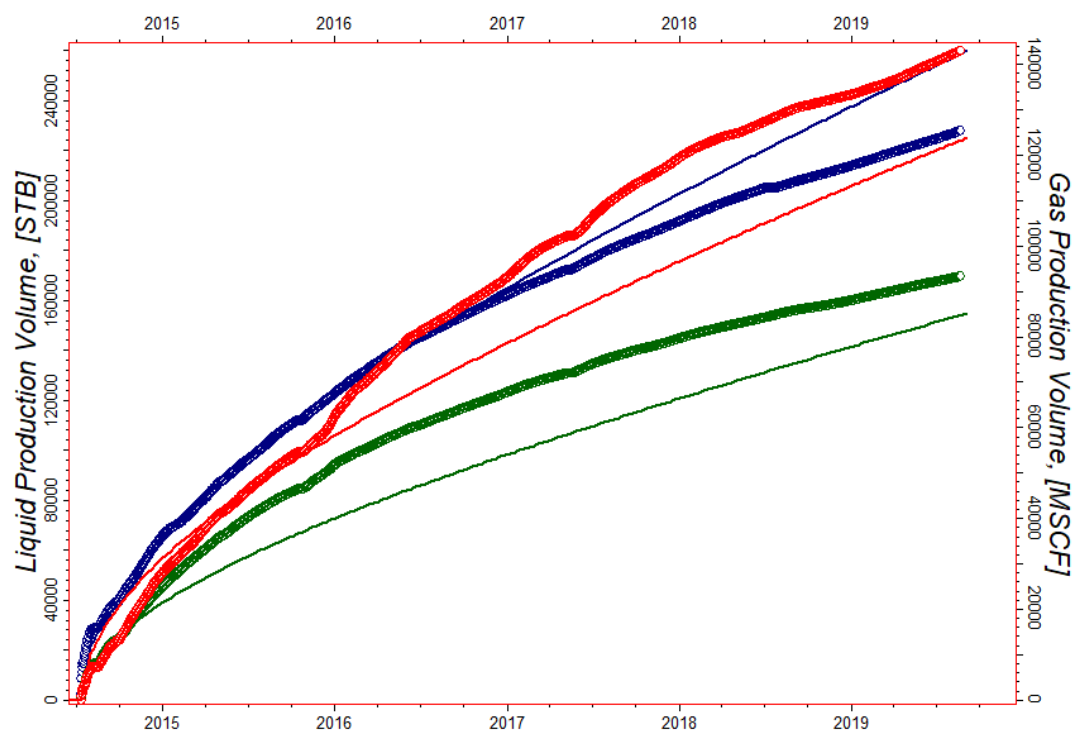


Figure 81: Sundheim 21-27-3H Separate Tank History Matched Cumulative Volumes

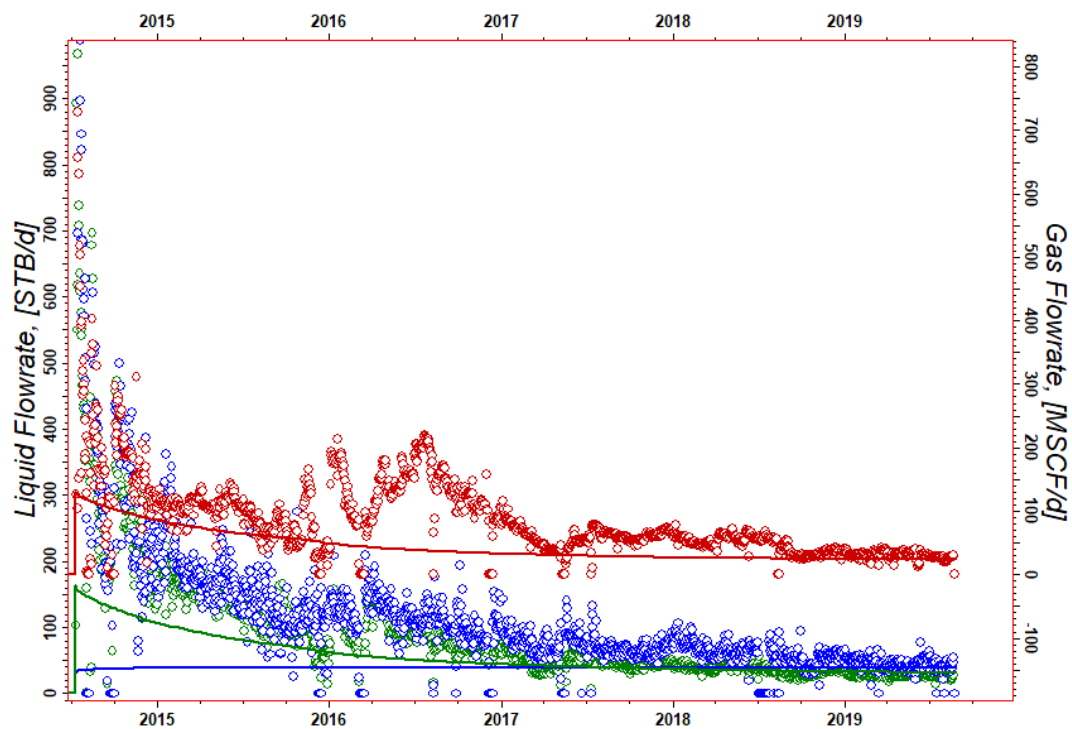


Figure 82: Sundheim 21-27-2H HFVM History Matched Rates

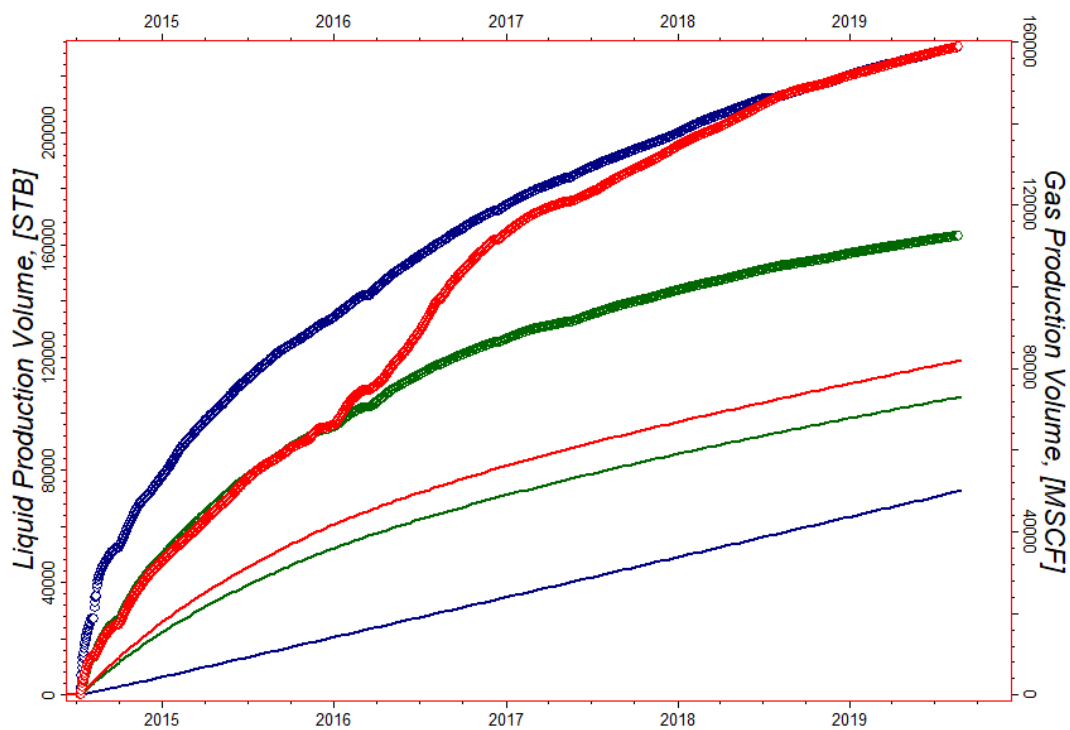


Figure 83: Sundheim 21-27-2H HFVM History Matched Cumulative Volumes

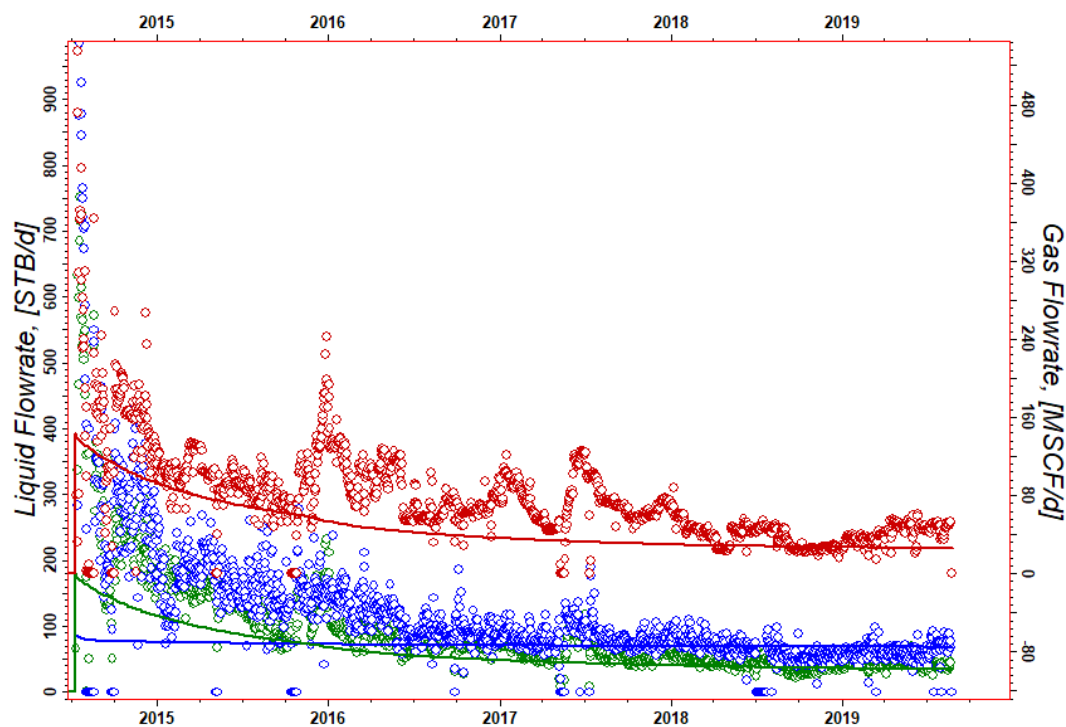


Figure 84: Sundheim 21-27-3H HFVM History Matched Rates

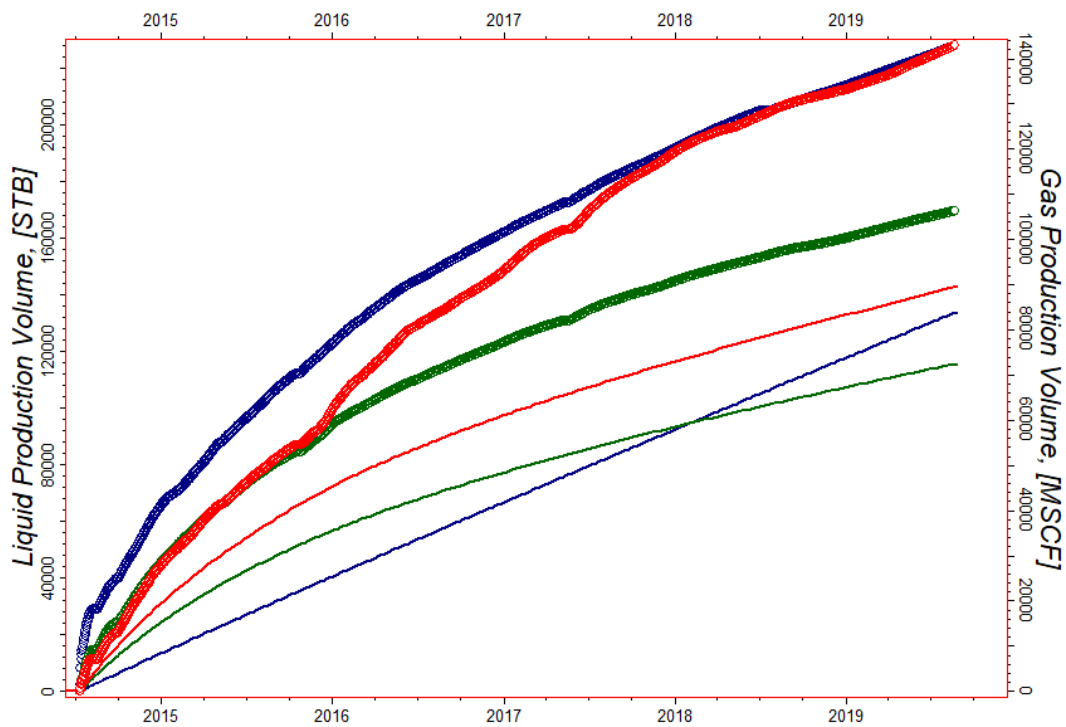


Figure 85: Sundheim 21-27-3H HFVM History Matched Cumulative Volume

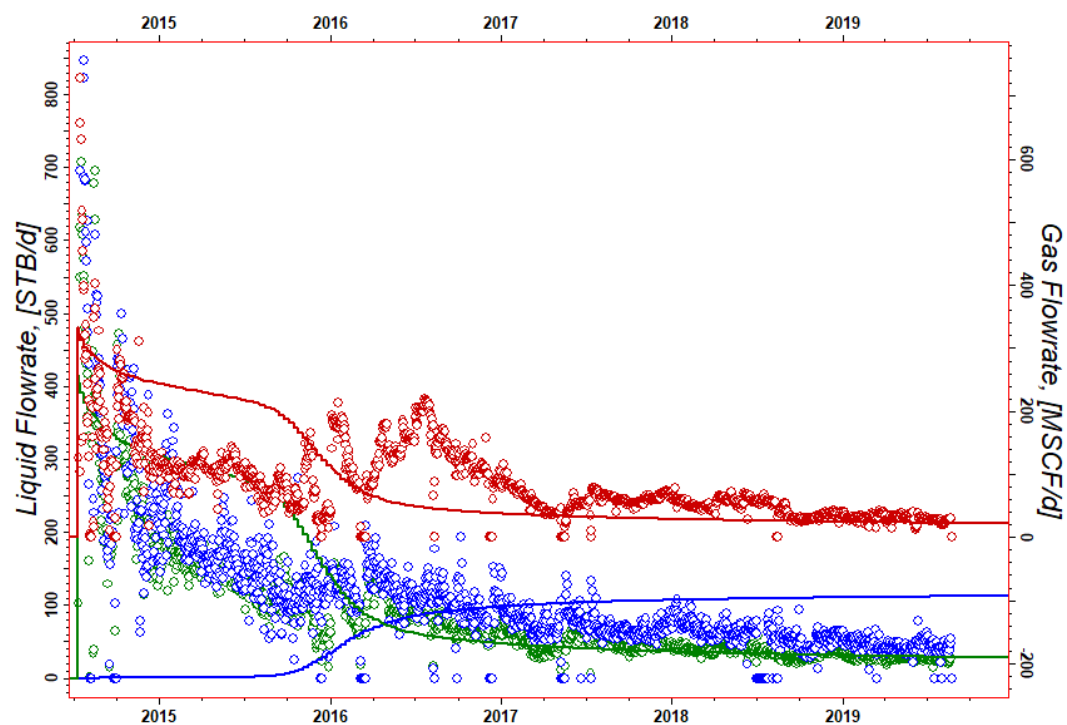


Figure 86: Sundheim 21-27-2H NFVM History Matched Rates

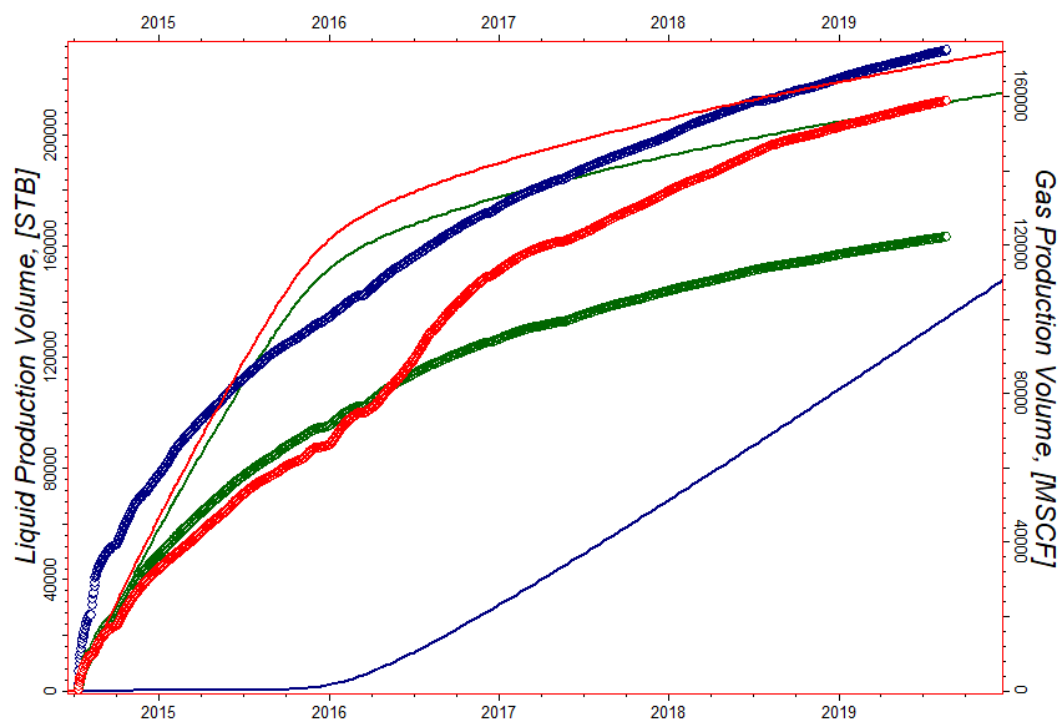


Figure 87: Sundheim 21-27-2H NFVM History Matched Cumulative Volumes

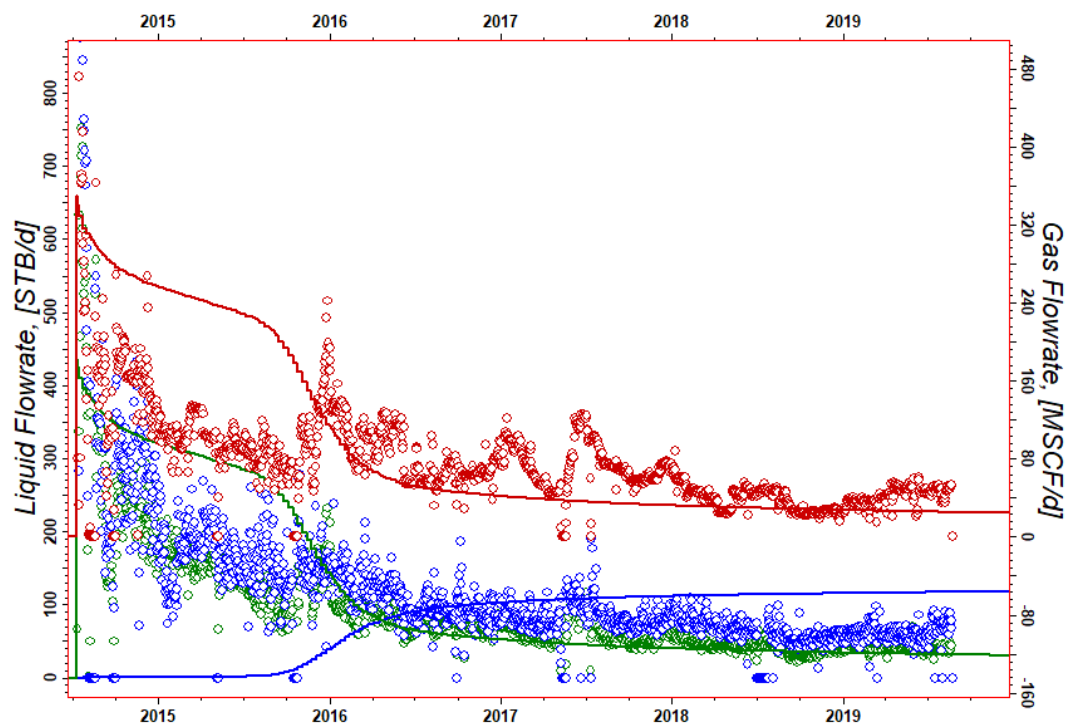


Figure 88: Sundheim 21-27-3H NFVM History Matched Rates

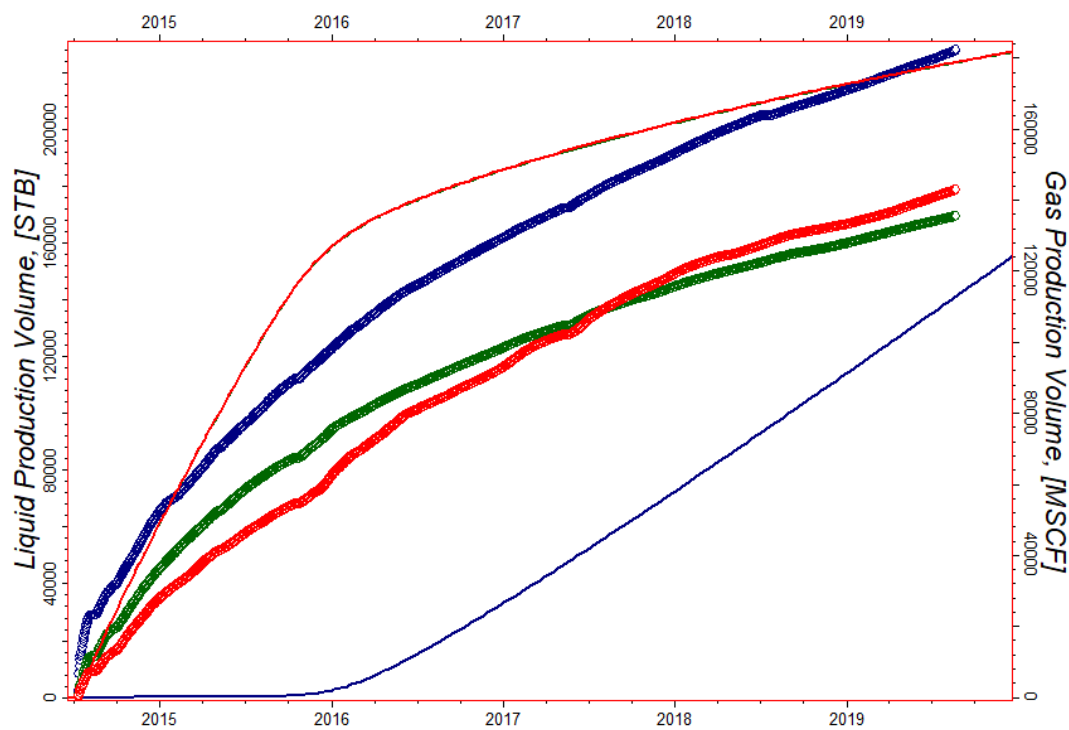


Figure 89: Sundheim 21-27-3H NFVM History Matched Cumulative Volumes

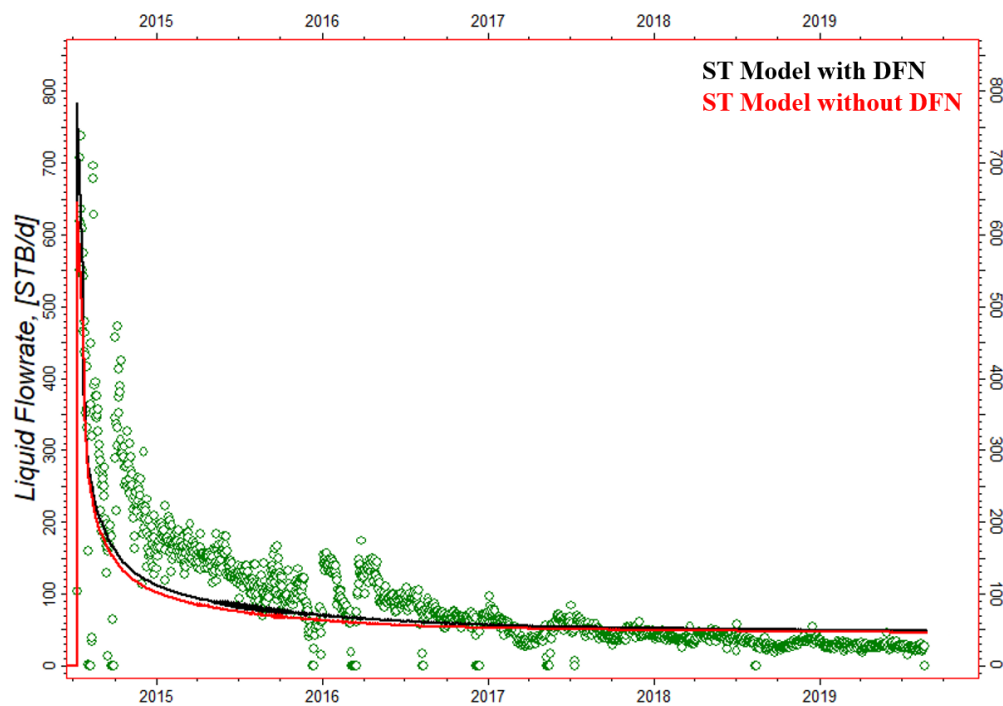


Figure 90: Sundheim 21-27-2H Simulated Oil Rates in the ST Model with and without Middle Bakken DFN

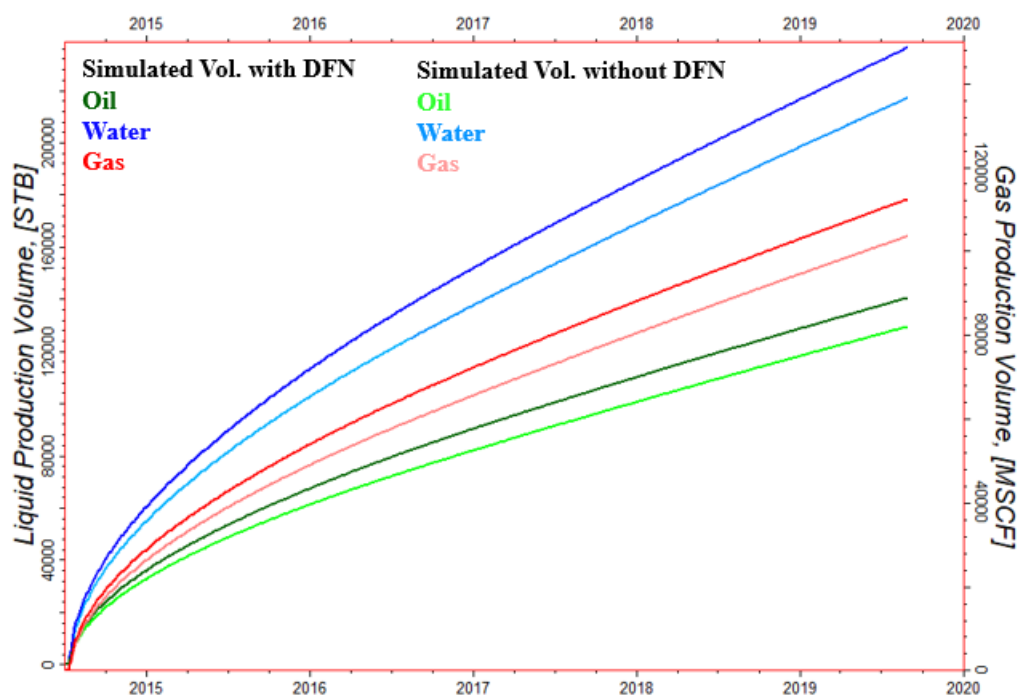


Figure 91: Sundheim 21-27-2H Simulated Cumulative Volumes in the ST Model with and without Middle Bakken DFN

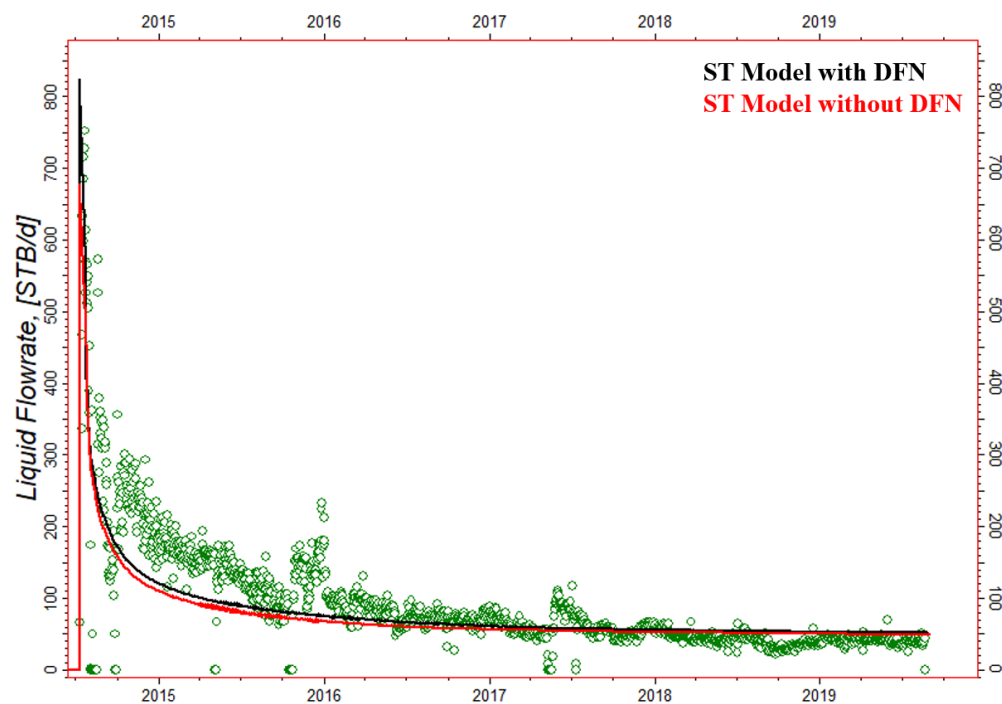


Figure 92: Sundheim 21-27-3H Simulated Oil Rates in the ST Model with and without Middle Bakken DFN

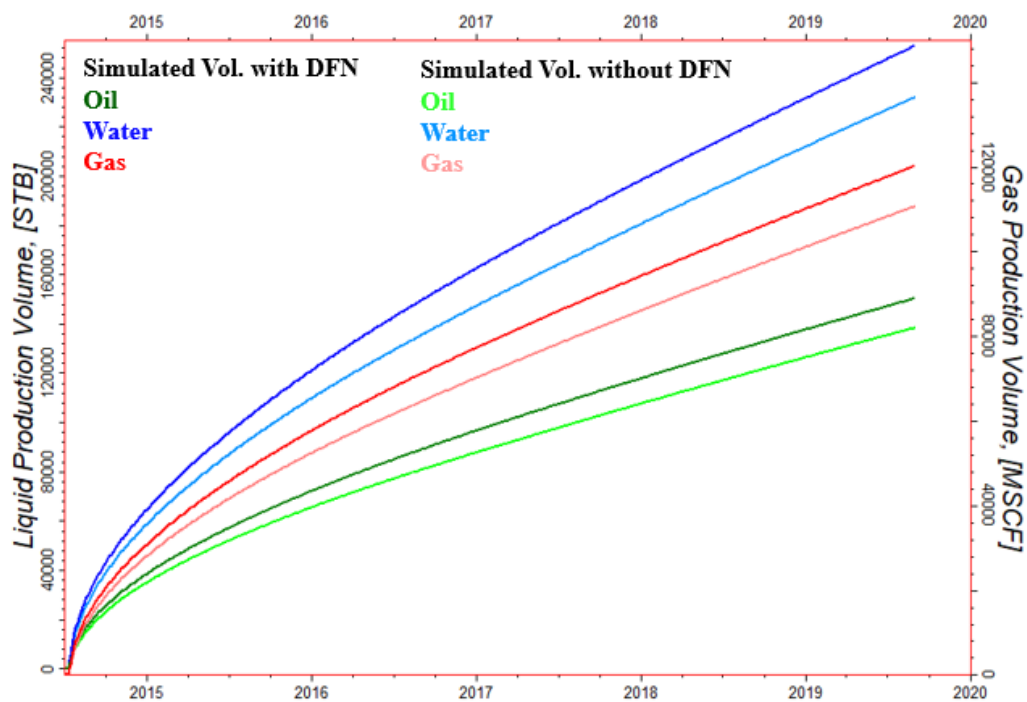


Figure 93: Sundheim 21-27-3H Simulated Cumulative Volumes in the ST Model with and without Middle Bakken DFN

Table VIII: Sundheim 21-27-1H Simulated Cumulative Volumes DFN Comparison

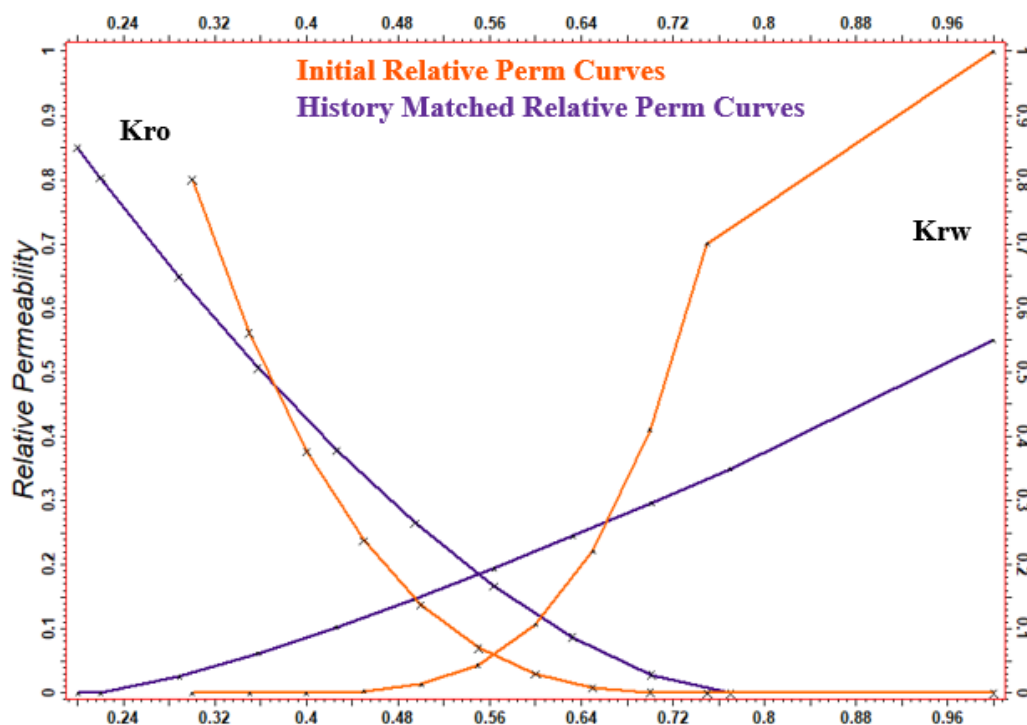
Sundheim 21-27-1H Simulated Cumulative Volumes			
Fluid Type	ST Model with DFN	ST Model without DFN	Percent Difference
Oil	158 MBO	145 MBO	8.2%
Water	265 MBO	244 MBO	7.9%
Gas	126 MMscf	116 MMscf	7.9%

Table IX: Sundheim 21-27-2H Simulated Cumulative Volumes DFN Comparison

Sundheim 21-27-2H Simulated Cumulative Volumes			
Fluid Type	ST Model with DFN	ST Model without DFN	Percent Difference
Oil	140 MBO	130 MBO	7.1%
Water	236 MBO	219 MBO	7.2%
Gas	112 MMscf	104 MMscf	7.1%

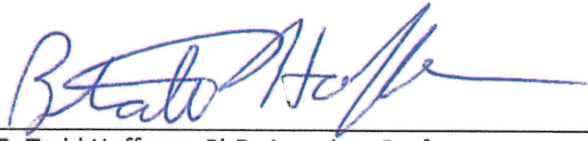
Table X: Sundheim 21-27-3H Simulated Cumulative Volumes DFN Comparison

Sundheim 21-27-3H Simulated Cumulative Volumes			
Fluid Type	ST Model with DFN	ST Model without DFN	Percent Difference
Oil	150 MBO	139 MBO	7.3%
Water	253 MBO	233 MBO	7.9%
Gas	120 MMscf	111 MMscf	7.5%

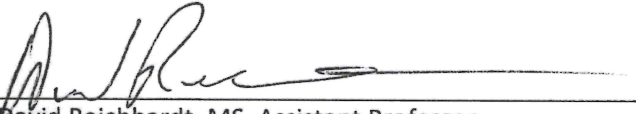
**Figure 94: Initial vs History Matched ST Model Relative Permeability Curves**

SIGNATURE PAGE

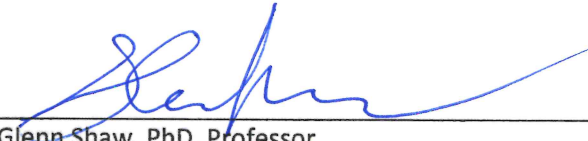
This is to certify that the thesis prepared by Jan Branning entitled "Modeling Unconventional Water Production in the Northeast Elm Coulee Field, Bakken Formation" has been examined and approved for acceptance by the Department of Petroleum Engineering, Montana Technological University, on this 1st day of May, 2020.



B. Todd Hoffman, PhD, Associate Professor
Department of Petroleum Engineering
Chair, Examination Committee



David Reichhardt, MS, Assistant Professor
Department of Petroleum Engineering
Member, Examination Committee



Glenn Shaw, PhD, Professor
Department of Geological Engineering
Member, Examination Committee